METABOLIC AND TRANSCRIPTIONAL REGULATION OF CITRULLINE IN WATERMELON

A Thesis

by

QIUSHUO SONG

Submitted to the Office of Graduate and Professional Studies of
Texas A&M University
in partial fulfillment of the requirements for the degree of

MASTER OF SCIENCE

Chair of Committee,	Vijay Joshi
Co-Chair of Committee,	Kevin M. Crosby
Committee Member,	Xuejun Dong
Head of Department,	Dan Lineberger

May 2020

Major Subject: Horticulture

ABSTRACT

Citrulline is a non-protein amino acid synthesized from ornithine and carbamoyl phosphate in plants. Experiments were performed to understand, (1) the partitioning of citrulline in watermelon plants during the development, (2) impact of environmental stresses (drought, heat, salt and nitrogen) on citrulline metabolism, (3) transcriptomic changes in the citrulline metabolism in response to drought and salt stress, and (4) the variability in seed-specific amino acids and proteins in watermelon germplasm. Based on the dynamic amino acid profiling of the watermelon plant during the development, fruit flesh and rind accumulated the highest amounts of citrulline. The moderate amount of citrulline in leaf and stem tissues suggested the possibility of translocation of citrulline from the vegetative (source) to fruit (sink) tissues. Citrulline accumulation was positively correlated with ornithine (precursor) and arginine (catabolic product). Rapid induction (38-fold in drought and 9.4-fold in salt stress) of citrulline in the vegetative tissues suggests its utility as a potential biomarker during drought and salt-stress induced responses. Heat stress significantly suppressed the synthesis of citrulline metabolism but activated the accumulation of N-rich amino acids (glutamine and asparagine), indicating the existence of citrulline-independent novel mechanisms of heat tolerance in watermelon.

Our data demonstrated that citrulline biosynthesis was regulated by nitrogen status and plays a role in translocating nitrogen based on the reduction of citrulline content in various tissues and down-regulation of genes, *AAT* and *CPS2* (citrulline biosynthesis genes) during nitrogen limitations in watermelon.

RNA-Seq analysis of drought and salt-induced watermelon plants identified over 3900 and 7600 differentially expressed genes, respectively. Consistent with our real-time quantitative

PCR studies, RNA-Seq analysis confirmed the up-regulation of biosynthetic genes (*AAT*, *AOD*, *OTC*, and *CPS2*) and down-regulation of catabolic genes (*ASS*, *ASL*, *ODC*, *OCD*) further supporting the increased accumulation of citrulline during drought stress.

A detailed survey showing significant variation in the content of various amino acids and total crude proteins across the watermelon germplasm opened up opportunities for genetic mapping and marker-assisted selection to enhance these traits in the cultivated varieties.

ACKNOWLEDGMENTS

I appreciate the guidance and support provided by Dr. Vijay Joshi (advisor, my committee chair) in designing and overseeing the research and writing of the thesis. I also appreciate the assistance provided by Dr. Kevin Crosby (committee member, Department of Horticultural Sciences) and Dr. Xuejun Dong (committee member, Department of Soil and Crop Sciences). I want to thank Dr. Umesh Reddy, and Venkata Lakshmi Abburi (West Virginia State University) for their assistance in GWAS analysis of seed amino acids and proteins.

I appreciate the help provided by lab member James DiPiazza in fieldwork and sampling, Dr. Madhumita Joshi for qRT-PCR performance, and Amit Kumar Mishra, and HarAmrit Gill for sample collection.

I thank the Excellence Fellowship/Departmental assistantship provided by the Department of Horticultural Sciences.

Last but not least, I appreciate all the mental and financial support from my family and friends throughout my master studies program.

CONTRIBUTORS AND FUNDING SOURCES

Contributors

This work was supervised by a thesis committee consisting of Dr. Vijay Joshi and Dr. Kevin M. Crosby of the Department of Horticultural Sciences and Dr. Xuejun Dong of the Department of Soil and Crop Sciences.

Qiushuo Song designed and performed the proposed research experiments under the supervision of Dr. Vijay Joshi. Qiushuo Song conducted experiments treatments, physiological measurements, sample collection, metabolic analysis, and transcriptomic expression analysis. James DiPiazza helped to fill in pots with sandy soil for drought experiments and to fertilize field plants for N limited supply experiment. Dr. Madhumita Joshi assisted in qRT-PCR performance. GWAS technical assistance is from Dr. Umesh Reddy, Venkata Lakshmi Abburi (West Virginia State University). Dr. Xuejun Dong (committee member) provided technical guidance for monitoring the drought stress treatments. The committee members, Dr. Joshi (advisor, committee chair), Dr. Crosby (co-advisor, committee member), and Dr. Dong, contributed to editing the thesis.

Funding Sources

The Excellence Fellowship/Departmental assistantship provided by the Department of Horticultural Sciences, Texas A&M AgriLife Research. This research was carried out using the funds made available by Dr. Joshi through the Hatch project (#TEX09647).

NOMENCLATURE

NPAAs	Non-proteinogenic amino acids
ASS	Arginine succinate synthase
NO	Nitric Oxide
NOS	NO-synthase enzyme
OTC	Ornithine carbamoyl transferase/ transcarbamoylase
CP	Carbamoyl-P
CPS	Carbamoyl phosphate Synthase
ASL	Argininosuccinate lyase
UPLC	Ultra-performance liquid chromatography
LC-MS	Liquid chromatography-mass spectrometry
UPLC-MS/MS	Ultra-performance liquid chromatography-tandem mass spectrometry
GC	Gas chromatography
CE	Capillary electrophoresis
AQC	6-aminoquinolyl-N-hydroxysuccinimidyl carbamate
NGS	Next-Generation Sequencing
FPKM	Fragments Per Kilobase of transcript per Million mapped reads

TABLE OF CONTENTS

Page

LIST OF FIGURES

Page

LIST OF TABLES

Page

CHAPTER I

INTRODUCTION OF CITRULLINE AND ITS DEVELOPMENTAL ACCUMULATION IN WATERMELON

1.1 Introduction

1.1.1 Background of citrulline

Citrulline, one of the non-proteinogenic amino acids (NPAAs), was isolated from watermelon (*Citrullus vulgaris*) [1] and hence was named after its *species* [2]. Citrulline is widespread in many living organisms, including animals, microorganisms, and plants.

In humans, citrulline is synthesized during the urea cycle and formation of nitric- oxide (NO) as a metabolic intermediate [3]. Citrulline is produced in the gut, released into the blood, and then turned back into arginine in the kidney [4]. This circulation results in the production of nitric oxide. Nitric oxide causes vasodilation or widening of the blood vessels to transport blood and thereby accelerating the distribution of blood oxygen throughout the body efficiently. For this reason, citrulline possesses substantial medical and therapeutic benefits, such as preventing arteries from hardening, reducing aortic blood pressure, lowering cholesterol to improving lipid profiles, and assisting in weight management [5]–[9]. Chemically. Citrulline ($C_6H_{13}N_3O_3$) is a colorless solid at ambient temperature and relatively soluble in water [3]. Commercially, citrulline is produced through fermentation using specialized microbial strains. L-citrulline production is achieved by engineering citrulline metabolic pathways, such as suppressing the expression of the repressor gene (argR) and argininosuccinate synthase gene (argG), promoting the overexpression of genes such as the ornithine acetyltransferase gene (argJ) [10], N-acetyl L-glutamate kinase ($argB^{fbr}$) and L-ornithine carbamoyl phosphate transferase (argF) [11].

In plants, citrulline metabolism and transport have been mostly studied in *Arabidopsis thaliana* and *Cucurbitaceae* species. The fruits of the members of the *Cucurbitaceae* family are considered to contain relatively large amounts of citrulline. Citrulline accumulates abundantly in *Cucurbitaceae* family members, such as buffalo gourd (*Cucumis foetidissima* Kunth), bitter gourd (*Momordica charantia*) cantaloupe (*Cucumis melo* L. Reticulatus Group), cucumber (*Cucumis sativus*), pumpkin (*Cucurbita pepo* L. subsp. *pepo*), squash (*Cucurbita pepo*), melon (*Cucumis melo*), horned melon (*Cucumis metuliferus*), mouse melon (*Melothria scabra*), and watermelon (*Citrullus lanatus*) [12], [13]. However, domestic watermelons accumulate six to nine times higher citrulline than their close relatives such as cucumber and pumpkin [14]. Citrulline concentration in watermelon fruits can reach up to 100-300 mmol per kg dry weight [15]. Besides fruits, citrulline has been detected in other watermelon tissues such as seeds, seedlings, stems, leaves, flowers and roots [16]. It has been suggested that the abundance of citrulline in watermelon might be regulated spatially and developmentally. Citrulline accumulation didn't show significant changes during the early fruit development but showed a steady increase during fruit maturity [15], [17], [18]. No correlation was observed between citrulline content and fruit shape, size, flesh color, rind color, or soluble solids content and ploidy level [19]. In muskmelon (*Cucumis melo* L.), Mitchell and Madore [20] found that citrulline was the primary component of all detected amino acids in leaf and phloem sap samples during the light period. The high amount of citrulline in the phloem sap suggested the possibility of citrulline transport from the leaf (source) to fruits (sink) through the phloem (vasculature) [20].

There are three main enzymes involved in citrulline metabolism in mammals: arginine succinate synthase (ASS), NO-synthase enzyme (NOS), and ornithine carbamoyl transferase (OTC). However, citrulline metabolism in plants is more complex. A detailed pathway of

citrulline metabolism is represented in Fig. 1. Anabolic enzyme Ornithine transcarbamoylase (OTC) takes part in the final step of citrulline biosynthesis by catalyzing carbamoyl-P (CP) and ornithine to synthesize citrulline in plants [21]. The RNAseq analysis [18] revealed that the progressive accumulation of citrulline towards fruit maturity was not due to the enhanced biosynthesis, as the expression of OTC during fruit development was relatively constant. Instead, regulated catabolism was suggested to explain the steady increase in citrulline. Citrulline is catabolized to L-argininosuccinate via Argininosuccinate synthase (ASS) and then to arginine via argininosuccinate lyase (ASL) [22]. Expression of both ASS and ASL genes were down-regulated in flesh tissues during fruit development [18], [23]. It has been demonstrated that citrulline could be recycled via arginine catabolism by nitric-oxide synthase (NOS) in animals [24]. But the presence of the NOS pathway is not experimentally demonstrated in plants [25], [26].

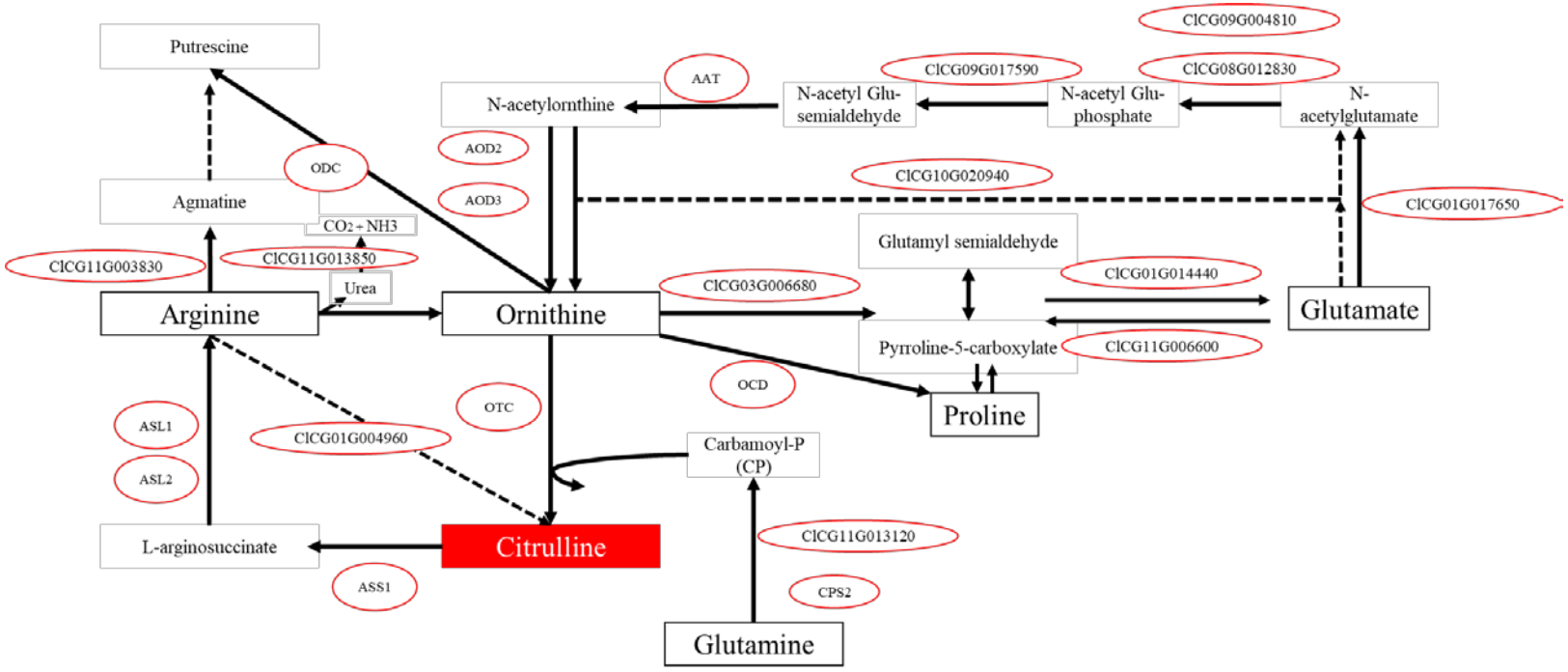

Figure 1. Citrulline metabolic pathways in plants based on a review by Joshi and Fernie [27]**. The gene IDs (ClCG#) were retrieved from the watermelon genome (cultivar "Charleston Gray") database in the International Cucurbit Genomics Initiative (ICuGI), and the abbreviations of gene names represent genes investigated in real-time PC**

1.1.2 Detection of citrulline and related amino acids using UPLC-MS/MS

Liquid chromatography-mass spectrometry (LC-MS), is an analytical chemistry technique that combines the liquid chromatography (LC) capability of physical separation with mass spectrometry (MS) capability of mass analysis. In liquid chromatography, differential partitioning between stationary and mobile phase causes the various constitutes in the mixture to travel at different speeds leading to an efficient separation while mass spectrometry measures the ion mass-to-charge ratio. Although several techniques have been used for the determination of amino acid content from biological samples, there is a continuing need for improved accuracy, precision, and higher throughput. Amino acids are separated utilizing high-performance liquid chromatography, gas chromatography (GC) or capillary electrophoresis (CE) before detection by absorbance, fluorescence, or mass spectrometry (MS). Water Corporation's UltraPerformance LC® (UPLC®, Waters Corp., Milford, MA) has emerged as an improvement over traditional LC for analytes detection and large amounts of samples screening due to higher resolution, greater sensitivity, and a shorter sample run-time.

Among the various amino acid detection techniques, Waters corporation's AccQ•Tag technology has continued to gain acceptance [28]–[30]. It utilizes 6-aminoquinolyl-N-hydroxysuccinimidyl carbamate (AQC) to transform primary and secondary amines into highly stable fluorescent derivatives. The AccQ•Tag technology can be used in conjunction with ultra-performance liquid chromatography (UPLC), and MS approach using an HPLC separation on a C18 column followed by detection with a mass spectrometer offering new opportunities for faster analysis [31], [32].

Citrulline metabolism in plants is not well understood. A detailed analysis of tissue-specific partitioning, developmental regulation, long-distance transport, expression analysis of

genes associated with its biosynthesis and catabolism mechanism of citrulline would help to understand its functional relevance in plants. Besides being naturally rich in citrulline, with the advent of the published genome [18] along with availability of the genetic mapping resources [33], [34], next-generation sequence (NGS) data [18], [23], [35], [36], natural genetic diversity within species [37], [38], and the genomic databases (International Cucurbit Genomics Initiative; ICuGI), watermelon would be an ideal model system to improve our understanding of its regulation. In Chapter 1, a protocol has been optimized using an analytical platform that combines ultra-performance liquid chromatography with tandem mass spectrometry (UPLC-MS/MS) to detect citrulline and other 44 amino acids and was used to study the changes in the accumulation of citrulline in watermelon throughout the development in different types of tissues.

1.2 Materials and Methods

1.2.1 Germination and growth condition

Seeds of two commercial watermelon varieties- Crimson Sweet and Charleston Gray were sown in 96-well plug trays (25’’length × 15’’ width × 2’’ depth) in a greenhouse at the Texas A&M AgriLife Research & Extension Center at Uvalde, TX. The environmental factors inside the greenhouse were monitored using a centralized control system (Wadsworth, Arvada, CO) with a cycle of 16 h light, followed by 8 h darkness. The temperature and relative humidity were maintained at 30±5℃ and 70±5%, respectively.

Approximately 6-week-old healthy seedlings of cultivars- Charleston Gray and Crimson Sweet with 9 replicates (4 replicates for further metabolic analysis and the rest for back-up) were transplanted into field beds covered with black mulch at Texas A&M AgriLife Research &

Extension Center at Uvalde, TX. After transplanting, plants were watered appropriately based on actual soil moisture status and were fertilized with urea (46-0-0, HELENA) every week starting from one week after transplanting until harvesting. Total fertilized N summed up to 150±10 lb./acre.

1.2.2 Sample collection and physiological measurements

As is shown in Fig. 2, samples (1) seeds, (2) developing seedlings (cotyledon), (3) fully opened leaves (first true leaf), (4) stems, (5) leaf I (~14-week-old), (6) leaf II (~16-week-old), (7) flowers, (8) rinds, and (9) flesh tissues of mature fruits, were collected from 3-5 independent plants from each replication at 8 time-points beginning 10 days after germination until the fruit maturity. Additionally, a phloem sap was collected from the internode and petiole at harvesting. As is shown in Fig. 3 (picture for collection position), sap samples oozing out up to 10 min from the cut end were collected using a pipette in 1.5ml of microcentrifuge tubes and stored at -80℃. The samples for both amino acid analysis and RNA extraction were collected and flash-frozen in liquid nitrogen.

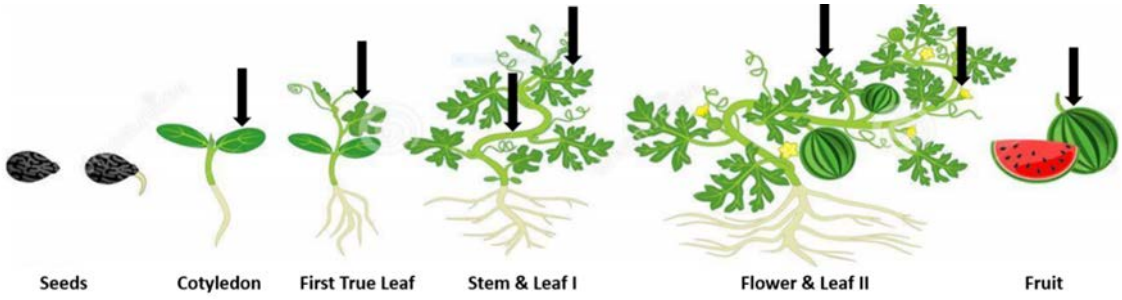

Figure 2. Timeline of sample collection at various developmental stages. The original color picture under the black arrow was downloaded from Dreamstime®(https://www.dreamstime.com/).

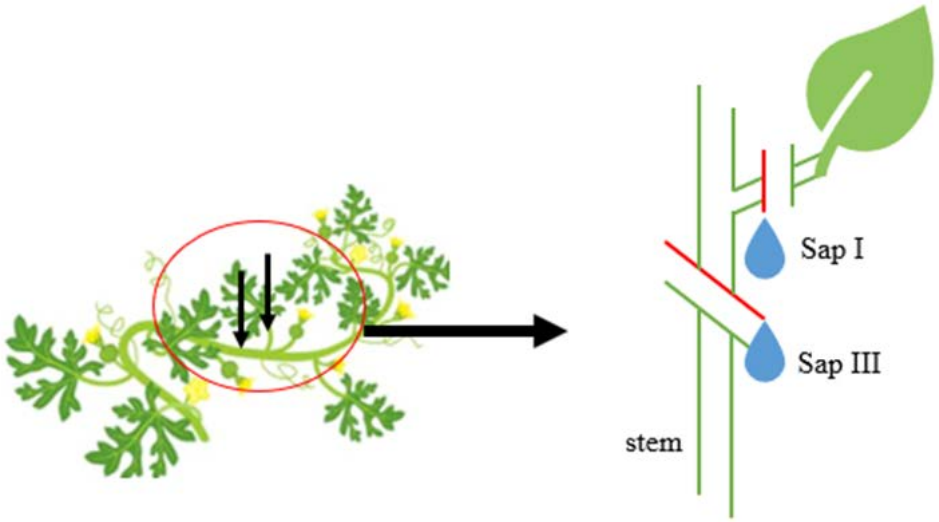

Figure 3. Phloem sap sampling position. The light black arrows represent the cutting positions for collecting sap I and sap III. These positions were amplified and simplified in the right-hand panel. The red straight lines indicate the cutting surface for sap collection.

1.2.3 Extraction method for free amino acids

Approximately 20 mg frozen tissue samples collected into 2 ml microcentrifuge tubes were homogenized into fine powder in a paint shaker (Harbil model 5G-HD paint shaker) using 3 mm stainless steel beads (Demag stainless steel balls, Abbott Ball Company, CT, USA) to quantify free amino acids. Amino acids were extracted using an established protocol [16] by suspending the homogenized samples in 100mM cold HCl extraction buffer, followed by incubation on ice (~ 20 minutes) and then centrifuging at a speed of 14,609 × g for 20 minutes at 4℃. The supernatants were collected and filtered through a 96-well 0.45-µm-pore filter plate (Pall Life Sciences, USA). The eluents collected in 96-well trap plates were stored at -20℃ for further amino acid quantification.

1.2.4 Detection and quantification of amino acids using LC-MS

The filtered eluents were used for amino acid quantification with AccQ•Tag3X Ultra-Fluor™ derivatization kit (Waters Corporation, Milford, MA, USA) as per the manufacturer's protocol. Amino acid calibrators including 45 amino acids (listed in Table 1) and AccQ•Tag Ultra "3X" Derivatization Reagent were obtained from Kairos™ Amino Acid Kit (Waters Corporation, Milford, MA, USA). The LC-MS grade solvents Methanol and Acetonitrile were purchased from VWR (USA).

Table 1. List of 45 amino acids included in calibrators of Kairos™ Amino Acid Kit

Essential and Non-essential Amino Acids (20)	Other Amino Acids (25)
Alanine, Arginine, Asparagine, Asparagine, Aspartic acid, Cystine, Glutamine, Glutamic acid, Glycine, Histidine, Isoleucine, Leucine, Lysine, Methionine, Phenylalanine, Proline, Serine, Threonine, Tryptophan, Tyrosine, Valine	Hydroxyproline, Allo-isoleucine, Argininosuccinic acid, Beta-Alanine, Carnosine, Citrulline, Cystathione, Beta Aminoisobutyric acid, Gamma-Aminobutyric acid, Alpha Aminobutyric acid, Homocitrulline, Homocysteine, Hydroxylysine, S-Sulfocysteine, Taurine, 1-Methyl Histidine, 3-Methyl Histidine, Kynurenine, Alpha Aminoadipic acid, Anserine, Ornithine, Phosphoethanolamine, Ethanolamine, Glycyl Proline, Ethanolamine

Lyophilized amino acid powder of six amino acid calibrators representing different concentrations (5.0pmol/µl to 1000pmol/µl) was reconstituted with 2mL of 0.1M HCl according to the manufacturer's protocol. L-Norvaline (Sigma, St. Louis, MO) was used as an internal standard at a fixed concentration of 25pmol/µl.

The derivatization of calibrators or samples was carried out with AccQ•Tag3X Ultra-Fluor™ derivatization kit (Waters Corporation, Milford, MA, USA), including AccQ•Tag3X reagents. 5µL of an amino acid standard solution or sample extract was mixed with 35µL of AccQ•Tag3X Ultra borate buffer, and the chemical reaction was initiated by adding 10µL of AccQ•Tag3X reagent which had previously dissolved with 1.5 mL of AccQ•Tag3X Ultra reagent diluent. The reaction was incubated at 55℃ for 10 minutes.

UPLC-ESI-MS/MS analysis was performed using a Waters Acquity H-class UPLC system equipped with Waters Xevo TQ mass spectrometer by using electrospray ionization (ESI) probe. The Waters Acquity H-class UPLC system was composed of an autosampler, a binary solvent manager, a Waters® ACQUITY UPLC® Fluorescence (FLR) detector, a column heater and a Water's AccQ•Tag Ultra column (2.1mm i.d.×140 mm, 1.7µm particles). The mobile phase consists of water phase (A) (0.1% formic acid v/v) and acetonitrile (B) (0.1% formic acid v/v) with a stable flow rate at 0.5 mL/min and column temperature setting of 55℃. The gradient of non-linear separation was set as following: 0-1 min (99% A), 3.2 min (87.0% A), 8 min (86.5% A), and 9 min (5% A). Finally, 2µL of the derivatized sample was injected on to the column for analysis. IntelliStart software (Waters Corp, Milford, MA) was used to optimize each amino acid Multiple Reaction Monitoring (MRM) transitions, collision energy values and cone voltage. ESI source was set to 150°C with gas desolvation flow rate at 1000 L/h, gas flow cone at 20 L/h, desolvation temperature at 500 °C, capillary voltage at 2.0 kV, gas collision energy varied from

15 to 30 V and cone voltage at 30 V for detecting all amino acids. MRM was operated in positive mode. Water's MassLynx™ software was used for instrument monitoring and data acquisition. The data integration, calibration curves and quantitation (0.45-90 pmol/µl) were carried out with TargetLynx™ Application Manager (Waters Corporation, Milford, MA, USA).

1.3 Results and Discussion

1.3.1 Detection of citrulline and other amino acids using UPLC-MS-MS

Fluorescence (FLR) and total ion chromatograms of 45 amino acids were monitored and viewed in Waters MassLynx^{TM} software. Among the three amino acids represented in Fig. 5, Arginine showed up first, followed by citrulline and then ornithine.

To quantify amino acid using Waters TargetLynx^{TM}, calibration was carried out for all 45 amino acids using TargetLynx software. Each amino acid was detected based on the calibration curves. The calibration curves of citrulline, arginine, and ornithine are shown in Fig. 6. R^2 coefficients for all amino acids were higher than 0.95 indicating strong linear fits. The standard curves were generated using 6 calibrators (standard solutions) to allow quantification of amino acids ranging from 0.45 to 90 pmol/µl. The UPLC-ESI-MS/MS determination of AQC derivatives of 46 amino acids including internal standard was achieved by operating the mass spectrometer (Fig. 4) in the MRM mode. The main product from the collision-induced dissociation of all AQC derivatives was the ion m/z 171, formed upon derivatization. Therefore, the MRM-MS method was developed to include the transition m/z [M + H]+ > 171 for each derivatized amino acid at the corresponding optimized collision energy and cone voltage. Table 2 shows the list of optimized MRM transition, cone, collision energy and scan windows of 46 amino acids (including internal standard Norvaline).

Table 2. Application of MRM transitions, cone, collision energy and scan windows for Kairos™ amino acids

Compounds	MRM Transition	Cone (V)	Collision (V)	Scan window (min)
Ethanolamine	232.20>171.10	30	20	3.14-4.14
Glycine	246.20>171.10	30	20	3.16-4.16
L-Ornithine	237.10>171.10	30	15	4.29-5.29
Lysine	244.10>171.10	30	15	4.67-5.67
Hydroxylysine	252.10>171.10	30	15	3.99-4.99
Phosphoethanolamine	312.20>171.10	30	15	2.72-3.72
Histidine	326.20>171.10	30	20	1.82-2.82
Hydroxproline	302.20>171.10	30	20	2.23-3.23
Asparagine	303.20>171.10	30	20	2.64-3.64
1-Methyl Histidine	340.20>171.10	30	20	2.54-3.54
3-Methyl Histidine	340.20>171.10	30	20	2.34-3.34
Arginine	345.20>171.10	30	20	2.76-3.76
Taurine	296.20>171.10	30	20	2.94-3.94
Serine	276.20>171.10	30	20	2.99-3.99
Aspartic Acid	304.20>171.10	30	20	3.30-4.30
Glycyl Proline	343.20>171.10	30	20	4.23-5.23
Homocitrulline	360.20>171.10	30	20	3.88-4.88
Glutamic Acid	318.20>171.10	30	20	3.49-4.49
Citrulline	346.20>171.10	30	20	3.41-4.41
Sarcosine	260.20>171.10	30	20	3.46-4.46
Threonine	290.20>171.10	30	20	3.67-4.67
β-Alanine	260.20>171.10	30	20	3.60-4.60
Alanine	260.20>171.10	30	20	3.91-4.91
α-Aminoadipic Acid	332.30>171.10	30	20	4.02-5.02
γ-Aminobutyric Acid	274.20>171.10	30	20	3.94-4.94
β-Aminoisobutyric Acid	274.20>171.10	30	20	4.21-5.21
α-Aminobutyric Acid	274.20>171.10	30	20	4.61-5.61
Cystathionine	282.10>171.10	30	15	4.31-5.31
Proline	286.20>171.10	30	20	4.21-5.21
Cystine	291.10>171.10	30	15	4.66-5.66
Valine	288.20>171.10	30	20	5.82-6.82
Homocysteine	305.20>171.10	30	15	8.79-9.79
Allo-isoleucine	302.20>171.10	30	20	9.03-10.03
Leucine	302.20>171.10	30	20	9.10-10.10

Table 2 Continued

Compounds	MRM Transition	Cone (V)	Collision (V)	Scan window (min)
Isoleucine	302.20>171.10	30	20	8.93-9.93
Glutamine	317.20>171.10	30	20	3.01-4.01
Tyrosine	352.20>171.10	30	20	5.23-6.23
Methionine	320.20>171.10	30	20	5.58-6.58
Phenylalanine	336.20>171.10	30	20	9.15-10.15
S-Sulfocysteine	372.20>171.10	30	20	3.11-4.11
Carnosine	397.20>171.10	30	25	2.81-3.81
Anserine	411.20>171.10	30	20	3.00-4.00
Kynurenine	379.20>171.10	30	25	8.97-9.97
Tryptophan	375.20>171.10	30	20	9.17-10.17
Argininosuccinic Acid	461.20>171.10	30	30	3.08-4.08
Norvaline	288.15>171.10	30	20	6.20-7.20

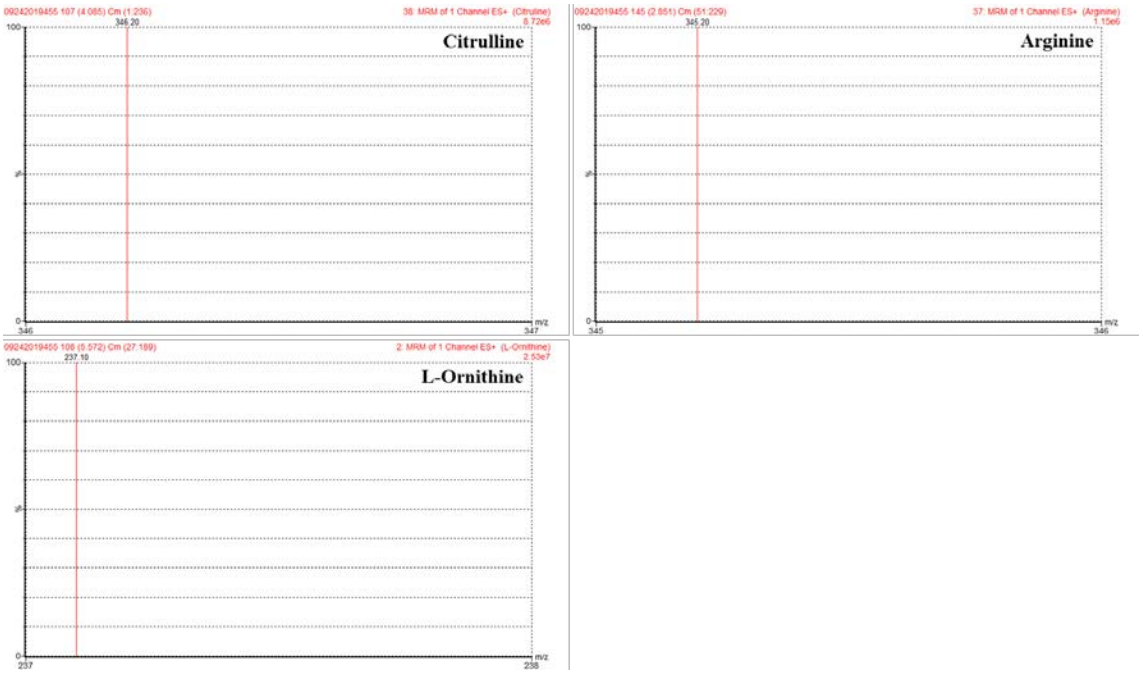

Figure 4. MS chromatograms showing parent ions each for citrulline, arginine and ornithine.

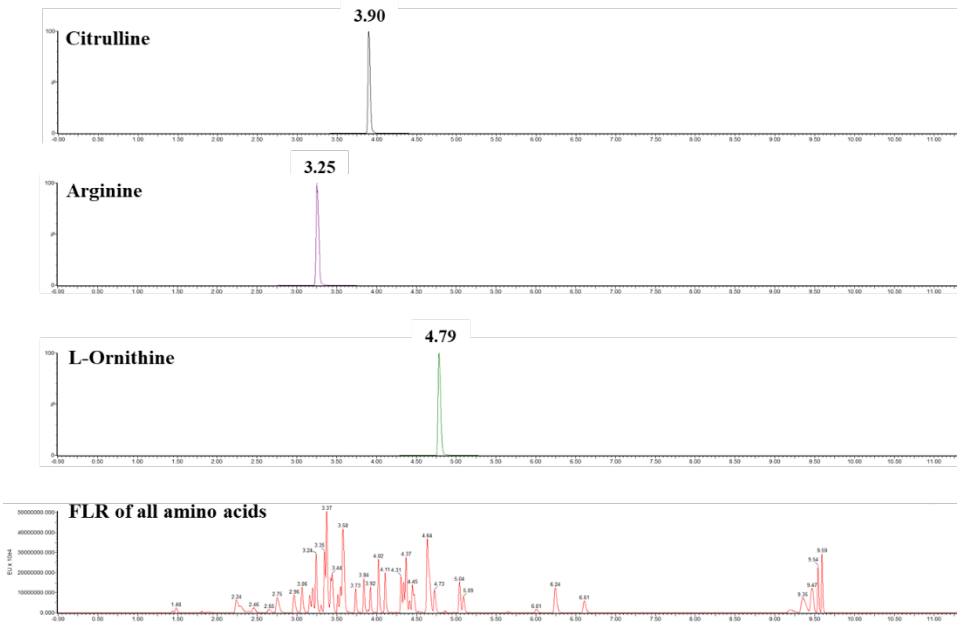

Figure 5. Fluorescence (FLR) of 45 amino acids and total ion chromatogram (TIC) shows the retention time of citrulline, arginine, and ornithine. The number on top of peaks represents the time of each amino acid.

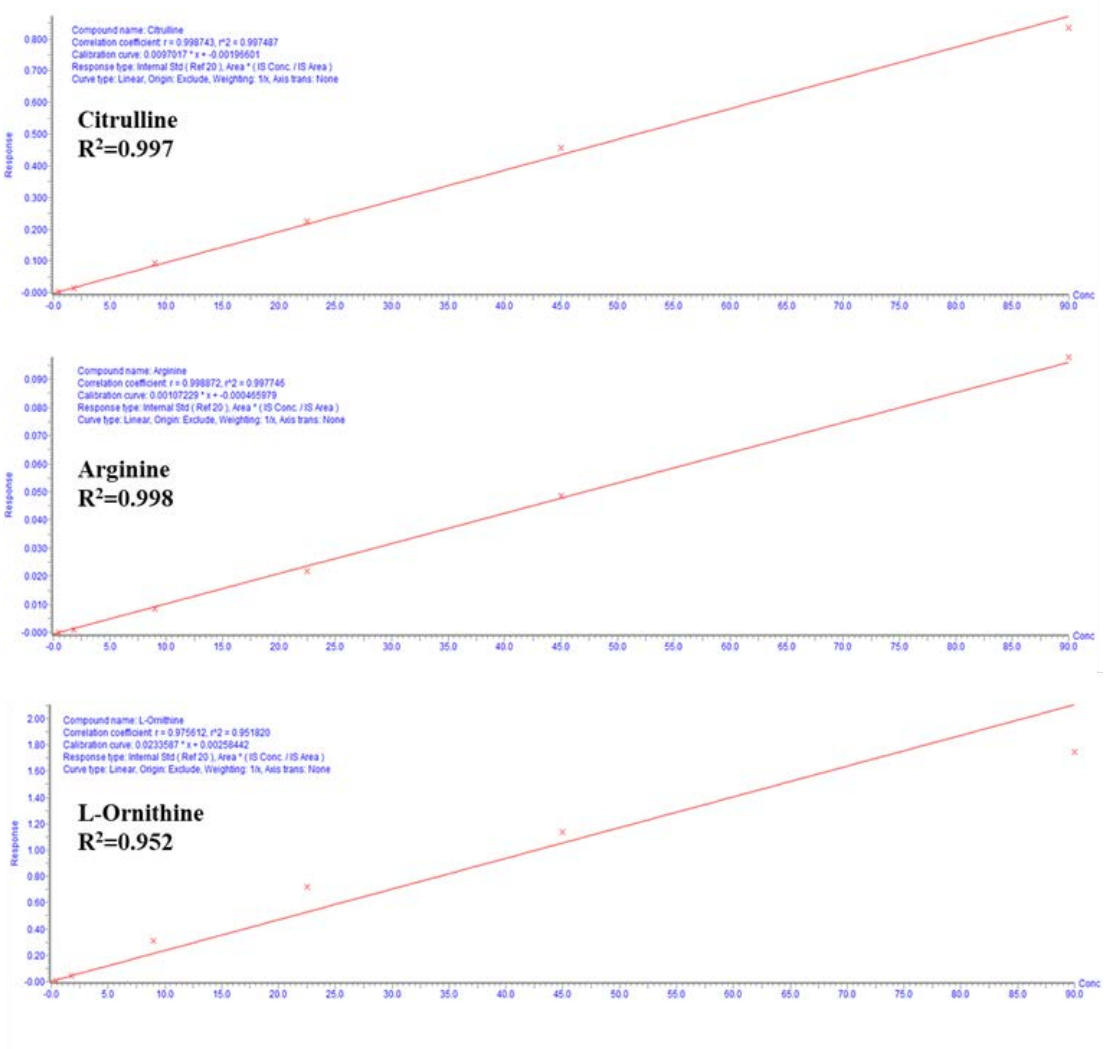

Figure 6. Calibration curves of 3 amino acids (citrulline, arginine, and ornithine). R^2 coefficients indicating the goodness of fit of the model.

1.3.2 Dynamics of citrulline content during development

1.3.2.1 Spatial partitioning of citrulline

To understand the developmental changes in citrulline accumulation, various tissue samples including seed, leaf, stem, flower, fruit rind, and pulp was collected from plants of two watermelon cultivars Crimson Sweet and Charleston Gray at multiple developmental stages as shown in Fig 2. The total citrulline contents in these tissues are shown (Fig. 7). Citrulline

abundance was minimal in seeds and seedling stages (cotyledons and first true leaves) compared to vegetative stages (leaf I and leaf II).

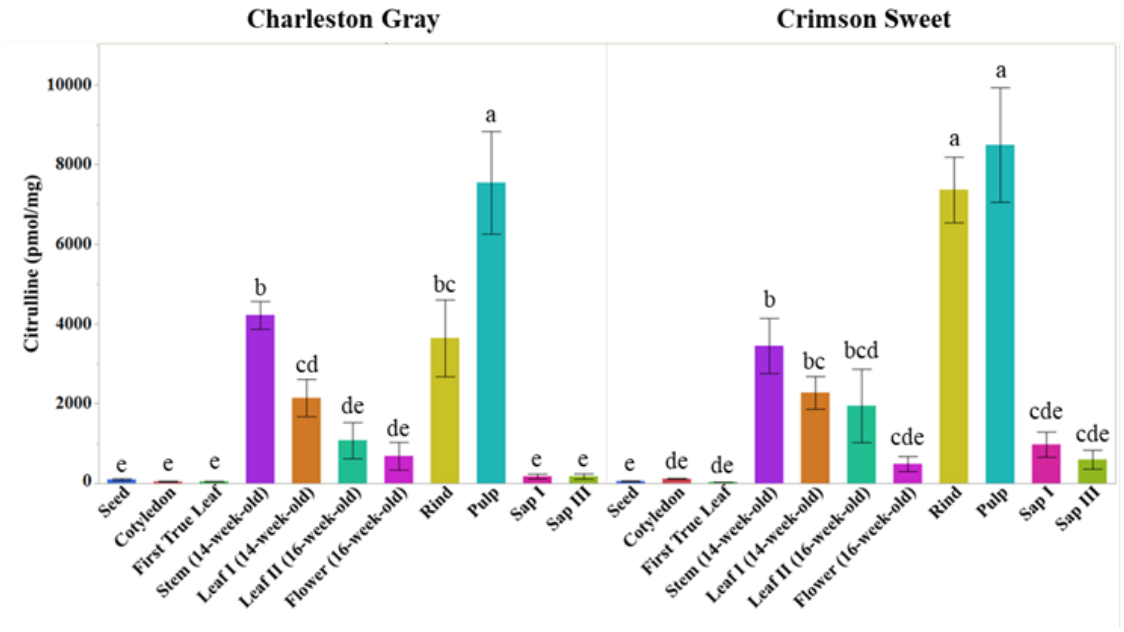

Figure 7. Dynamics of citrulline accumulation (pmol/mg FW) in different tissues during development in watermelon cultivars. Charleston Gray and Crimson Sweet. Student's t-test was conducted for comparison within tissues in each variety. The error bars show the means ± SE (n=3 or 4), and different letters indicate significant differences ($p < 0.05$).

There was no significant difference in citrulline accumulation between 14-week Leaf I and 16-week-old Leaf II tissues. Unlike vegetative tissue, citrulline accumulation in flower tissue was much lower. Both fruit rind (exocarp) and pulp (mesocarp) tissue accumulated the highest amount of citrulline in the matured fruits. These observations indicated a progressive increase in citrulline content, which peaked at the physiological harvesting in fruits in both varieties. Accumulation of citrulline in late vegetative tissue suggests the possibility of citrulline transport from leaves to developing fruits. However, the citrulline content in both sap samples didn't show as high amounts as that in the stem tissues. Besides the high accumulation of citrulline in fruit

tissue, a relatively high amount of citrulline in stem tissue in both the cultivars supported the possible vascular transport of citrulline.

The accumulation of citrulline in fruits during ripening is consistent with other studies [15], [17], [18], [39]. In contrary to the previous studies reporting higher citrulline content in rind [19], [40], [41], citrulline was significantly higher in the pulp in *cv.* Charleston Gray fruits. Variations in citrulline content in rind and flesh are also influenced by genotypic and environmental factors [15]. Based on citrulline partitioning across tissues, it appears that citrulline may be synthesized elsewhere and transported to the developing watermelon fruits. The stable levels of citrulline in the mature fruits could be a composite outcome of decreased catabolism, increased biosynthesis, long-distance transport, and partitioning across the rind and flesh tissues of the fruits.

1.3.2.2 Contribution of Citrulline's precursor and byproduct

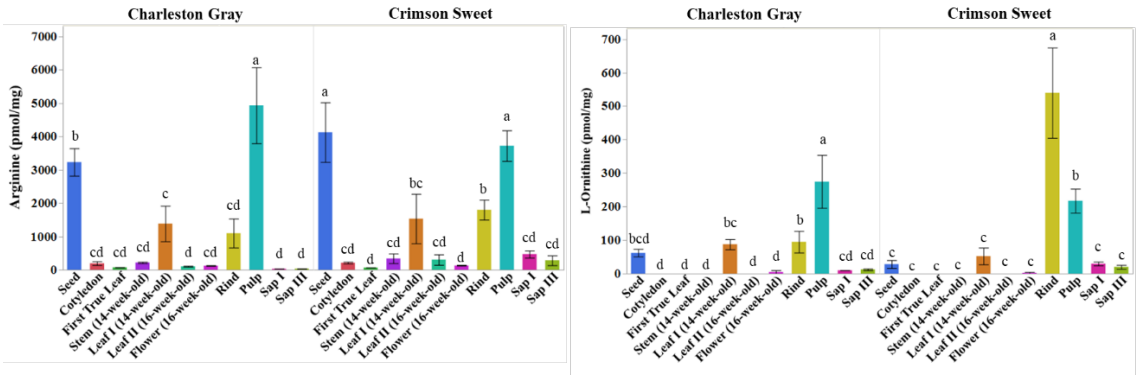

Figure 8. Partitioning and amount (pmol/mg) of Arginine (citrulline's byproduct) and L-Ornithine (citrulline's precursor) in different plant tissues during development. The student's t-test was conducted for comparison within tissues in each variety. The error bars show the means ± SE (n=3 or 4), and different letters indicate significant differences ($p < 0.05$).

To investigate the regulation of synthesis and catabolism of citrulline during growth, the profiles of other amino acids closely associated with citrulline metabolism were evaluated (Fig.

8). Ornithine, a precursor of citrulline, takes part in the last step of citrulline synthesis while arginine, a catabolic by-product, is associated with the penultimate step of citrulline catabolism. Except for seeds and vascular tissues (stem), the accumulation trend of arginine and Ornithine was positively correlated with that of citrulline. Similar to Citrulline accumulation (Fig.7), fruit tissues (rind and pulp) accumulated the highest amount of arginine and ornithine. The accumulation of citrulline precursor (ornithine) and catabolic product (arginine) has been shown to correlate positively with its progressive accumulation in the flesh [16], suggesting the existence of a regulatory mechanism to maintain citrulline homeostasis in the flesh tissues. The contents of ornithine and arginine were less consistent in the rind but showed increased accumulation at maturity.

Unlike citrulline, arginine was relatively abundant in seed (more details of seed amino acids are provided in Chapter 4) and leaf I tissue of both varieties whereas L-Ornithine was comparably abundant in these two tissues only in cv. Charleston Gray. Even though no significant difference of citrulline observed in leaf I and leaf II tissues, arginine and ornithine accumulation between leaf I and leaf II were significantly different in both the varieties. Leaf I tissue, as younger leaf tissues, accumulated more arginine and ornithine than did the older leaf II tissue.

1.4 Conclusion

In this chapter, we optimized a protocol for the detection of free amino acids from watermelon tissues using UPLC-MS-MS-based high throughput protocol. The method would allow the detection of ~45 protein and non-protein amino acids in less than 10 minutes. The detection limits for citrulline from varied tissues ranged from 30 to 11430 pmol/mg. The linear

detection limits for most amino acids ranged from 0.45 to 90 pmol/µl. The protocol warrants the detection of a range of amino acids with high reproducibility and accuracy.

We characterized the dynamic perturbation in citrulline accumulation during the watermelon development. Amino acid profiling of plant tissues during the plant development confirmed the highest accumulation of citrulline in the fruit flesh and rind tissues followed by vegetative tissues like leaves and stem. Citrulline accumulation was positively correlated with the precursor (ornithine) and by-product (arginine) amino acids in fruits. The results showed genotypic differences in the partitioning of citrulline and related amino acids in fruit and other tissues. A moderate amount of citrulline accumulation in leaves and stem tissues suggested the possible transport of citrulline from the source (vegetative tissue) to the sink (developing fruits).

CHAPTER II

SIGNIFICANCE OF CITRULLINE IN MULTIPLE ABIOTIC STRESSES

2.1 Introduction

Abiotic stresses affect growth, development, productivity, and quality of plants. Plants undergo a series of physiological, morphological, molecular and biochemical adjustments to sustain through stress-induced damages. Several known and unknown genes and biological pathways are involved in tolerance to various abiotic stresses [42]–[46].

Watermelon production around the world is severely affected due to the prevalence of environmental stresses such as drought stress, extreme temperature, and salinity. The biochemical or molecular mechanisms underlying these responses in watermelon to the various abiotic stresses remain largely unknown. In this chapter, we performed experiments to understand the biological relevance of citrulline during four abiotic stresses – (1) Drought, (2) Heat, (3) Salt and (4) nitrogen stress.

2.1.1 Plant response to drought stress

Water limitation is a serious environmental factor impairing the productivity and yield of agricultural crops [47]. Based on the present yield condition, drought stress was predicted to cause 30% reduction in global crop production by 2025 [48], [49]. Cucurbitaceous crops are particularly sensitive to drought as many members of the family accumulate over 85% to 90% water in fruits and hence suffer under drought conditions. It was reported that yield loss of watermelon (*Citrullus vulgaris*) reached 29.5-33.5% and total soluble solids (TSS) was affected significantly after being treated with 50% level of deficit irrigation throughout the whole

developing season [50]. Germination, leaf area, the establishment of the stem, proliferation of root, and water use efficiency can be negatively affected by drought stress [51]–[53]. The leaf net CO_2 uptake decreases due to the closure of stomata when subject to desiccation or water shortage. The decline of the concentration of CO_2 in chloroplasts could lead to the following consequences: (1) a reduction in PS II photochemical yield; (2) an increased activity of ribulose 1,5-bisphosphate oxygenase; and (3) a decrease of enzymes activity, such as nitrate reductase and sucrose phosphate synthase [54]. However, with the increasing demand of nutritious and high-quality vegetables, and the reduced supply of high-quality underground water for irrigation [55], improving the drought tolerance of watermelon is of paramount importance. Numerous studies on developing drought tolerance of watermelon were performed [40], [56], [57] and the drought tolerance of wild watermelon was reported to be related to the water status maintenance and a metabolic accumulation of amino acids, especially citrulline [57], suggesting the importance of citrulline in response to drought stress.

2.1.2 Plant response to heat stress

High temperature has a substantial negative effect on crop production [58] and is a serious threat to global food security [59]–[61]. Each 1ºC increase in temperature above optimum might induce crop yield loss of up to 17% [62]. Heat stress damages the intermolecular interaction associated with plant/fruit development [63]. In terms of structural changes, heat stress during the early growth stage leads to alterations of chloroplast protein complexes and enzyme activities [64], damages to microtubules organization, cell membrane, cytoskeleton affecting cell elongation, differentiation, expansion, and membrane permeability [65]–[67]. The damage to photosynthetic membranes is induced by swelling and distorted stacking grana

accompanied by leakage of ions which are otherwise allocated to photosystems [47], [68]. The thermal stress causes increased chlorophyllase activity along with the decreased amount of photosynthetic pigments, photosynthesis and respiration activity [69]. The negative effects due to heat stress have been demonstrated in the members of *Cucurbitaceae* species, such as melon [70], cucumber [71] and watermelon [72]. The optimal temperature for growth and photosynthesis ranges 15-32℃ and 25-30℃, respectively, in the case of cucumber (*Cucumis sativus L*.) [71]. The thermal stress results in damages to photosynthesis [73], metabolism of carbon and nitrogen [74], [75], membrane lipid [76] and root development [77] in cucumber. The yield loss due to the heat stress in cucumber is greater at seedling stages than reproductive stages [78]. Significant decrease of photosynthesis rate, transpiration rate, stomatal conductance, PSII photochemistry quantum yield (ΦPSII), maximum efficiency of PSII (F_v/F_m), photochemical quenching (qP) and electron transport rate has been reported in watermelon seedlings (*Citrullus lanatus*) due to high temperature stress [72]. And stress-induced proteins are accumulated inside plants under high temperature conditions, such as heat-shock proteins (Hsps) which are triggered by extreme heat [79] but necessary for protecting the overall balance of cellular proteins [80], [81].

The temperature fluctuations can be sensed by plants with a series of sensors located in numerous cellular compartments [82]. Due to heat stress, biosynthesis and compartmentalization of metabolites are disturbed, which in turn activate the production of antioxidants and osmolytes [82]. The production of osmolytes plays a role in increasing the stability of protein and membrane bilayer structure [83], such as sugar alcohols (polyols), or ammonium compounds [84], proline and hydrogen peroxide in wheat [85] and amino acids arginine and asparagine [86].

2.1.3 Plant response to salt stress

Salinity adversely affects the productivity of several vegetables [87]–[89] including seed germination [90]. It has been demonstrated that salinity resulted in the reduction of biomass, total soluble solids (TSS) as well as yield (16% to 20%) in watermelon [91], the inhibited germination of seeds of tomato [92], mustard [93] and mung bean [94] and the decrease of seedling length and leaf number in maize [95] and soybean [96]. The excess salt disturbs the salt-water balance within the plant, causing dehydration and accumulation of salts in the sap and tissues. The physiological consequences of excessive salts include (1) reduced water potential of the root; (2) toxicity effect of Na^+ and Cl^- ions; and (3) nutrient imbalance induced by depression of uptake and transport [97]–[99]. The progressive reduction of growth occurs due to the decreased osmotic potential of external solutions along with a deficiency of key nutrients [100]. For example, increased exchangeable Na^+ in the soil causes the reduction of Ca^{2+} absorption and nutritional imbalance. Moreover, in salt susceptible plants such as tomato [101] and pea [102], the salinity inhibits the activity of PSII [103]–[107]. To keep the osmotic balance between the vacuole and external medium, osmolytes which are non-toxic and compatible with cytoplasmic enzymes, are required [108], such as proline in halophytic plants [109], glycine betaine in Chenopodiaceae and Poaceae [110] and beta-alanine in Limonium [111], [112]. It has been shown that the overexpression of genes associated with osmolyte metabolism enhanced tolerance to salt stress [113], [114]. Plants at the early reproductive stage were reported to be more sensitive under salt stress [49]. In addition, salinity induced the reduction of stomatal conductance [115] and photosynthetic rate caused by decreased photosynthetic pigment contents (chlorophyll, xanthophyll and carotenoid) in mung bean [116] and rice [117].

2.1.4 Physiological response to N limitation

Nitrogen plays an important role in plant growth, development and yield of crop due to its fundamental function as a constituent of many cell components, photosynthesis apparatus, and membranes proteins [118], [119]. External nitrogen application improved multiple crop growth parameters, such as grain weight [120], tillers [121] and grain yield [122]. Watermelon has a high demand for nitrogen due to the element's important role in maintaining yield, fruit quality and disease resistance. Around 40 kg/ha of N application induced up to 14 ton per ha yield increase of watermelon (*c. lanatus*) fruits [123] and the dry weight of seedlings was reduced 29% after treated with low N condition after 2 weeks in watermelon [124].

Photosynthesis and photosynthate allocation can be affected by N availability [125] as well. The photosynthetic assimilation efficiency was reported to be reduced by 74% after low concentration of N application and the photochemical activity (F_v/F_m) of low N treated seedlings was lower than control in watermelon [124].

Nitrogen use efficiency (NUE) includes the efficiency of three steps- uptake, transport, and utilization. Nitrogen is primarily absorbed in the form of NO_3^- and NH_4^+ through roots transporters [126]. And NO_3^- is converted into NH_4^+ via cytosolic nitrate reductase following which the conversion from NH_4^+ to glutamine via glutamine synthetase (GS) happened and then the N is transferred to glutamate amino position via glutamate synthase (GOGAT) [127]. These N-rich compounds are precursors of proteins, amino acids or other metabolites essential for the development and growth of plants [125], [128]. The metabolism of amino acid serves as an essential role in N transport from vegetative tissue to reproductive grain [129], [130]. The increased activities of multiple enzymes, such as alanine aminotransferase, asparagine synthetase and glutamine synthetase can improve NUE [131], [132].

2.1.5 Citrulline metabolism and abiotic stresses

Under drought stress conditions, citrulline became one of the most efficient scavengers of hydroxyl radicals among these compatible solutes, including mannitol, glycine betaine and proline [133]. As water deficit stress progressed, citrulline became the primary component (~50%) in the free amino acids pool [134]. And it was suggested that the accumulated citrulline in watermelon leaves might act as antioxidative protection for cells under drought stress [56], [133] and the drought-induced citrulline metabolism possibly served as a biochemical indicator of drought tolerance in cucurbits [135].

The transcripts/genes closely associated with biosynthesis of citrulline and proline were significantly up-regulated in response to both drought and salt stress [136] suggesting these osmolytes' role as an adaptive feature and further confirming citrulline's function as a biomarker of both drought and salt tolerance [137] in melon [135]. Citrulline was proposed to be a by-product of stress-related NO signal [138] and potential scavenger of hydroxyl radicals induced by osmotic stresses [133].

Under high-temperature condition, citrulline was assumed to play an important role in scavenging the elevated photorespiratory NH_4^+ and acting as an efficient osmolyte [139]. Citrulline accumulation was induced up to six-fold by the overexpression of photorespiration responsive enzymes in Arabidopsis, and the correlation between citrulline and the enzyme activity was strong (r=0.94) [140]. And citrulline was reported to be accumulated when supplemented with NH_4NO_3 due to the transport of photorespiratory ammonium to accumulate arginine and citrulline via CPS mediated pathway in Arabidopsis [141].

Under N limitation conditions, citrulline is regarded as a major portion of nitrogen storage and possible long-distance transporter of nitrogen in plants [142]. In Cucurbitaceous

species, citrulline has been reported to act as a fundamental carrier of organic nitrogen [143], [144]. As is well known, there is a rapid interconversion reaction of citrulline, arginine and ornithine taking place. In this reaction process, urea is split out from arginine and then is further hydrolyzed to ammonia and CO_2 which are both then fixed with citrulline and arginine from ornithine through reaction pathways [143]. The above processes indicate that both citrulline and ornithine function as intermediates in the synthesis process of arginine, and citrulline is presumed to be used in the synthesis of proteins [143].

2.2 Materials and Methods

2.2.1 Drought stress experiment

2.2.1.1 Watermelon varieties, growth condition and treatment method

Seeds of commercial watermelon varieties- Crimson Sweet and Charleston Grey seeds were sown in 96-well plug trays (25’’length × 15’’ width × 2’’ depth) in a greenhouse at the Texas A&M AgriLife Research & Extension Center in Uvalde, TX. The environmental factors in the greenhouse were monitored using a control system (Wadsworth, Arvada, CO) with a cycle of 16 h light, followed the 8 h of the dark period. The temperature and humidity were maintained at 30±5℃ and 70±5%, respectively.

Approximately 8-week-old Crimson Sweet seedlings were transplanted to 5-gallon heavy-duty round nursery pots (28cm width × 26cm height) at a depth of 2.5 inches leaving one seedling in every pot for the drought stress experiment located in a high-tunnel greenhouse (hoop-house) at Texas A&M AgriLife Research & Extension Center in Uvalde, TX. A total of 10 pots each were assigned for control (well-water) and drought stress experiments. Before transplanting, all pots were filled with ~ 22 lb of Sandy Soil Mix (Absorb-N-Dry), irrigated

completely and then covered with plastic films overnight to avoid evaporation. All pots were water-saturated and then weighed to estimate the amount of water per pot by averaging the weight increase of these 10 pots. Soil moisture sensors (Decagon 5TE VWC, METER) were inserted at a depth of 6 inches in 2 out of 10 pots for both the treatments. The 5 sensors were all connected with a data logger (EM 50 Data Logger, METER) for recording, monitoring and downloading the information of water content per pot. All pots received an equal volume of fertilizer (Peter® Professional 20-20-20) the same amount and once to twice a week during the entire period of the experiment. For irrigation, well-watered pots were frequently watered to maintain 90±5% of field capacity (FC) while drought treatment pots were subjected to progressive soil drying by withholding watering to maintain the soil FC at 30±5% determined based on the data from EM 50 Data Logger (METER).

2.2.1.2 Osmotic potential measurement from leaf tissues

For the drought stress experiment, leaf discs collected with a 0.25- inch- diameter punch were packed with alumina foils and quickly frozen in liquid nitrogen for the measurement of osmotic potential from both the treatments. To measure the osmotic potential of leaf tissues, the frozen discs samples were placed on the sample plate and then loaded into a vapor osmometer (Wescor VAPRO Osmometer 5520, Logan, Utah, USA). Osmometer readings ($mmol \cdot kg^{-1}$) were converted to MPa as per the manufacturer's instructions. The differences in the osmotic potentials between the samples were analyzed using student's t-test ($p\text{-value} < 0.05$).

2.2.1.3 Photosynthesis parameters measurements

A portable gas analyzer (LI-6400 XT, LI-COR Bioscience, NE) was used to measure the leaf photosynthetic rate (Photo), stomatal conductance (Cond), intercellular CO_2 (Ci) and transpiration rate (Trmmol) with parameters (Photosynthetic Active Radiation, PAR,1000μmol

m^{-2} s^{-1};CO_2 concentration, 400 ppm; leaf temperature, 20°C; VPD, 1 kPa; flow, 500µmol s^{-1}). Chlorophyll content was measured with a chlorophyll meter (SPAD-502 Plus, Minolta, Japan) and quantum yield (QY) of Photosystem II (PSII) in the dark-adapted state was obtained with a FluorPen (PAR-FluorPen FP 110/D., Photon Systems Instruments, Czech Republic) by following the instrument manual. The physiological measurements were takin periodically each 8, 24, and 53 days after treatment.

2.2.2 Heat stress and citrulline metabolism

The seedlings of watermelon varieties “Charleston Gray” and “Crimson Sweet” (seeds purchased from American Seed Company Inc, Spring Grove, PA) were used for a heat stress experiment. Before initiation of high-temperature treatment, plants were grown in a temperature-controlled growth chamber under constant temperature adjusted to 20±1℃, 65±5% humidity and 16h light/ 8h dark photoperiod with a light intensity of 250 µmol•m^{-2}•s^{-1}. Six-week-old watermelon seedlings (three fully expanded leaves stage) of both the cultivars with four replicates were transferred into another growth chamber (PGR15, Conviron, Canada) with a temperature of 40±1℃ and with the same cycle of 16h light/ 8h dark. Both leaf and root tissues were sampled at the end of heat shock from seedlings each with 4 replicates. The seedlings not exposed to heat stress were used as control and were also sampled after 8 hours.

2.2.3 Salt stress and citrulline metabolism

Seedlings of the same two varieties (Charleston Gray and Crimson Sweet) grown in a non-nutrient sandy/stone soil (Quick Dry Infield Conditioner, Turface Atheletics™, USA) under similar conditions as described in the section (2.1.1) were used for salt stress study. Six-week-old

seedlings with three fully expanded leaves were subjected to salinity stress. The seedlings with four replicates for each treatment were carefully lifted out from Turface media, washed under running water and were incubated in 50mL Conical-Bottom tubes (VWR®, Radnor Corporate Center, USA) containing (1) 300 mM NaCl (2) MilliQ water (Barnstead™ Smart2Pure™ Water Purification System, Thermo Scientific, Waltham, MA). Chlorophyll fluorescence was measured at the end of the experiment using a portable Fluorometer (PAR-FluorPen FP 110/D; Photo Systems Instruments, Czech Republic) after dark adaption for 30 mins. This measurement initiated from 1 hour after initiation of the treatment and was continued every after 2 hours. The maximum photochemical efficiency of PSII (F_v/F_m) was calculated according to the manufacturer's protocol. After 7 hours of exposure to salt stress, leaf and root tissue samples were collected from seedlings each with 4 replicates for both treatment and flash-frozen by liquid nitrogen before storing at -80°C for further processing.

2.2.4 Impact of N limitation on citrulline metabolism

Before initiating the N-deficiency field experiment, soil samples were collected at 10 random locations at a depth of 6 inches from the field at Texas A&M AgriLife Research & Extension Center in Uvalde, TX. The samples were analyzed for basic soil analysis, such as pH, phosphorus, potassium, calcium, magnesium, sulfur, sodium, and especially nitrate-N at Texas A&M AgriLife Extension Service Soil, Water and Forage Testing Laboratory (http://soiltesting.tamu.edu).

Approximately 6-week-old Charleston Grey and Crimson Sweet seedlings were transplanted field plots on 3-feet-wide raised beds covered with plastic mulch. Plants were irrigated and fertilized using sub-surface drip lines located at 4-6 inches below the center bed.

The experimental area spanned over 78 feet × 120 feet area containing 6 rows placed 12 feet apart. Plants of both the varieties were transplanted in alternate order keeping 3 rows each for high and low N treatments keeping 3 feet plant to plant distance. The rows under high and low N treatment were 12 feet apart. The frequency and amount of irrigation were determined per the weather data and soil moisture. A total of 150±10 lb/acre of nitrogen in the form of Urea (46-0-0, HELENA®) was gradually applied for high N treatment. The low N treatment received 40±5 lb/acre N fertilizer. The N doses defining nitrogen treatments were decided based on remnant soil N and previous field experiments. To monitor N content in the soil, soil samples were collected from the watermelon field at a depth of 6-inch-deep every week from transplanting until harvest.

2.2.4.1 Measurement of physiological traits

The nitrogen content from petiole saps was measured by cutting the petiole and squeezing it to drip sap on the sample testing groove of the Nitrate Pocket Tester (Horiba LAQUAtwin NO3-11 Compact Water Quality Nitrate Ion Meter). Fresh leaves located in the middle position of vines were harvested, oven-dried, and analyzed for total nitrogen, nitrate, and ammonium analysis. A portable gas analyzer (LI-6400 XT, LI-COR Bioscience, NE) was used to measure photosynthetic parameters as described earlier (2.1.3).

2.2.5 Amino acids extraction of tissues from all three experiments

In order to detect and quantify amino acids, approximately 20 mg fresh tissue samples were collected into 2 ml microcentrifuge tubes accompanied with 3mm stainless steel beads (Demag stainless steel balls, Abbott Ball Company, CT, USA) and then homogenized into fine powder with the help of a shaker machine (Harbil model 5G-HD paint shaker). Total free amino

acids were extracted by suspending the homogenized samples in 10μL of 100mM cold HCl extraction buffer per mg of tissues, incubating on ice for around 20 minutes and then centrifuging at a speed of 15,000 x g for 20 minutes at 4℃. The clean solutions of the amino acid extracts were collected by filtering the supernatant obtained above through 96-well 0.45-μm-pore filter plate (Pall Life Sciences, USA). The derivatization of the filtrate was conducted with AccQ•Tag3X Ultra-Fluor™ derivatization kit (Waters Corporation, Milford, MA, USA) following the manufacturer's protocol.

2.2.6 Total RNA extraction and qPCR from drought and salt stress experiments

Total RNA was extracted from leaf tissue (drought stress) and seedlings (salt stress) with the Quick-RNA™ Miniprep Kit (Zymo Research Corporation, Irvine, CA) and cleaned up DNA with DNase I (Zymo Research Corporation, Irvine, CA) according to the manufacturer's protocol. Then the quality and quantity of extracted RNA was checked by a spectrophotometer (Denovix DS-11+ spectrophotometer, Wilmington, Delaware, USA).

The total RNA treated with DNase was used to synthesize cDNA using iScript™ Reverse Transcription Supermix (Bio-Rad Laboratories, Inc, Hercules, USA). Gene expression analysis was carried out using Bio-Rad CFX96 Real-time PCR (qPCR) instrument and SsoAdvanced™ Universal SYBR® Green Supermix (Bio-Rad Laboratories, Inc, Hercules, USA). Relative gene expression levels were determined using a standard curve method, and the value for each target gene was then normalized against the mean of expression values of reference genes. The watermelon β-actin and α-tubulin5 genes [145] were used as the internal controls, and the relative expression levels (Cq values) for each gene were normalized to that of β-actin

transcription by taking an average of three biological replicates. The primers for qPCR used in this chapter are listed in Appendix A Table 9.

2.3 Results and Discussion

2.3.1 Drought stress experiment

2.3.1.1 Validation of drought stress treatment

Before transplanting seedlings into pots, the soil moisture sensors were calibrated by correlating readings (m^3/m^3) from the data logger with actual water content (%) in a pot which was calculated as the percentage of actual water weight divided by water weight in saturated status. Based on the calibration, the actual water content in all pots was estimated. The percent of water data are shown in Table 3. The soil moisture levels were collected at three-time points beginning initiation of stress treatment. The plants under drought stress maintained around 35±5% soil moisture while the control plants in saturated pots maintained a steady level of 95±5% soil moisture.

Table 3. Soil moisture status monitored by sensors (Decagon 5TE VWC, METER). The data are the means ± SE (n=3 or 4), and different letters represent significant differences ($p < 0.05$). DAT, days after initiation of drought stress treatment

	1st Sampling 8 DAT	2nd Sampling 24 DAT	3rd Sampling 53 DAT
Water Vapor Content (WVC) Reading			
Well-watered (Control)	0.209 ± 0.011^a	0.194 ± 0.007^a	0.174 ± 0.001^a
Treated (Drought)	0.093 ± 0.011^b	0.081 ± 0.006^b	0.097 ± 0.006^b
Available Water Content (%)			
Well-watered (Control)	$99 \pm 1\%^a$	$99 \pm 2\%^a$	$98 \pm 2\%^a$
Treated (Drought)	$34 \pm 2\%^b$	$30 \pm 1\%^b$	$36 \pm 1\%^b$

2.3.1.2 Osmotic potential of leaf tissues for stress confirmation

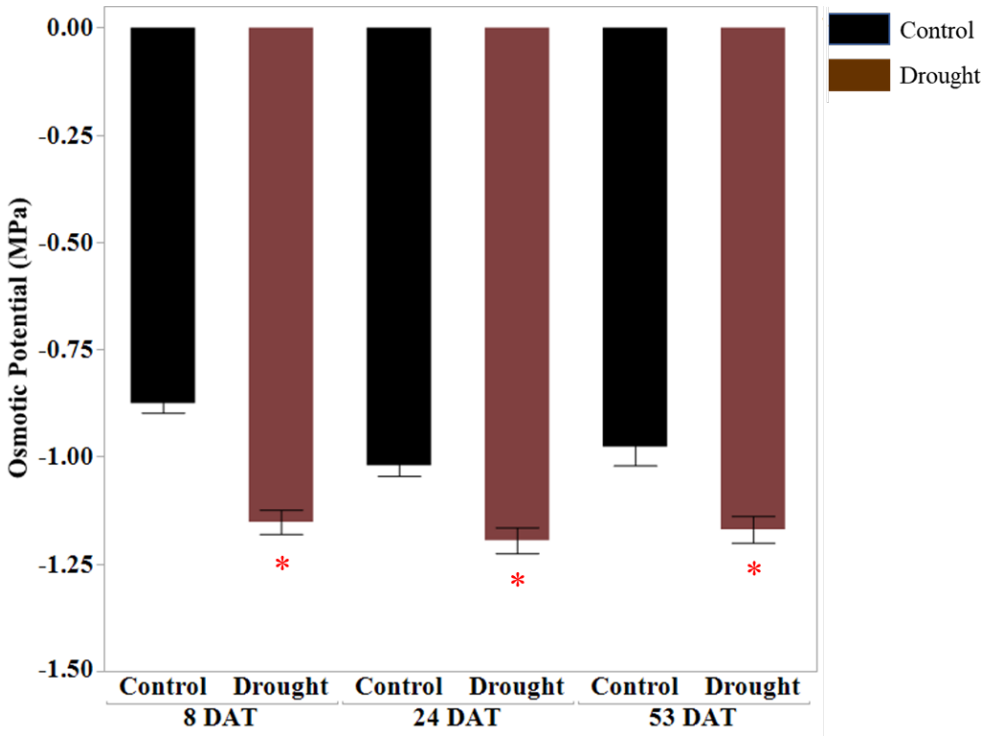

Figure 9. Osmotic potential (MPa) of leaf tissues from three different developmental times. The error bars represent the means ± SE (n=3 or 4) and asterisks (*) represent significant differences ($p < 0.05$). DAT, days after treatment (drought).

Osmotic potential (Ψ_s) deriving from the dissolved solutes in cell sap is closely associated with solute concentration but oppositely proportional to the water volume of plant cells. Ψs is a negative quantity of osmotic pressure and decreases under dehydration or water-deficit condition due to the concentrated solutes. The technique of dew point temperature depression by using an osmometer (Wescor Vapro Osmometers 5520, Logan, Utah, USA) was used for the determination of cell solution's osmotic potential. According to the Vapro Osmometers manual, at 25 °C, the coefficient of unit conversion from mmol/kg to MPa is -0.0025 which means, for instance, 400 mmol/kg is equal to -1.0 MPa.

The 0.25- inch- diameter punches of leaf discs packed in aluminum foils were flash-frozen in liquid nitrogen to maintain plant cell structure and trap water inside cells. When measuring the osmotic potential, leaf discs were placed on the sample holder and rapidly inserted into the enclosed measuring chamber (Wescor Vapro osmometers 5520) to avoid thawing. Then osmolality readings were recorded repeatedly until an equilibrium was reached [146]. Samples for the analysis were collected at three different time points, respectively, before anthesis, during anthesis, during fruiting. The significant difference in osmotic potential (MPa) between drought treatment and well-watered plants was confirmed in all three development stages using a student's t-test (p-value<0.05) (Fig. 9). Ψs of drought treated plant samples are more negative than well-watered samples, which is consistent with dehydration-induced decreases in Ψs demonstrated in several crops [147], [148].

2.3.1.3 Physiological measurements

Photosynthetic parameters-Photo (net CO_2 assimilation rate), Cond (Stomatal conductance), Ci (Intercellular [CO_2]) and Trmmol (Transpiration rate) were measured and determined at three different developmental stages (vegetative, anthesis and reproductive) using a gas analyzer (LI-6400 XT, LI-COR Bioscience, Lincoln, NE). The results showed a significant decrease in Photo, Cond and Trmmol at all three-time points in drought-stressed plants. In the early vegetative state (8 DAT, Leaf I), the Ci of drought-treated plants was significantly lower than that of control plants (Fig. 10). But during sustained drought stress (after the stage of anthesis and reproductive), Ci increased in drought-stressed plants. This rise in Ci can result from nonstomatal limitation, which also leads to the depression of Photo [149]. This biphasic characteristic has been demonstrated in several crops [150]–[153]. As Cond (stomatal conductance) dropped or approached to a minimum, a strong nonstomatal inhibition initiated

leading to the increase of Ci [154]. Our results are in agreement with these reports that Ci might not be the only limiting factor for CO_2 assimilation rate in stressed plants [155]. Studies have demonstrated that Ci could remain constant despite a decrease in photosynthetic rate [156], [157].

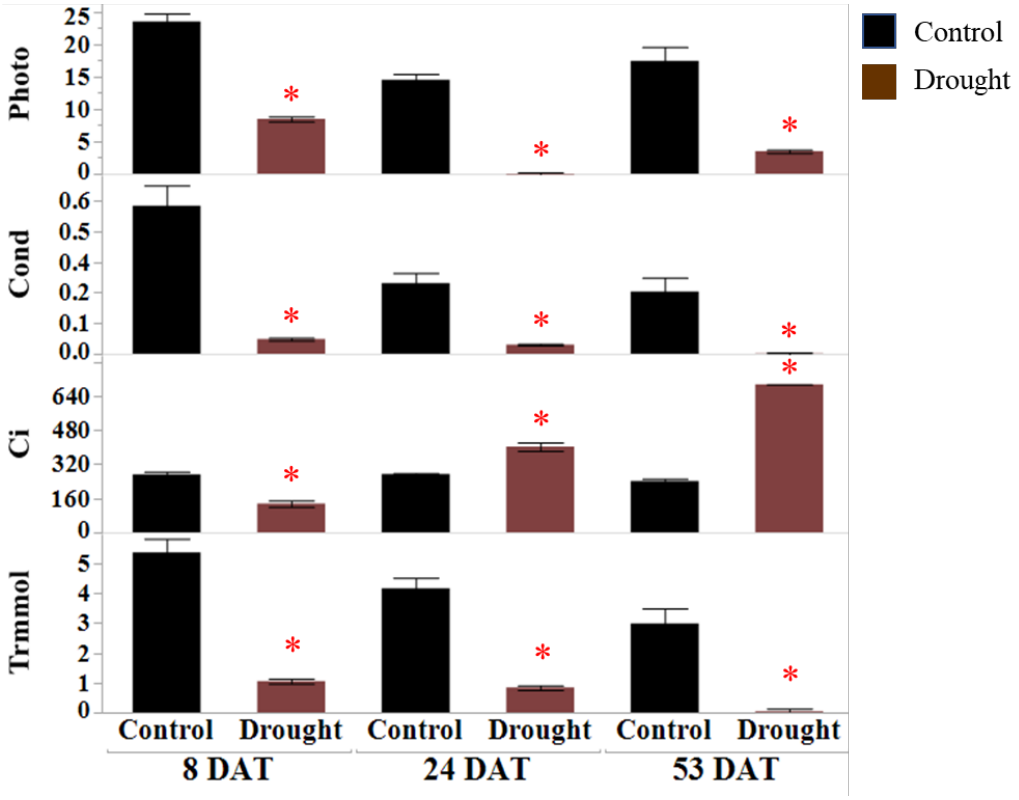

Figure 10. Gas analyzer measurements of drought-stressed leaves.
Net photosynthesis (Photo, µmol CO_2 m^{-2} s^{-1}), stomatal conductance (Cond, mol H_2O m^{-2} s^{-1}), intercellular CO_2 (Ci, µmol CO_2 mol air^{-1}) and transpiration rate (Trmmol, mol m^{-2} s^{-1}) were measured at 8, 24 and 53 DAT. The values represent means ± SD (n=3 or 4) and asterisks (*) represent significant difference ($p < 0.05$). DAT, Days after initiation of drought treatment.

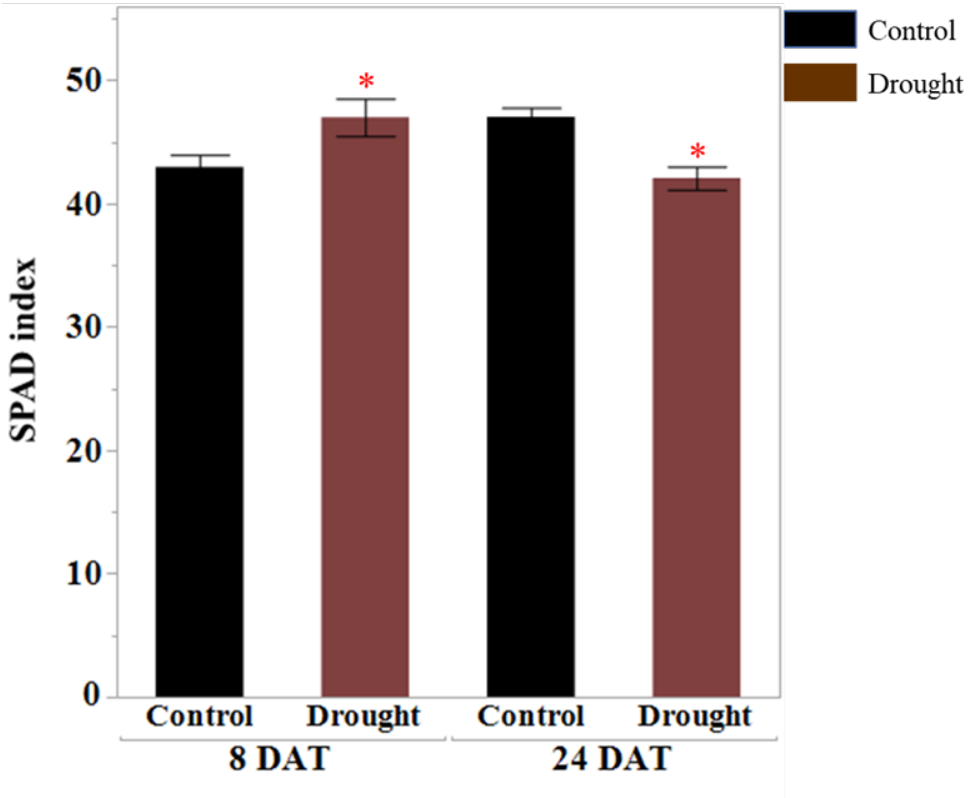

Figure 11. Chlorophyll content in watermelon leaves measured by chlorophyll meter (SPAD-502 Plus) in the drought stress experiment. The error bars represent the means ± SE (n=3 or 4), and asterisks (*) represent significant differences ($p < 0.05$). DAT, Days after initiation of drought treatment.

Chlorophyll content of the leaf tissues was measured by using a chlorophyll meter instrument (SPAD-502 Plus, Chiyoda, Tokyo, Japan) at three-time points (vegetative stage, anthesis, and reproductive stage). In the early phase (8 DAT, vegetative stage), it is significant and higher in chlorophyll content in drought-stressed plants (Fig. 11). At the later stage of sustained drought stress (24 DAT), drought-stressed plants had less chlorophyll content. Several studies have demonstrated a loss of chlorophyll due to water deficit stress most likely resulted from chloroplast damage induced by reactive oxygen species (ROS) [158]–[161].

2.3.1.4 Metabolic changes induced by drought stress

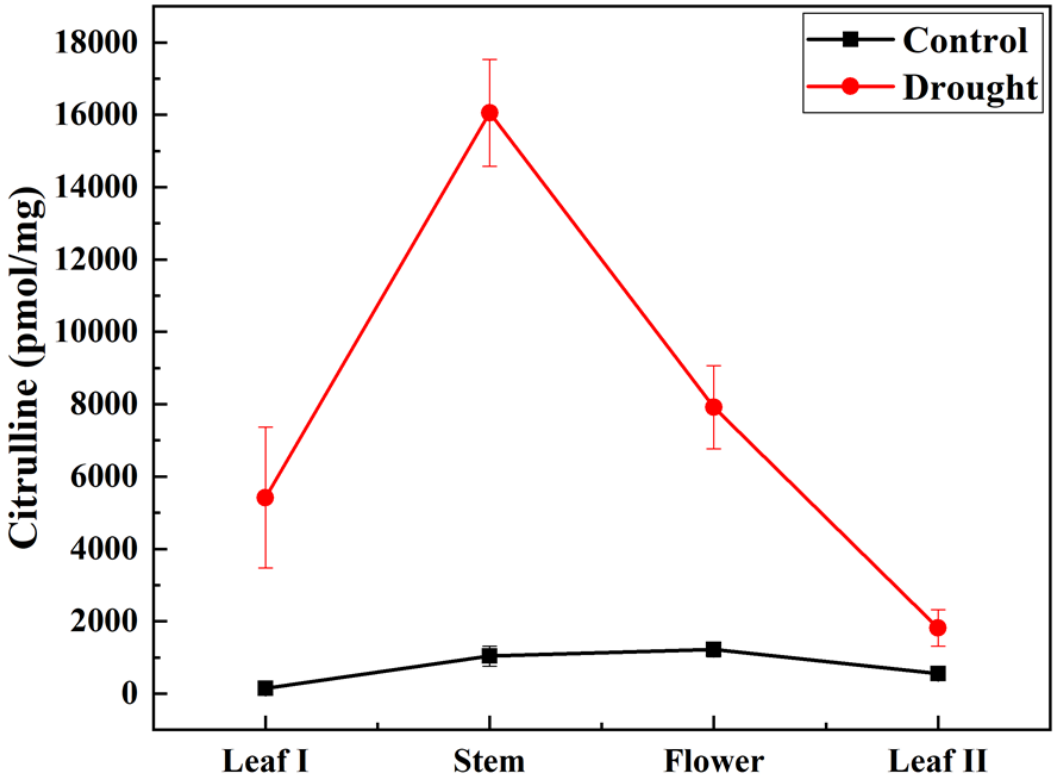

Figure 12. Changes of citrulline content in different plant tissues after treated with drought stress at the stage of First True Leaf. Leaf I represents 14-week-old leaf tissue while Leaf II is 16-week-old.

Amino acid contents in tissues of drought-stressed and control plants are summarized in Table 4. After the initiation of drought stress, citrulline content in all tissue types increased dramatically due to drought stress (Fig. 12). This can be explained by citrulline's potential function as a strong hydroxyl radical scavenger. Drought-induced accumulation of citrulline has been demonstrated [161]–[164].

Table 4. Various content of amino acids detected in different tissues under drought stress. The represented data are the means ± SE (n= 4) and red star (*) represents significant difference ($p < 0.05$). Leaf I represent 14-week-old leaf tissues while Leaf II is 16-week-old.

Tissue	Leaf I		Stem		Flower		Leaf II	
Treatment	control	drought	control	drought	control	drought	control	drought
unit	pmol/mg							
Arginine	107.5 ± 21.0	1487.5 ± 702.3	125.0 ± 21.8	3492.5 ± 757.4*	187.5 ± 22.5	1337.5 ± 353.4*	365.0 ± 252.2	1707.5 ± 916.4
Asparagine	102.5 ± 4.8	170.0 ± 10.8*	120.0 ± 7.1	1137.5 ± 99.1*	1312.5 ± 240.4	2880.0 ± 836.0	100.0 ± 20.4	222.5 ± 65.4
Glutamine	250 ± 60.4	535.0 ± 55.0*	2362.5 ± 396.6	25915.0 ± 4243.9*	4857.5 ± 682.7	11865.0 ± 2738.6*	640.0 ± 175.9	1727.5 ± 547.5
Serine	522.5 ± 78.4	1397.5 ± 146.4*	650.0 ± 73.6	2477.5 ± 26.9*	1187.5 ± 123.5	2755.0 ± 311.7*	380.0 ± 107.3	915.0 ± 192.6
Glutamic Acid	2325.0 ± 215.8	6392.5 ± 637.2*	982.5 ± 53.3	2525.0 ± 172.9*	3897.5 ± 223.1	7620.0 ± 364.3*	3150.0 ± 523.9	3952.5 ± 683.7
Aspartic Acid	1050.0 ± 94.6	1602.5 ± 220.1	1222.5 ± 38.2	1632.5 ± 43.1*	2312.5 ± 148.2	4490.0 ± 304.3*	1542.5 ± 282.3	2415.0 ± 571.1
Citrulline	142.5 ± 39.7	5420.0 ± 1950.0*	1035.0 ± 277.7	16057.5 ± 1479.1*	1220.0 ± 200.6	7917.5 ± 1152.5*	550.0 ± 182.3	1815.0 ± 500.0
Glycine	197.5 ± 24.6	477.5 ± 105.5*	180.0 ± 33.2	2565 ± 86.1*	357.5 ± 66.0	967.5 ± 147.8*	322.5 ± 67.5	495.0 ± 84.2
Alanine	1620.0 ± 135.4	1547.5 ± 115.5	750.0 ± 38.9	4377.5 ± 403.2*	1625.0 ± 139.4	4217.5 ± 745.9*	572.5 ± 125.1	1172.5 ± 185.4*
GABA	1727.5 ± 147.2	2087.5 ± 202.8	857.5 ± 64.2	3302.5 ± 276.7*	1500.0 ± 92.0	2502.5 ± 240.2*	1500.0 ± 228.5	3212.5 ± 346.4*
Proline	137.5 ± 22.5	332.5 ± 47.7*	65.0 ± 2.9	1685.0 ± 95.0*	1822.5 ± 268.7	10625.0 ± 1338.5*	185.0 ± 40.9	332.5 ± 49.6
L-Ornithine	0.0	90.0 ± 50.5	0.0	1672.5 ± 351.8*	0.0	25.0 ± 6.5*	0.0	152.5 ± 129.2
Lysine	90.0 ± 43.4	490.0 ± 198.5	35.0 ± 5.0	1300.0 ± 107.9*	150.0 ± 20.4	402.5 ± 20.6*	97.5 ± 20.2	335.0 ± 89.3*

The fold-change induction in citrulline varied in different tissue types. In leaf I tissue, citrulline increase was 38-fold while in the stem, it increased by 16-fold. It is plausible to assume that citrulline synthesis primarily occurs in leaves and translocated via long-distance through the stems. These results are consistent with our data from Chapter I showing the presence of a significant amount of citrulline in tissues other than the leaf. Citrulline was the most abundant among all drought-stress induced amino acids relative to control. These observations are consistent with the drought-induced accumulation of citrulline in C. colocynthis, showing almost 49% of total amino acids [134], suggesting that citrulline plays a bigger role during drought stress in the vegetative tissues of watermelon.

Besides citrulline, accumulation of GABA and Proline, the classic biomarkers associated with drought stress [165], increased 2-fold up in drought-stressed leaf tissues (Table 4). A relatively minor increase in these amino acids further substantiates the greater role of citrulline in conferring drought resistance in watermelon during drought stress.

2.3.1.5 Transcriptomic activity influence caused by drought

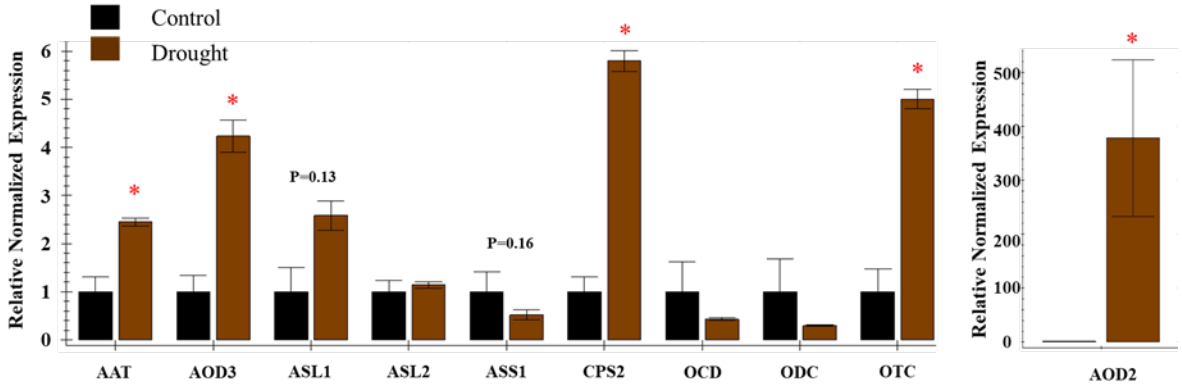

Figure 13. Relative expression profiles of genes involved in the citrulline metabolic pathways in leaf I tissues under drought stress. The error bars are the means ± SE (n=3), red stars (*) represent significant differences between treated and control tissues ($p < 0.1$). AAT, N-acetylornithine; AOD2 and AOD3, N-acetylornithine deacetylase; ASL1 and ASL2, Argininosuccinate lyase; ASS1, Argininosuccinate synthase; CPS2, Carbamoyl phosphate synthase; ODC, Ornithine decarboxylase; OCD, Ornithine cyclodeaminase; OTC, Ornithine carbamoyltransferase.

The relative expression of 10 major genes tightly associated with synthesis and catabolism pathway of citrulline mechanism was investigated, including 5 citrulline catabolic related genes (*ASS1*, *ASL1*, *ASL2*, *ODC*, *OCD*) and 5 citrulline synthetic related genes (*AAT*, *AOD2*, *AOD3*, *CPS2*, *OTC*). The qPCR analysis confirmed the expression of N-Acetylornithine aminotransferase (*AAT*), which catalyzes the reversible conversion of N-acetylglutamate 5-semialdehyde to N-acetylornithine in the presence of glutamate, was highly induced in drought-stressed leaves. Consistent with the induced expression of N-acetylornithine deacetylases genes in the drought-stressed leaves of C. colocynthis [166], both the N-acetylornithine deacetylases genes (*AOD2* and *AOD3*) were induced in the leaf tissue in response to drought stress. Expression of *OTC* catalyzing the ultimate step of citrulline synthesis and *CPS2* involved in the regeneration of carbamoyl phosphate moieties were both up-regulated. Taken together,

synchronized upregulation of citrulline biosynthesis and downregulation in leaf tissue explains the drought-induced accumulation of citrulline.

2.3.2 Effect of heat stress on amino acids accumulation

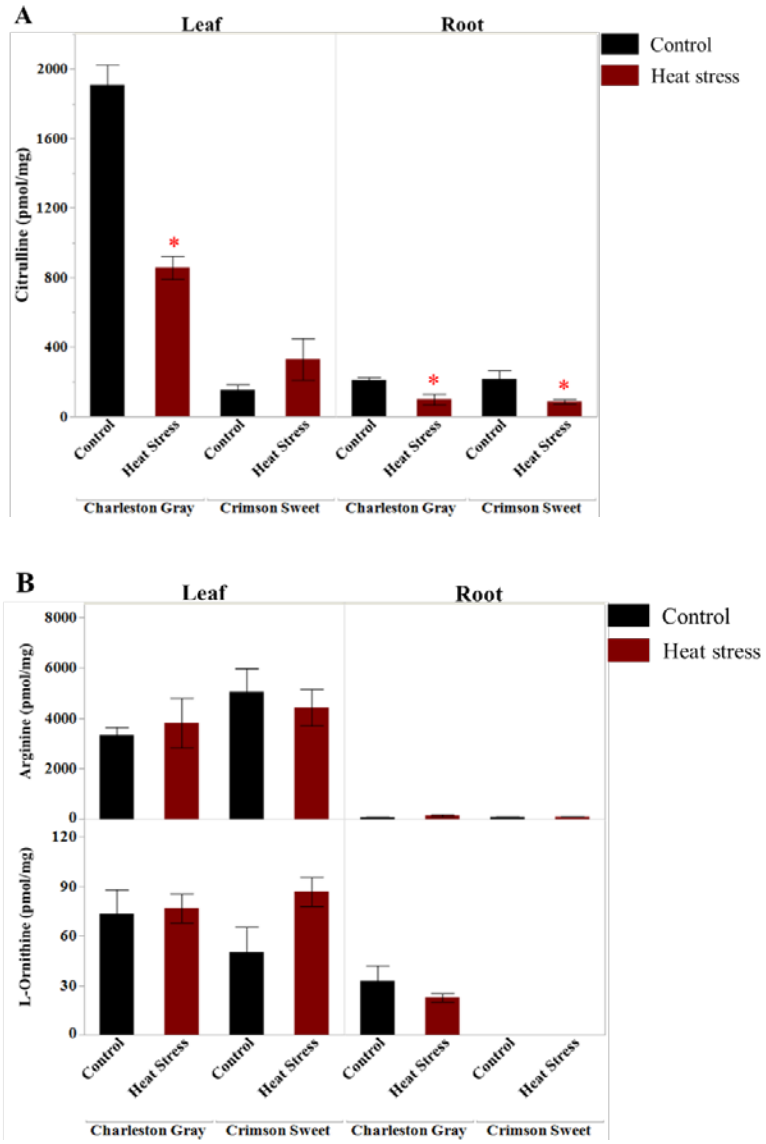

Figure 14. Accumulation (pmol/mg) of Citrulline (A) as well as its byproduct and precursor (B), respectively, Arginine and L-Ornithine, in seedlings' leaf and root tissues under heat stress. The error bars are the means ± SE (n=3 or 4). Red stars (*) represent significant differences between treated and control tissues ($p < 0.05$).

Citrulline content in the seedlings due to heat stress in “the cultivar Charleston Gray” leaf and root tissues was significantly lower than the controls (Fig. 14A). Amounts of L-Ornithine and Arginine, associated with citrulline synthesis and catabolism, respectively, showed no significant differences after heat stress treatment (Fig. 14B).

Table 5. Other related amino acids detected in seedlings leaf and root tissues under heat stress. The represented data are the means ± SE (n=3 or 4), and red star (*) represents a significant difference ($p < 0.05$).

Variety	Charleston Gray				Crimson Sweet			
Tissue	Leaf		Root		Leaf		Root	
Treatment	Control	Heat stress	Control	Heat stress	Control	Heat stress	Control	Heat stress
unit	pmol/mg							
Asparagine	110.0 ± 5.8	223.3 ± 20.3*	55.0 ± 2.9	85.0 ± 8.7*	103.3 ± 8.8	273.3 ± 31.8*	50.0 ± 0.1	57.5 ± 3.3
Glutamine	976.7 ± 237.3	3086.7 ± 474.0*	450.0 ± 25.5	452.5 ± 140.0	716.7 ± 116.7	2206.7 ± 421.9*	390.0 ± 45.5	282.5 ± 37.1
Glutamic Acid	4546.7 ± 145.3	5790.0 ± 505.2	720.0 ± 5.8	1100.0 ± 121.4*	4096.7 ± 229.8	6056.7 ± 379.7*	867.5 ± 60.7	942.5 ± 131.3
GABA	536.7 ± 97.4	536.7 ± 164.6	660.0 ± 80.4	965.0 ± 121.6	793.3 ± 99.4	673.3 ± 57.8	840.0 ± 94.4	760.0 ± 153.4
Proline	170.0 ± 20.8	216.7 ± 3.3	60.0 ± 4.1	50.0 ± 4.1	623.3 ± 213.4	243.3 ± 31.8	62.5 ± 7.5	45.0 ± 10.0

In contrast, amino acids, including Asparagine, Glutamine and Glutamic Acid, were induced by heat stress (Table 5). Like drought stress, heat stresses cause either increases or decreases in the total pool of several amino acids [167]. Consistent with our results, Arabidopsis plants showed elevated of glutamine due to heat stress and a combination of drought and heat stress [167]. Our data suggest that heat stress inhibits the citrulline and proline biosynthesis, while the synthesis of glutamine is preferred over proline synthesis during the heat stress. Asparagine is primarily biosynthesized by asparagine synthetase (AS) which is a glutamine-dependent enzyme in plants. The accumulation of asparagine in watermelon seedlings due to heat stress is in agreement with the increased expression of asparagine synthetase (*HAS2*) in sunflower (*Helianthus annuus*) leaves under heat stress [168] and in Purslane (*Portulaca oleracea* L.) [169].

Our data indicate that heat stress tolerance in watermelon is most likely regulated by citrulline-independent mechanisms. Enhanced levels of asparagine and glutamine may suggest the significance of nitrogen metabolism in heat tolerance.

2.3.3 Salt stress experiment

2.3.3.1 Effect of salinity on chlorophyll fluorescence of PSII system

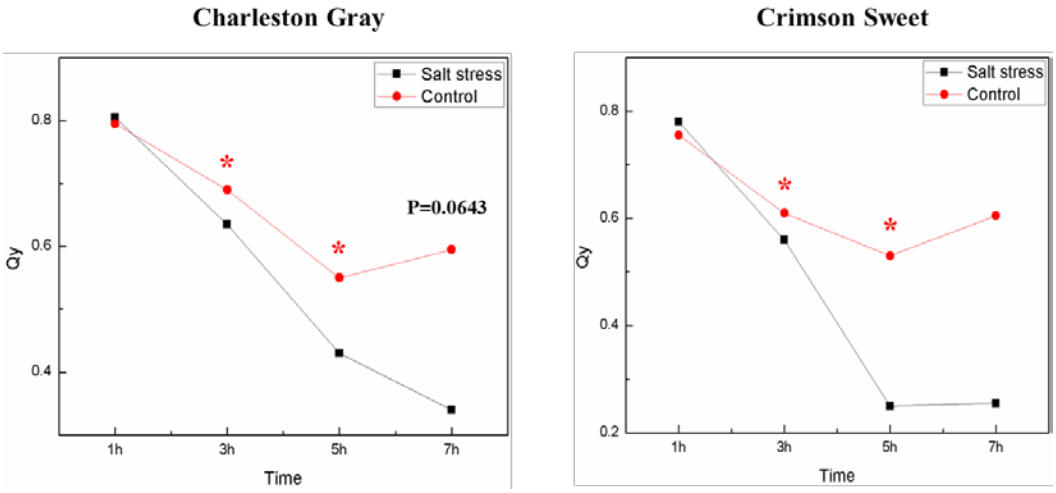

Figure 15. Chlorophyll fluorescence of PSII achieved by FluorPen (PAR-FluorPen FP 110/D) in the dark-adapted *cv*. Charleston Gray and *cv*. Crimson Sweet leaves under salt stress. Red star (*) represents significant difference ($p < 0.05$). Q_y, equal to F_v/F_m in the dark-adapted samples, photosystem II efficiency.

We studied how short-term exposure of watermelon seedlings to salt stress changes the behavior of photosystem II (PSII) and citrulline metabolism. Six-week-old seedlings of cultivars, Charleston Gray and Crimson Sweet, were subjected to 7-hour salt treatment with 300mM NaCl solution. We monitored PSII performance with FluorPen in the watermelon leaves by measuring the dark-adapted (F_v/F_m) (Fig. 15) and light-adapted (F_v'/F_m') (Fig. 16) fluorescence traits affected by the heat treatment.

Measurements of photosystem II efficiency of watermelon seedlings of varieties (Charleston Gray and Crimson Sweet) exposed to 300mM NaCl (Fig. 15), showed a consistent reduction in the PSII efficiency (Q_y) in dark-adapted leaf samples. The decrease in Q_y in treated plants was much more rapid than the control ones over time. Early decrease in Q_y in our experiment is consistent with reports showing inhibition of PSII activity due to salt stress [170]–[172].

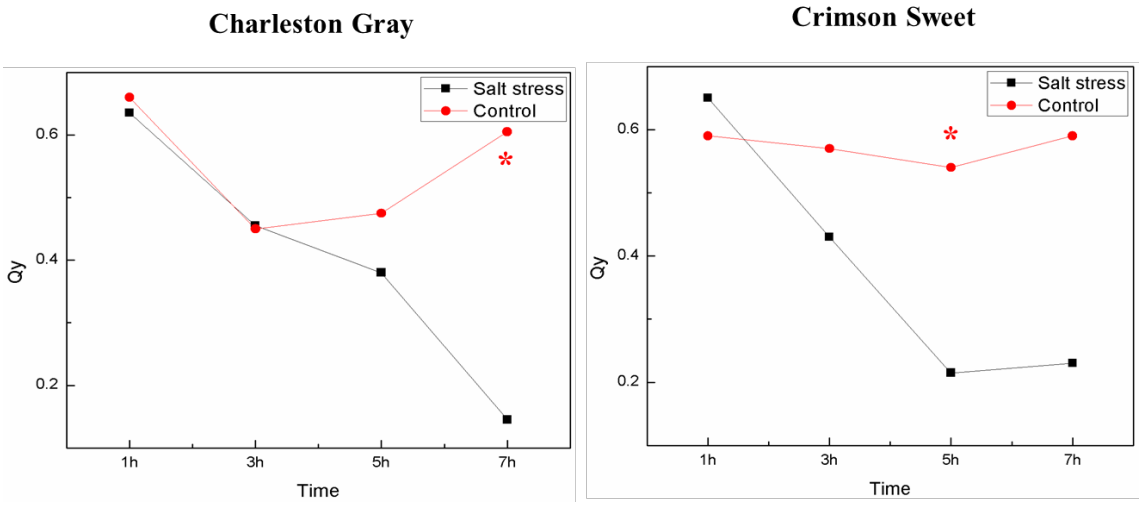

Figure 16. Chlorophyll fluorescence of PSII achieved by FluorPen (PAR-FluorPen FP 110/D) of *cv*. Charleston Gray and *cv*. Crimson Sweet leaves in the light condition under salt stress. Red star (*) represents significant difference ($p < 0.05$). Q_y, equal to F_v'/F_m' of samples in light condition, photosystem II efficiency.

In the light-adapted leaves (Fig. 16), Q_y of salt-stressed tissues was dramatically lower than that of control plants, confirming a negative effect on the quantum yield of PSII electron transport by salinity stress after seven hours of exposure.

2.3.3.2 Changes in the amino acid contents due to salt stress

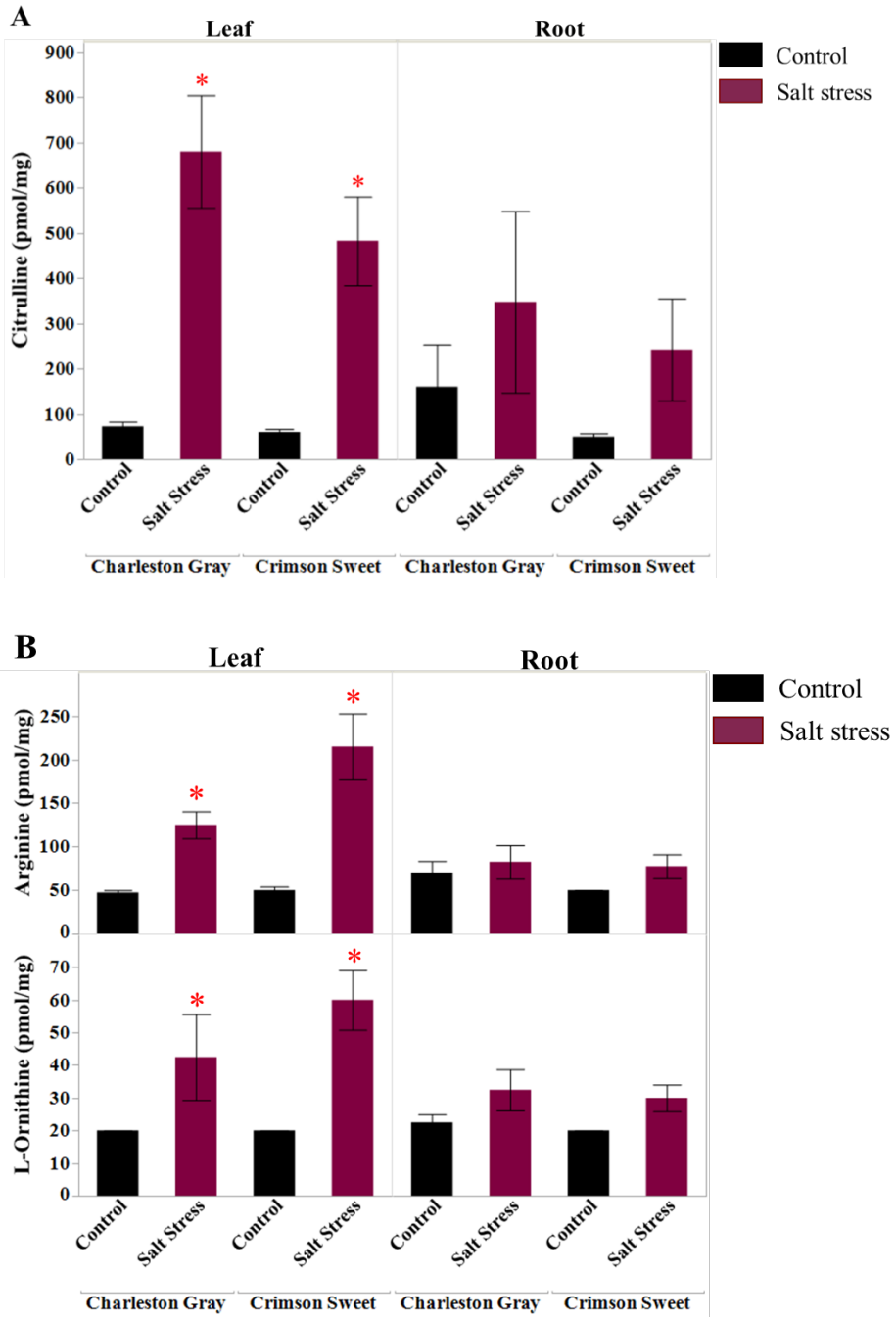

Figure 17. Accumulation (pmol/mg) of Citrulline (A), Arginine, and L-Ornithine (B) in seedling leaf and root tissues after salt treatment applied for 7h. The error bars are the means ± SE (n=3 or 4). Red stars (*) represent significant differences between treated and control tissues ($p < 0.05$).

During salt stress, plants accumulate high concentrations of compatible osmolytes such as polyols, organic acids, and nitrogen-containing compounds (NCC) [173] such as amino acids. In response to the salt stress, the levels of citrulline in leaf tissues were enhanced dramatically 10-fold and 8-fold higher in Charleston Gray and Crimson Sweet varieties, respectively (Fig. 17A). No significant changes were seen in the citrulline content of the root tissues ruling out the possibility of its localized synthesis or transport. Our results are in agreement with the study [174] which showed enhanced citrulline accumulation but contradicts the finding showing no changes in citrulline content in wild watermelon plants [57] due to salt stress. On the other hand, progressive salinization significantly enhanced citrulline content in melon leaves [175] consistent with our results. Increased citrulline was also accompanied by enhanced levels of arginine and ornithine in seedlings exposed to salt stress (Fig. 17B).

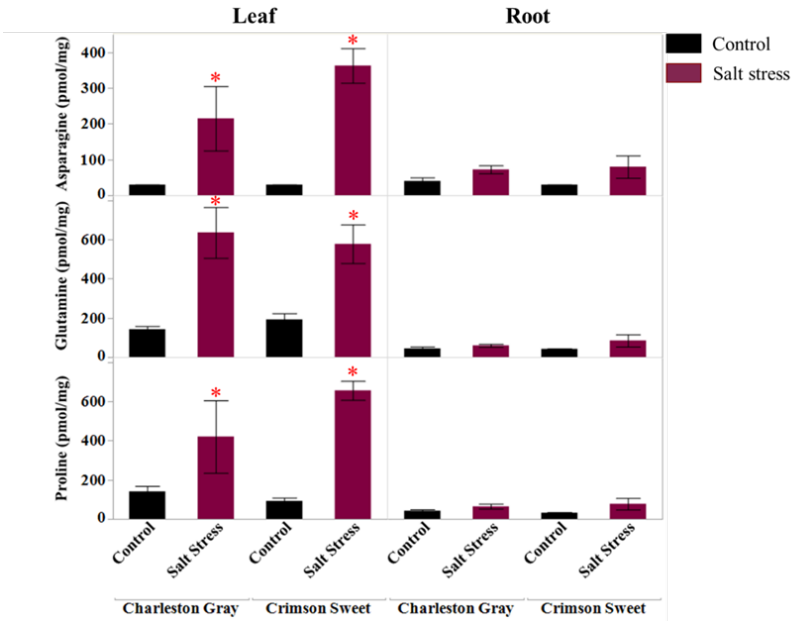

Figure 18. Other related amino acid accumulation (pmol/mg) including Asparagine, Glutamine, and Proline in seedling leaf and root tissues after salt treatment applied for 7h. The error bars are the means ± SE (n=3 or 4). Red stars (*) represent significant differences between treated and control tissues ($p < 0.05$).

Besides citrulline, amino acids such as, proline, glutamine and asparagine also showed a significant increase (Fig.18). A similar observation was reported in wheat and soybean [176], [177]. Consistently high levels of citrulline and proline suggest their utility as biochemical markers for salt tolerance in watermelon [174], [178]. It is expected that similar to proline, citrulline could play a role in regulating useable N accumulation and osmotic adjustment and membrane stability [179], [180] to mitigate the effects of salt stress [181].

2.3.3.3 Salinity effect on the relative expression of citrulline-related genes

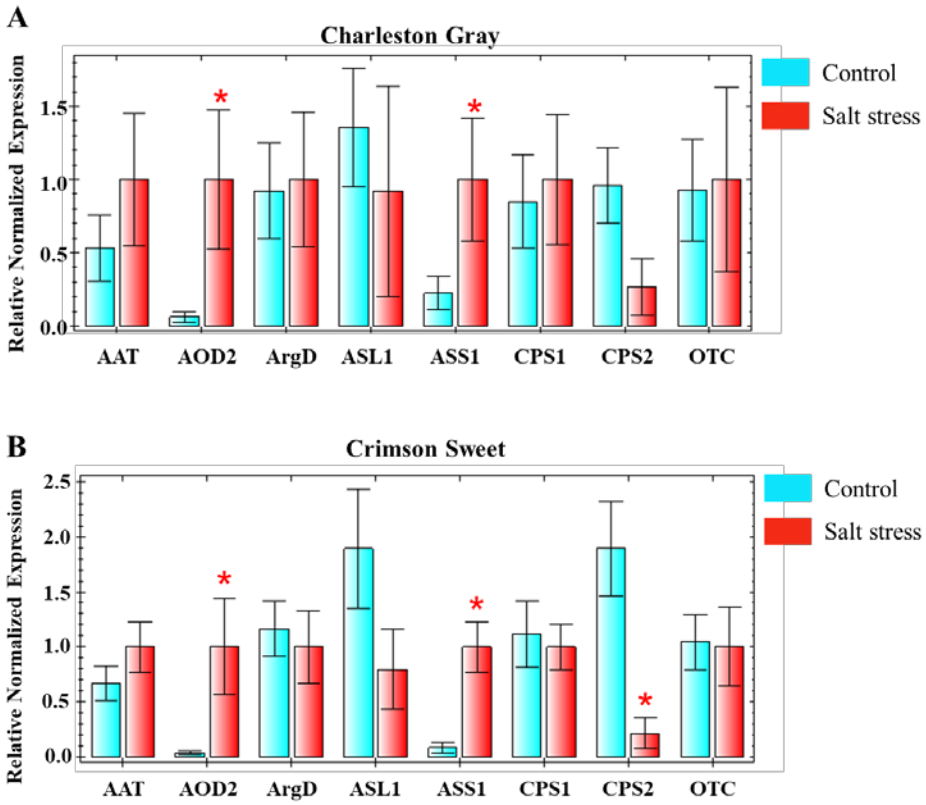

Figure 19. Relative expression profiles of genes involved in the citrulline metabolic pathways in seedling leaf tissues of Charleston Gray (A) and Crimson Sweet (B) under salt stress. The error bars are the means ± SE (n=3), red stars (*) represent significant differences between treated and control tissues ($p < 0.05$). AAT, N-acetylornithine; AOD2, N-acetylornithine deacetylase; ArgD, Arginine decarboxylase; ASL1, Argininosuccinate lyase; ASS1, Argininosuccinate synthase; CPS1 and CPS2, Carbamoyl phosphate synthase; OTC, Ornithine carbamoyltransferase.

The relative expression analysis of major citrulline metabolism-associated genes (*AAT, AOD2, ArgD, ASL1, ASS1, CPS1, CPS2* and *OTC*) was performed to understand the impact of salt stress on citrulline metabolism using leaf tissues of both the cultivars. In *cv.* Crimson Sweet (Fig. 19B), the expression of *AOD2* and *ASS1*, were significantly induced in salt-stressed samples while the expression of *CPS2* was down-regulated. The induction in the expression of *AOD2* in salt-treated samples explains the enhanced accumulation of citrulline. However, the reduced expression of *CPS2* and increased expression of *ASS1* were unexpected changes. Our current understanding of citrulline metabolism in plants indicates unidirectional synthesis from ornithine and glutamine via carbamoyl phosphate. However, the regeneration of citrulline through the involvement of nitrate oxide synthase (NOS) cannot be ruled out. In that case, increased arginine content in salt-stressed leaves justifies citrulline synthesis and upregulation of *ASS1*. The other possibility is that excessive citrulline or glutamine may feedback inhibit *CPS2* activity, which however, would require a detailed enzyme characterization.

2.3.4 N stress experiment

2.3.4.1 Nitrogen content in the soil

The nitrogen deficit was validated based on the consistently significant lower total soil inorganic nitrogen (Fig. 20A) and NO_3-N (Fig. 20B).

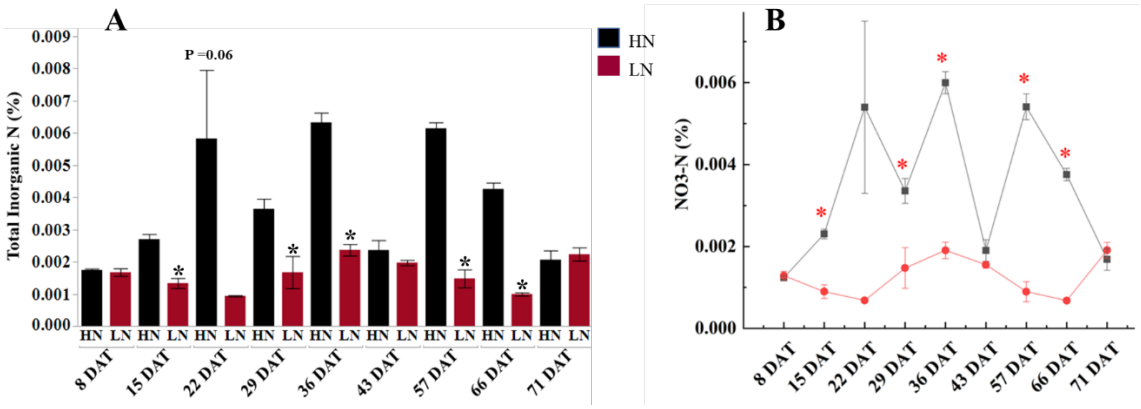

Figure 20. Nitrogen status of the soil.
A. Total inorganic nitrogen content (%) and B. NO_3^- in soil samples were measured on a weekly basis. The values represent means ± SD (n=3) and asterisks (*) represent significant differences ($p < 0.05$) between control (HN) and N deficit (LN) treatment. DAT = Days after initiation of nitrogen deficit treatment.

Total Inorganic N content showed differences between control and N depletion treatment from 15 DAT until 66 DAT. NO_3-N was consistently lower in the N-depleted soil.

2.3.4.2 Nitrogen content in petiole sap

Plants possess mechanisms for scavenging the fixed nitrate (NO_3^-) and ammonium (NH_4^+) ions rapidly from the soil solution. Under the increased soil nutrient concentration that happens after fertilization, the nitrate and ammonium absorption by root tissue may exceed the plant capacity of assimilating these ions, resulting in the accumulation of these ions within plants' tissues [182].

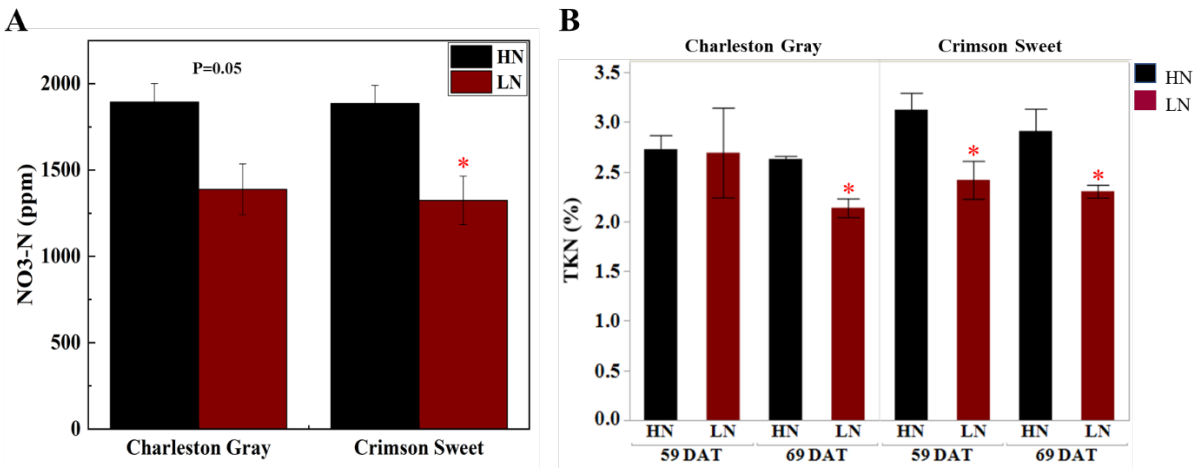

Figure 21. Nitrate content in phloem sap (A) and total nitrogen in leaf tissue (B).
(A) NO3-N content (%) in plant petiole sap collected 69 DAT from cv. Charleston Gray and cv. Crimson Sweet grown under high (HN) and N deficit (LN) treatments.
(B) Total nitrogen (TKN) from leaf tissues collected 59 and 69 DAT from cv. Charleston Gray and cv. Crimson Sweet grown under high (HN) and N deficit (LN) treatments.
The values shown are means ± SD (n=3), and asterisks (*) represent significant differences between treatments ($p < 0.05$). DAT = Days after initiation of nitrogen deficit treatment.

Both the NO_3-N concentration of leaf petiole sap (Fig. 21A) and TKN content of lyophilized leaf samples (Fig. 21B) of both cultivars showed significant differences between control (HN) and N-deplete treatment (LN) at later developmental stage (69 DAT) (p-value<0.1), validating difference in the N status of the soil among treatments.

2.3.4.3 Determination of physiological parameters

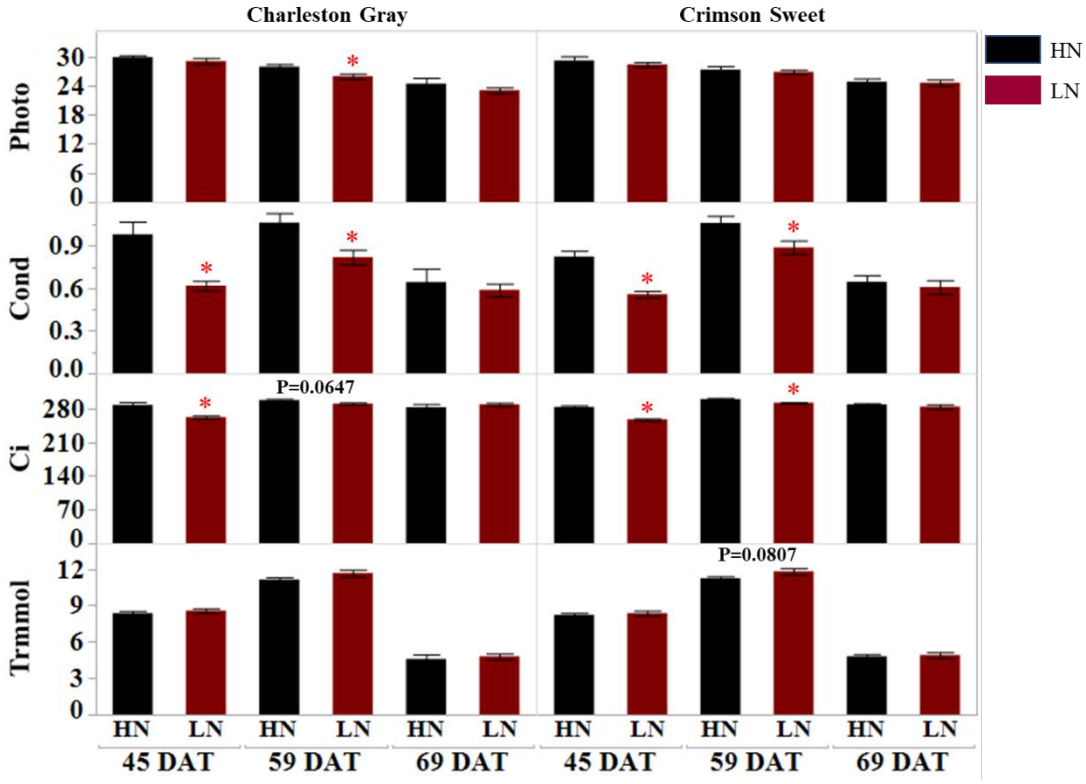

Figure 22. Net photosynthesis (Photo, µmol CO_2 m^{-2} s^{-1}), stomatal conductance to water vapor (Cond, mol H_2O m^{-2} s^{-1}), intercellular CO_2 (Ci, µmol CO_2 mol air^{-1}) and transpiration rate (Trmmol, mol m^{-2} s^{-1}) in watermelon leaves under N limitation stress. The X-axis week number represents the time after treatment (transplanting). The error bars represent the means ± SE (n=9) and asterisk (*) represent significant differences between control (HN) and N deficiency treatment (LN) (p<0.05).

The physiological parameters were measured at three developmental stages i.e., vegetative, anthesis and reproductive, to understand the impact of N status on the photosynthetic ability of plants. No significant changes occurred in photosynthetic rate during all three developmental stages among treatments (Fig. 22). Decreased stomatal conductance (Cond) and intercellular CO_2 (Ci) at 45 and 59 DAT did not compromise the photosynthetic rate due to nitrogen limitation.

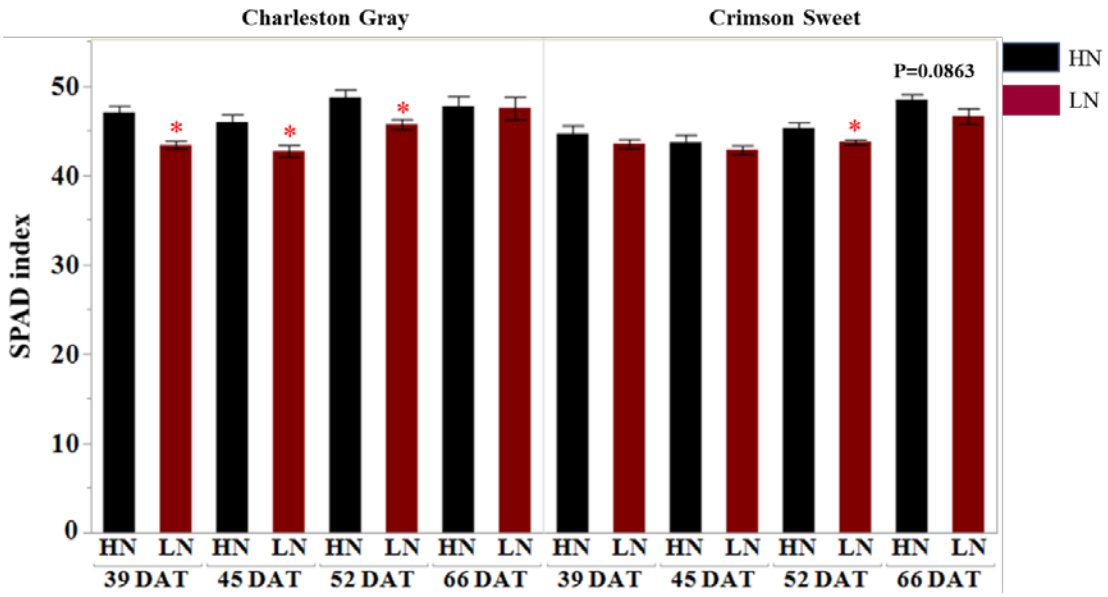

Figure 23. Chlorophyll content index (SPAD) in watermelon leaves under N limitation stress. The X-axis week number represents the time after treatment (transplanting). The error bars represent the means ± SE (n=9) and asterisks (*) represent significant differences between control (HN) and N deficiency treatment (LN) ($p<0.05$).

A significant reduction in chlorophyll content was observed during the early vegetative stage in N-stressed plants of *cv*. Charleston Gray samples and late vegetative stage in case of *cv*. Crimson Sweet (Fig. 23). Chlorophyll concentration is an important physiological indicator of plant N status.

2.3.4.4 Amino acids change under N deficiency stress

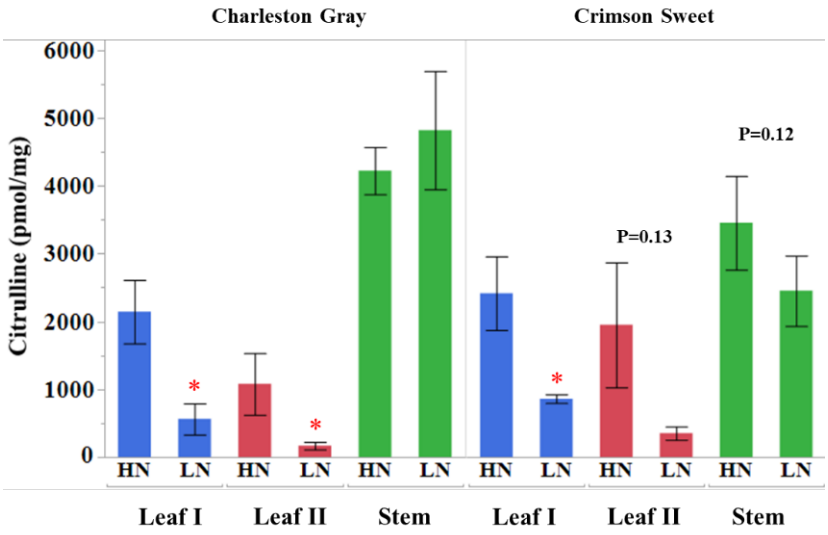

Figure 24. Citrulline accumulation in watermelon tissues during nitrogen deficit. Citrulline content of plant tissues collected during early 45 DAT (Leaf I and stem) and extended 69 DAT (Leaf II) nitrogen deficit treatment is shown on the vertical axis. The values represent means ± SD (n=3 or 4). The asterisk (*) represents significant differences between high (HN) and nitrogen deficit (LN) treatments ($p < 0.1$, Student's T-Test). DAT = Days after initiation of nitrogen deficit treatment.

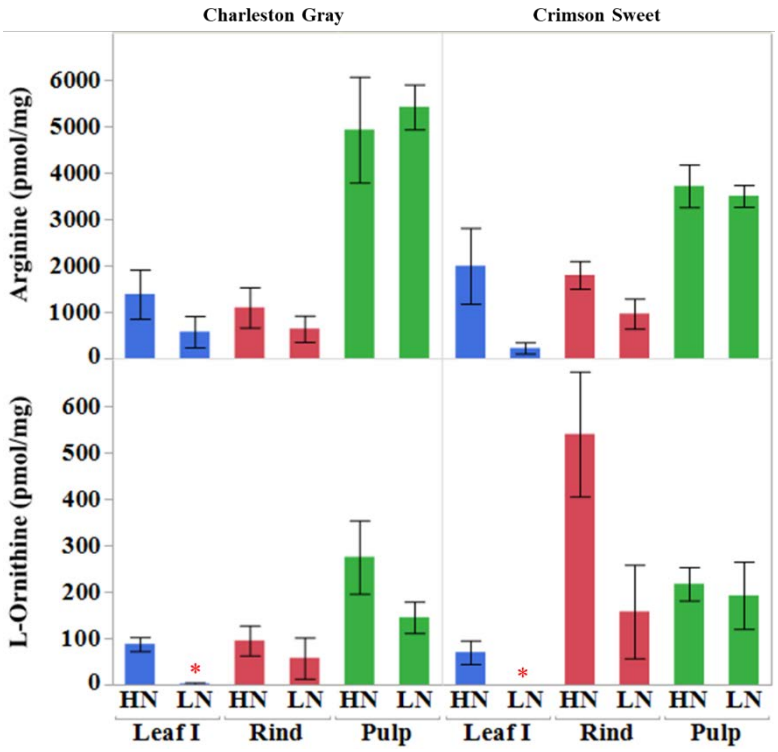

Figure 25. Partitioning of Citrulline, Arginine, and L-Ornithine in various watermelon tissues collected after limited N supply treatment. Leaf I represents 45 DAT leaf tissue while Leaf II is for 69 DAT. The error bars are the means ± SE (n=3 or 4). Red stars (*) represent significant differences between treated (LN) and control (HN) tissues ($p < 0.05$). DAT = Days after initiation of nitrogen deficit treatment.

N-rich amino acids play a major role in the storage and transport of endogenous N in plants [142]. However, limited research has been done to understand the mode of nitrogen transport in Cucurbitaceous crops. Our data indicated that the concentration of citrulline in N-stressed leaf I tissues (Fig. 24) was dramatically low. Citrulline content in the leaf tissues was altered significantly, vis-à-vis the availability of nitrogen. The citrulline in leaf tissues collected 45 and 69 days (leaf I and leaf II, respectively) after initiation of nitrogen stress was reduced by 5 to 6-fold in cultivar Charleston Gray and 2 to 6-fold in Crimson Sweet (Fig. 24). Ornithine content was only detectable in leaves during the early stages of plant development and was reduced by several folds in both the cultivars due to nitrogen stress (Fig. 25). Arginine content

was reduced by 8-fold due to nitrogen stress in the cultivar Crimson Sweet at 45 days after the initiation of nitrogen stress. Besides aspartate and glutamine, which reduced significantly due to nitrogen stress, most other amino acids showed a trend of reduced accumulation due to nitrogen stress in leaf tissues (Fig. 26). The changes were less consistent in the stem among the cultivars. In terms of comparative contribution, percent distribution of citrulline, arginine, or ornithine relative to all amino acids was significantly reduced due to nitrogen stress in the vegetative tissues of both cultivars (Fig. 27). Further, we also evaluated changes in the content of amino acids in the phloem sap due to nitrogen stress (Fig. 28). Although differences were insignificant in the case of cultivar Charleston Gray, the amounts of citrulline, arginine, and ornithine were significantly reduced in the cultivar Crimson Sweet subjected to nitrogen stress (Fig. 28B).

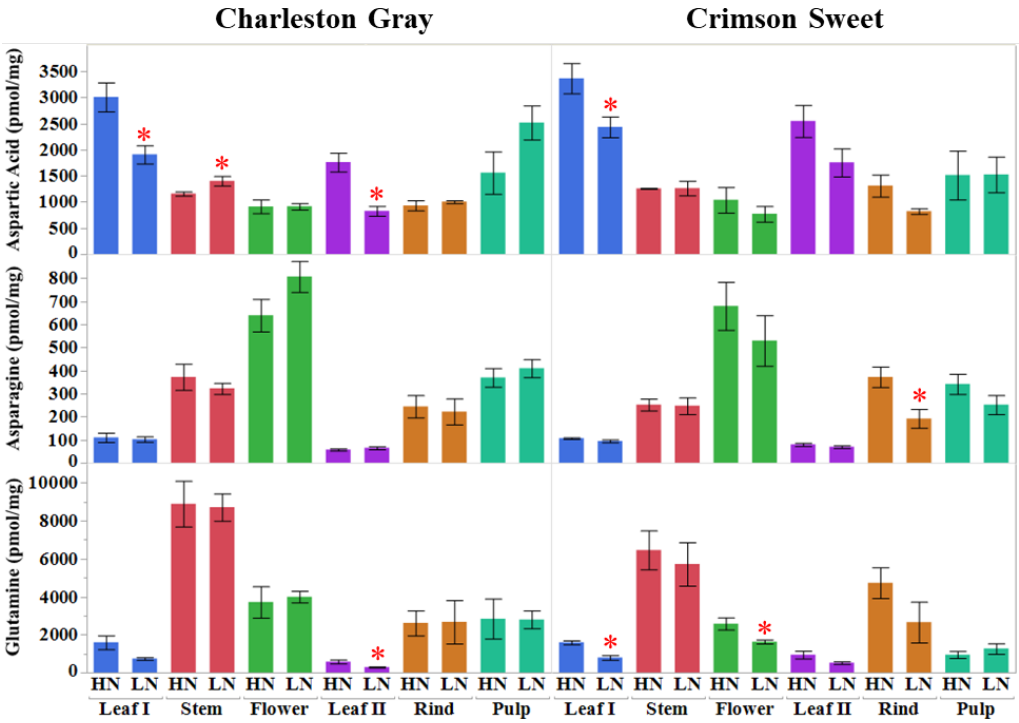

Figure 26. Other related amino acids, aspartic acid, asparagine, and glutamine accumulated in multiple tissues after N deficiency treatment throughout the whole development. The error bars are the means ± SE (n=3 or 4). Red stars (*) represent significant differences between treated (LN) and control (HN) tissues ($p < 0.05$).

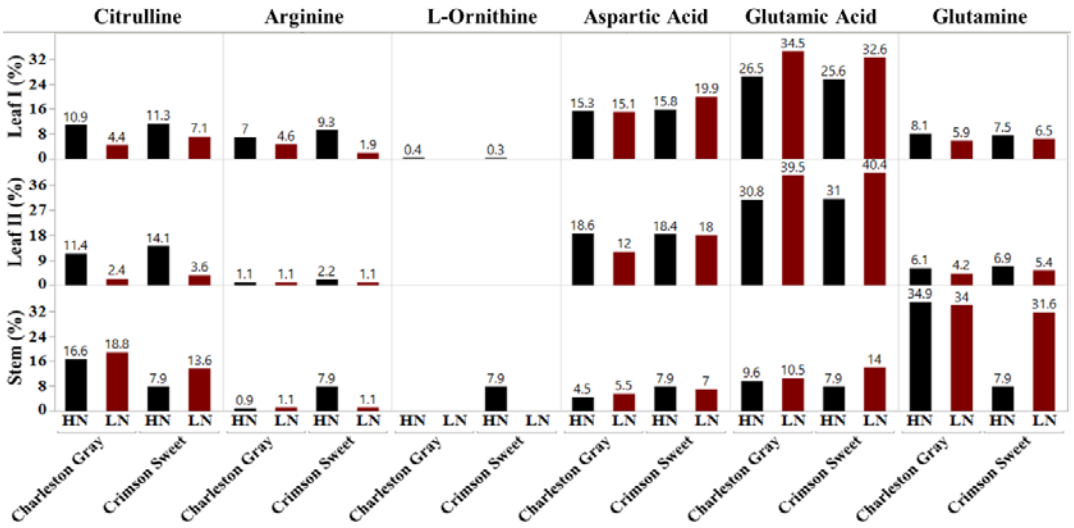

Figure 27. Percent distribution of amino acids in nitrogen depleted tissues.
Percent distribution of amino acids (citrulline, arginine, ornithine, aspartic acid, glutamic acid and glutamine) in leaves and stem tissues in nitrogen replete and deplete treatments. The values on top of the bar show percent contribution relative to other amino acids. High (HN) and N deficit (LN) treatments.

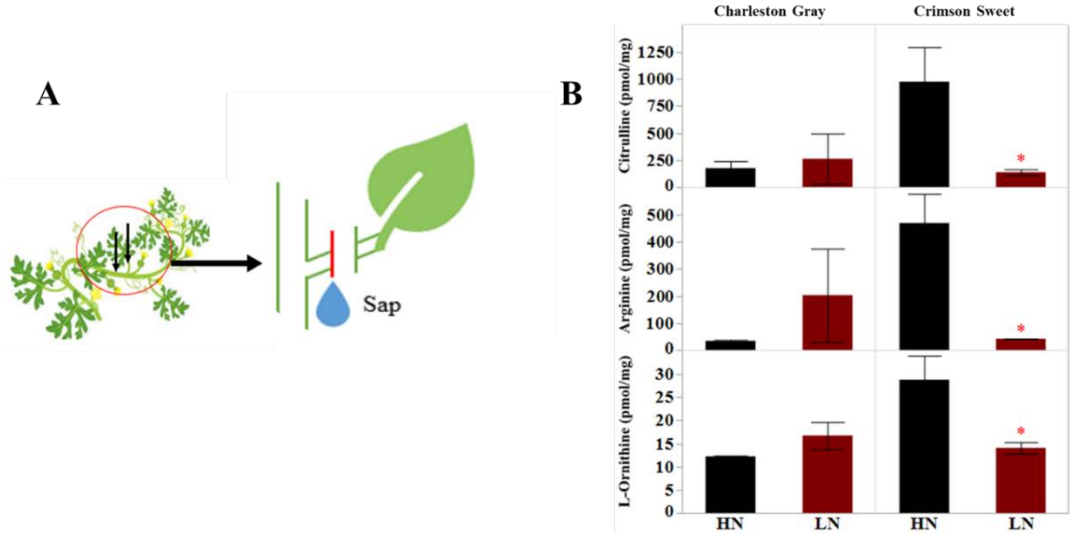

Figure 28. Citrulline accumulation in phloem sap from watermelon plants 69 DAT
(A) Phloem sap was collected 69 DAT after drought stress from the middle part of the leaf petioles located in the middle of vines (B) Citrulline, arginine and ornithine content in the phloem sap. The values represent means ± SD (n=3 or 4). The asterisk (*) represents significant differences between high (HN) and nitrogen deficit (LN) treatments ($p < 0.05$, Student's t-Test). DAT = Days after initiation of nitrogen deficit treatment.

2.3.4.5 Different relative genes expression under N limitation

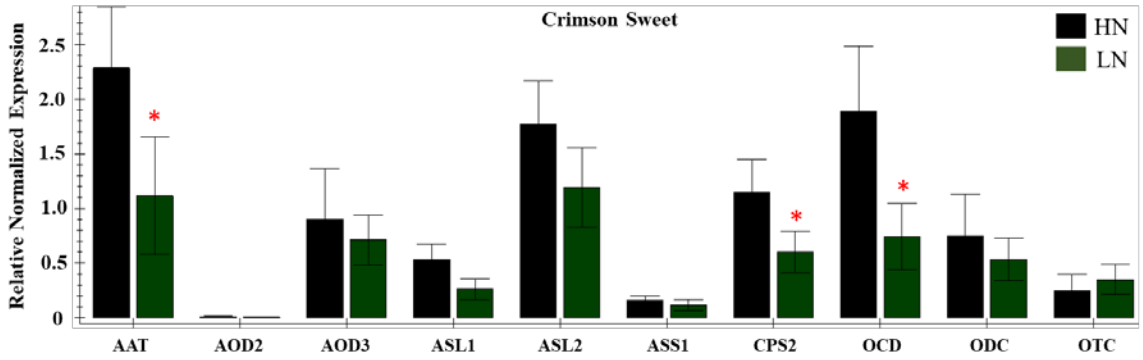

Figure 29. Relative expression profiles of genes involved in the citrulline metabolic pathways in leaf I tissues under N limitation stress. The error bars are the means ± SE (n=3), red stars (*) represent significant differences between treated and control tissues ($p < 0.1$). AAT, N-acetylornithine; AOD2 and AOD3, N-acetylornithine deacetylase; ASL1 and ASL2, Argininosuccinate lyase; ASS1, Argininosuccinate synthase; CPS2, Carbamoyl phosphate synthase; ODC, Ornithine decarboxylase; OCD, Ornithine cyclodeaminase; OTC, Ornithine carbamoyltransferase.

A subset of genes associated with citrulline metabolism was evaluated using the quantitative real-time gene expression analysis of leaf tissue using *cv.* Crimson Sweet (Fig. 29). The expression of *AAT* and *CPS2* associated with citrulline biosynthesis were downregulated. Unlike the drought-stressed plants, changes in the expression of other genes associated with citrulline metabolism were mostly unchanged due to nitrogen stress.

2.4 Conclusion

Our results demonstrated a rapid early induction (~38 fold) of citrulline within eight days of initiation of drought stress. Citrulline accumulation in leaf tissues further increased during prolonged stress, but its induction relative to control decreased (~16 fold). The early rapid induction of citrulline implicates its utility as a potential biomarker for drought-induced responses. The fold-change increases in arginine (catabolic product of citrulline) and ornithine

(precursor), consistent with the increase in citrulline and their high positive correlations with one another, emphasize the significance of the ornithine-citrulline-arginine pathway in watermelons during drought stress.

Citrulline metabolism was largely unaffected by heat stress. A significant increase in the accumulation of N-rich amino acids- Asparagine, Glutamine and Glutamic Acid indicates the possibility of exploring new targets in nitrogen assimilation to enhance heat tolerance.

Our data also demonstrated the rapid accumulation of citrulline in response to salt stress, supporting its potential as a biomarker for salinity-induced responses. Further studies to understand the biological relevance of citrulline would provide new insights for enhancing salt tolerance and in identifying targets for metabolic engineering.

Our data demonstrated that citrulline synthesis is regulated by the nitrogen status of the plant. The results (1) significant reduction in citrulline content along with ornithine or arginine in the leaf tissues (2) the percent distribution in the nitrogen depleted leaves and stems (10-18%), comparable to that of nitrogen carrying amino acids - aspartate and glutamate (3) reduction in the phloem sap (*cv.* Crimson Sweet), during nitrogen stress and (4) down-regulation of biosynthetic genes *AAT* and *CPS2*, all support the role of citrulline in translocating nitrogen in the vegetative tissues of watermelon.

CHAPTER III

RNA-SEQ ANALYSIS AND CITRULLINE METABOLISM IN DROUGHT AND SALT STRESS

3.1 Introduction

RNA-seq (whole transcriptome shotgun sequencing) analysis is based on next-generation sequencing (NGS) technology. RNA-seq is known as a tool for sequencing messenger RNA (mRNA) of a cell and generating millions of fragments of short-sequence called “reads”, in a single run. The number reads generated from a single RNA transcript represents a functioning assembly of that transcript’s abundance, since the density of reads can be utilized to measure the expression of transcript and gene with high accuracy [183]. The typical workflow of RNA-seq is summarized in Fig. 30.

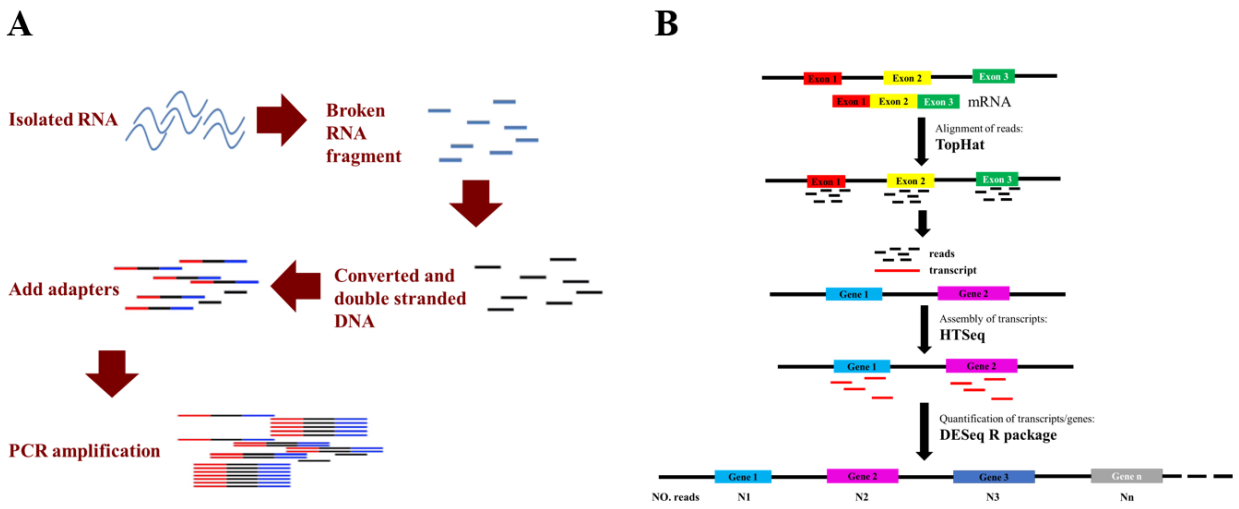

Figure 30. A typical workflow of reads library construction (A) and RNA-seq analysis performance (B).

The three major steps in the RNA-Seq analysis are (1) the alignment of reads and quality control; (2) the assembly of transcript or annotation using a reference genome; and (3) quantification of transcript and gene [184]. Two commonly applied tools can serve as all three roles, respectively TopHat (http://tophat.cbcb.umd.edu/) software and HTSeq (https://htseq.readthedocs.io/en/release_0.11.1/) package.

TopHat functions as a tool for aligning reads to the genome and discovering transcript splice sites as well [185] while counting the mapped reads was performed by HTSeq v0.6.1 [186]. DESeq R package (1.18.0) was used for differential expression analysis performance [187].

NGS technologies have been applied for transcriptome characterization, which is a cost-effective tool to enrich the knowledge in the genomics of a variety of crops. RNA-seq analysis has also been used in *Cucurbits* to study response to abiotic stresses in watermelon and melon [188]–[192].

3.2 Materials and Methods

3.2.1 Extraction of RNA, cDNA library preparation, and sequencing

The leaf tissues flash-frozen in liquid nitrogen were homogenized into fine powder by using a paint shaker (Harbil model 5G-HD paint shaker, USA) and 3mm stainless steel beads (Demag stainless steel balls, Abbott Ball Company, CT, USA).

Total RNA was extracted with the Quick-RNA™ Miniprep Kit (Zymo Research Corporation, Irvine, CA) and cleaned up DNA with DNase I (Zymo Research Corporation, Irvine, CA) according to the manufacturer's protocol. Then the quality and quantity of extracted

RNA was checked by a spectrophotometer (Denovix DS-11^{+} spectrophotometer, Wilmington, Delaware, USA).

3.2.2 Library preparation for Transcriptome sequencing

Twelve independent libraries were created by using a total of 12 RNA samples from 3 replicate leaf I tissue of *cv.* Crimson Sweet under the well-watered and drought-treated condition and from 3 individual leaf tissues of *cv.* Crimson Sweet under both control and salt-stressed condition. 1 µg of total RNA extract per sample was subjected to RNA sequencing library preparations by using NEBNext® Ultra™ RNA Library Prep Kit for Illumina® (NEB, USA) according to the manufacturer's protocol. The concentration of the library was quantified by a Qubit 2.0 fluorometer (Life Technologies), and then diluted to 1 ng/µl before checking the insert size on an Agilent Bioanalyzer 2100 system.

3.2.3 Data processing and analysis

3.2.3.1 Data processing, analysis, and mapping to reference genome:

The clustering of the index-coded samples was performed on a cBot Cluster Generation System using PE Cluster Kit cBot-HS (Illumina) according to the manufacturer's instructions. After cluster generation, the libraries were sequenced on an Illumina Hiseq platform, and 150 bp paired-end reads were generated. Raw reads of fastq format were processed to obtain clean reads by removing the adapter, reads containing ploy-N, and low-quality reads from raw data. At the same time, Q20, Q30, and GC content, the clean data were calculated. Watermelon reference genome (cultivar Charleston Gray) and gene model annotation files were downloaded from

CuGenDB (http://cucurbitgenomics.org/). Index of the reference genome was built using Bowtie v2.2.3 and paired-end clean reads were aligned to the reference genome using TopHat v2.0.12.

3.2.3.2 Gene expression quantification and DEG analysis

HTSeq v0.6.1 was used to count the reads mapped to each gene. FPKM (Fragments Per Kilobase of transcript per Million mapped reads) [193] of each gene was calculated based on the length of the gene and reads count mapped to this gene. Differential expression analysis was performed using the DESeq R package (1.18.0) Genes with P-value < 0.05 found by DESeq were assigned as differentially expressed.

3.3 Results and Discussion

3.3.1 Identification of DEGs associated with citrulline metabolism under drought stress

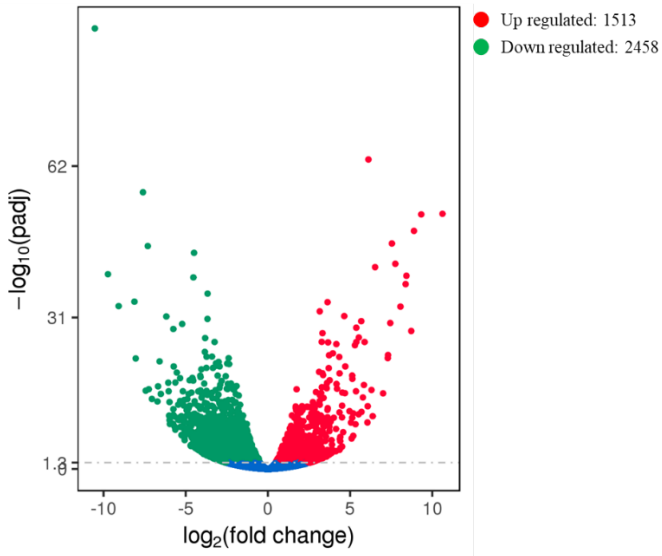

Figure 31. Volcano scattergram showing the amount of differentially expressed genes (DEGs, P-value<0.05) and non-DEGs under drought stress. Green points represent down-regulated DEGs, red points represent up-regulated DEGs and blue ones represent non-DEGs.

To understand the early transcriptomic changes induced by drought stress, we performed RNA-Sequencing (RNA-Seq) analysis of leaf tissue 8 days after the initiation of drought stress. A total of six libraries from leaf tissue were sequenced using the Illumina HiSeq platform. The volcano graph was generated by the R package (1.18.0). A total of 3971 genes were differentially expressed (DEGs), accounting for 20.1% of the total expressed genes (19742 genes). Of those 3971 genes, 1513 (38.1%) DEGs were up-regulated under drought stress while 2458 (61.9%) of them were down-regulated. The list of DEGs is attached as Appendix A Table 10.

A list of differentially expressed genes associated with citrulline metabolism [27] during drought stress is shown in Table 6. Based on the expression dynamics of genes closely associated with citrulline metabolism, we have proposed a model to explain possible regulation of citrulline in watermelon (Fig. 32). Consistent with our results from qPCR (Chapter II), the expression of N-acetylornithine deacetylase (*AOD2*) and Carbamoyl phosphate synthase (*CPS2*) was up-regulated. The expression of Ornithine carbamoyltransferase (OTC) was significant but the fold change increase was not consistent with our qPCR results. The expression of two other biosynthesis-related genes, N-acetylornithine aminotransferase (*AAT*) and N-acetylornithine deacetylase (*AOD3*) was also up-regulated, further confirming the increased citrulline accumulation in drought-stressed plants. The expression of putative Nitric-oxide synthase (NOS) was up-regulated although its existence in plants has not been experimentally demonstrated [25], [26]. The downregulations of citrulline catabolic genes, Argininosuccinate synthase (*ASS1* and ClCG03G003670), and ornithine catabolic genes, Ornithine decarboxylase (*ODC*) and Ornithine cyclodeaminase (*OCD*), further supports the citrulline abundance in water-stressed plants. Taken together, the up-regulation of genes associated with citrulline biosynthesis responsive and the

downregulation of genes involved in its catabolism explains the high accumulation of citrulline in drought-treated watermelon leaf tissues.

Table 6. List of up/down-regulated DEGs associated with citrulline metabolism under drought stress.

Up-regulated			Down-regulated		
Gene ID (Label)	**Description**	**log_2 Fold-Change**	**Gene ID (Label)**	**Description**	**log_2 Fold-Change**
ClCG09G012030 (AOD2)	N-acetylornithine deacetylase	7.4424	ClCG06G017780 (ASS1)	Argininosuccinate synthase	-1.5812
ClCG09G021680 (CPS2)	Carbamoyl phosphate synthase, large subunit	1.8449	ClCG11G006600	Pyrroline-5-carboxylate synthase	-1.6746
ClCG09G012020 (AOD3)	N-acetylornithine deacetylase	1.1365	ClCG05G008460 (OCD)	Ornithine cyclodeaminase	-1.9315
ClCG01G004960	Nitric-oxide synthase, putative	0.81193	ClCG03G003670	Argininosuccinate synthase	-2.2531
ClCG09G003180 (AAT)	N-acetylornithine aminotransferase	0.78922	ClCG08G013990 (ODC)	Ornithine decarboxylase	-2.4865
ClCG03G006680	Ornithine δ-aminotransferase	0.70555			
ClCG11G003830	Arginine decarboxylase	0.62965			

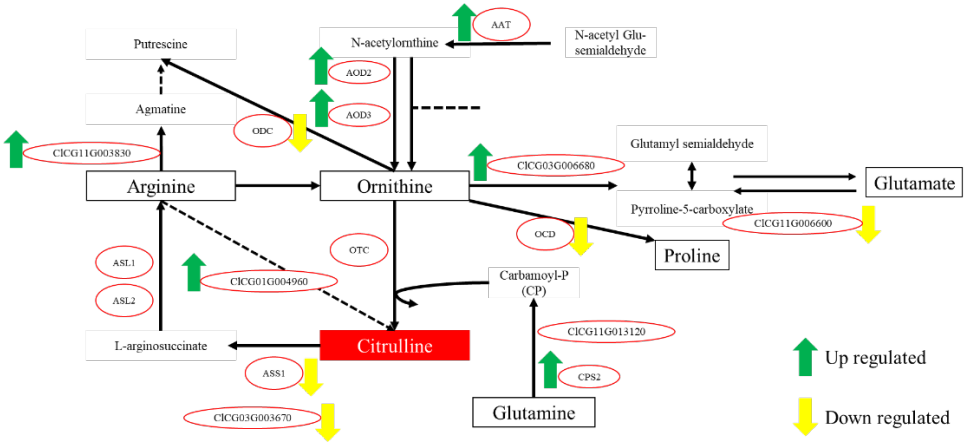

Figure 32. Up/Down regulations of genes associated with citrulline metabolism under drought stress in RNA-seq results. The green-up arrows represent up regulations of the genes at the right side while yellow down arrows show down regulations of genes on the left side. The labels inside red cycles represent gene ID and gene abbreviations used in qRT-PCR.

3.3.2 Identification of DEGs associated with citrulline metabolism under salt stress

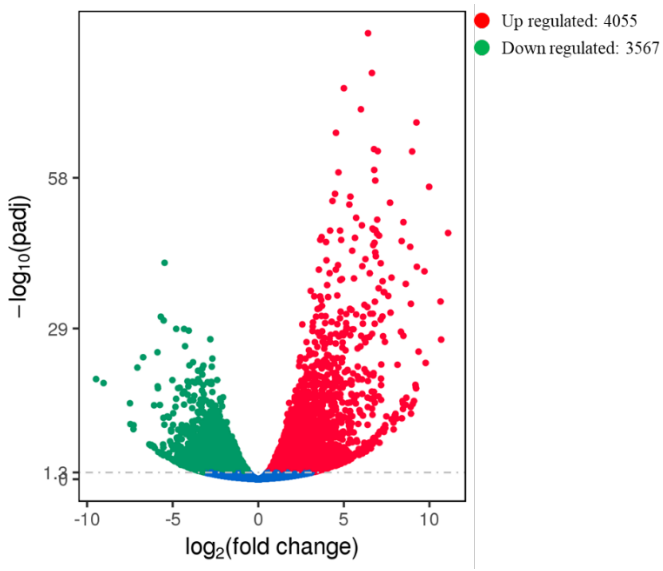

Figure 33. Volcano scattergram showing the amount of differentially expressed genes (DEGs, P-value<0.05) and non-DEGs under salt stress. Green points represent down-regulated DEGs, red points represent up-regulated DEGs and blue ones represent non-DEGs.

To understand the transcriptomic changes induced due to salt stress, we performed RNA-Seq analysis of seedlings exposed to salt stress. A total of six libraries were sequenced using the Illumina HiSeq platform. The RNA-Seq data identified a total of 7622 differentially expressed genes in response to salt stress, accounting for 39.0% total expressed genes (19557 genes). Out of total DEGs, 4055 (53.2%) of those DEGs were up-regulated while 3567 (46.8%) of them were down-regulated. The list of DEGs is presented in Appendix A Table 11.

The RNA-Seq data confirmed the induction of N-acetylornithine deacetylase (*AOD2*) and N-acetyl-γ-glutamyl-P-reductase (ClCG09G017590), both involved in the synthesis of citrulline. However, the upregulation of *ASS1* and *ODC* suggests the possibility of a citrulline-independent mechanism most likely through polyamine or proline synthesis in response to salt stress.

Table 7. List of up/down-regulated DEGs associated with citrulline metabolism under salt stress.

Up-regulated			Down-regulated		
Gene ID (Label)	**Description**	**log_2 Fold-Change**	**Gene ID (Label)**	**Description**	**log_2 Fold-Change**
ClCG09G012030 (AOD2)	N-acetylornithine deacetylase	4.1885	ClCG01G017650	N-acetyl Glu synthase	-1.0866
ClCG06G017780 (ASS1)	Argininosuccinate synthase	3.523	ClCG08G012830	N-acetylglutamate Kinase	-1.1651
ClCG08G013990 (ODC)	Ornithine decarboxylase	1.5285	ClCG09G004810	P-II	-1.1848
ClCG05G008460 (OCD)	Ornithine cyclodeaminase	1.3767	ClCG09G012020 (AOD3)	N-acetylornithine deacetylase	-1.3756
ClCG09G017590	N-acetyl-γ-glutamyl-P-reductase	1.2117	ClCG10G020940	N-acetylornithineglutamate acetyltransferase	-1.44
ClCG01G014440	P5C dehydrogenase	0.93856	ClCG11G013850	Urease	-1.5965
			ClCG03G006680	Ornithine δ-aminotransferase	-1.7134
			ClCG11G006600	Pyrroline-5-carboxylate synthase	-2.247
			ClCG09G021680 (CPS2)	Carbamoyl phosphate synthase, large subunit	-2.6234

3.4 Conclusion

Drought- and salt-induced global transcriptomic analysis in watermelon identified over 3900 and 7600 differentially expressed genes, respectively. These datasets would serve as a resource for identifying unique as well as conserved genes and pathways associated with both physiological processes. A model illustrating the possible regulation of citrulline supports activation of biosynthesis and down-regulation of citrulline metabolism during drought stress. However, expression profiles of genes showed non-overlapping patterns when compared with changes induced due to salt stress. Drought-induced activation of biosynthetic genes (*AAT*,

AOD, *OTC*, and *CPS2*) and down-regulation of catabolic (*ASS*, *ASL*, *ODC*, *OCD*) during drought stress aligns with increased citrulline. These results are consistent with the expression changes in the drought-stressed leaves of C. colocynthis [166]. The complexity of salt-induced responses was apparent based on the high number of DEGs, accounting for over 1/3 of the expressed transcriptome. It suggests that salt-induced responses are possibly spanned over several mechanisms rather than citrulline alone. Unlike drought stress, RNA-seq analysis of salt-stressed seedlings showed inconsistent expression patterns of genes associated with citrulline metabolism. Nonetheless, expression of *AOD2* involved in ornithine synthesis was consistently high in both drought and salt-stressed tissues.

CHAPTER IV

POLYMORPHISM OF SEED SPECIFIC AMINO ACIDS AND PROTEIN ACROSS WATERMELON GERMPLASM

4.1 Introduction

Seeds store a wide range of compounds, such as carbohydrates (especially starch), storage proteins, free amino acids, and storage lipids, contributing ~70% of the world's human caloric intake directly or indirectly as a feed [194]. The seed of most crops is an important nutritional source and target for manipulating protein and amino acid metabolism. Humans and farm animals cannot synthesize many essential amino acids and hence rely on their food sources. Developing countries, whose foods are mostly derived from crop plants, suffer from particular deficiencies in the essential amino acids and proteins leading to several health problems. Amino acids are not only used for the synthesis of storage proteins but also catabolized into the TCA cycle to generate energy [195]. Currently, animal feed is also supplemented with chemically synthesized amino acids which are very cost-intensive. Hence there is a commercial value in enhancing seed bound amino acids. Several transgenic approaches have been successfully used to improve amino acid balance in plant seeds [196], [197].

Watermelon seeds contain high amounts of seed proteins and various types of essential amino acids, as well as a non-protein amino acid, citrulline [198]–[200].

Watermelon is mostly used for the production of juices from fruit pulp, but the seed is mostly disposed of off while processing [201]. With up to 30-35% protein [199], [202], [203], and nutritionally adequate amino acid profile, watermelon seeds are also a valuable source of nutrition. Besides its nutritional potential, the proteins are hydrolyzed into amino acids during

germination, which in turn serves as an energy source to support seedlings growth [204]. Arginine, as citrulline's byproduct, is one of the predominant amino acids in watermelon seeds [205], [206].

Despite the availability of huge genetic variation, a detailed picture showing the extent of variability for seed amino acids and proteins across watermelon germplasm has not emerged. In this chapter, we have attempted to generate information on seed-specific amino acids and protein content in the watermelon germplasm available at the USDA germplasm repository. The protein and amino acid profiles generated through this experiment are being used for association mapping studies in collaboration with Prof. Umesh Reddy, West Virginia State University.

4.2 Materials and Methods

4.2.1 Seed samples preparation

Seeds of total 155 *Citrullus lanatus*, 54 *Citrullus mucosospermus* and 2 *Citrullus amarus* accessions obtained from the USDA Germplasm Resources Information Network (USDA-GRIN) were evaluated for protein content and amino acid distribution in this study. The seed coats of all the accessions were removed by plier or nail clipper and the intact endosperm was recovered. Approximately 20mg and 10mg of shelled watermelon seeds of each accession were placed in 2mL microcentrifuge tube in triplicates for amino acids and protein extractions respectively. The samples were flash-frozen in liquid nitrogen and homogenized to a fine powder using 5 mm Demag stainless steel balls (Abbott Ball Company, CT, USA) in Harbil model 5G-HD paint shaker.

4.2.2 Amino acids extraction and analysis

Free amino acids from watermelon seeds were extracted and detected using UPLC-MS/MS as per the protocol described in the Methods section of Chapter I.

4.2.3 Total protein extraction and analysis

The total proteins from homogenized seeds samples of each accession were extracted using a buffer consisting of 70mM Tris HCl, 25mM KCl, 1mM $MgCl_2$, 5mM EDTA, 5% glycerol, 0.1% Triton X-100 and 15mM β-mercaptoethanol (BME). The extracts were filtered using a 96-well 0.45-µm-pore filter plate (Pall Life Sciences, USA) and used to determine protein content using the Bradford Protein Assay Kit (AMRESCO® Inc.). 20 µl of extracts were incubated with 180 µl of buffer for 2 minutes in 96-well microplate (F-bottom, Greiner Bio-One, Kremsmünster, Austria) before measuring the absorbance at 595 nm in a spectrophotometer (Multiskan GO, Thermo Scientific, Waltham, Massachusetts, USA). Prior to the measurement of samples, 0.5 mg/mL BSA solution was used to prepare a standard curve to detect protein concentrations ranging from 0 to 100 µg/ml. The total proteins were calculated as 0 to 200 µg per mg.

4.3 Results and Discussion

4.3.1 Variation and association mapping in citrulline

4.3.1.1 Detection of citrulline and other free amino acids

We detected a total of 18 protein-bound and 3 non-protein (GABA, citrulline, ornithine) amino acids in the seeds of all watermelon accessions (Fig. 34). Glutamic acid (29.16%) followed by arginine (19.26%), were the most abundant amino acids in seeds. Accumulation of

nitrogen-rich amino acids, arginine and glutamate in watermelon seeds have been reported [199], [200]. The mean, SD and the co-efficient of variation (CV) for all seed bound amino acids are listed in Table 8. The range of phenotypic variation differed among amino acids; the highest coefficient of variation (CV) was observed for citrulline, followed by tryptophan; and the lowest coefficient of variation was observed for glutamic acid. The highest arginine and citrulline content were seen in the accession PI 435990 (23233.3 pmol/mg) and PI 276658 (6993.3 pmol/mg) (Fig. 35).

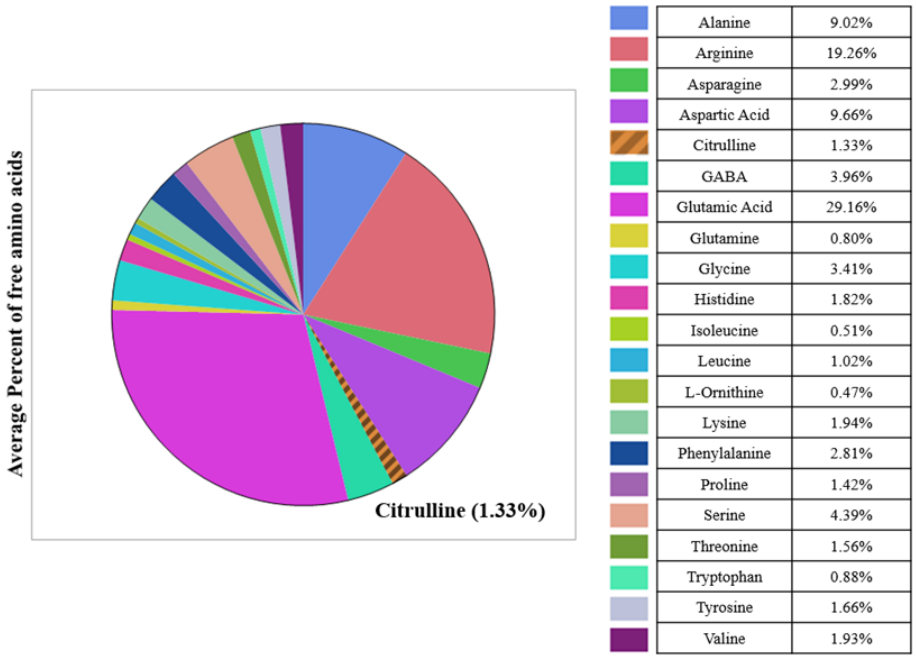

Figure 34. Percentage of average free amino acids contents accumulated in all watermelon accessions seeds.

Table 8. The mean, SD, variance and the co-efficient of variation (CV) for seed bound amino acids

Compounds	Mean	Std Dev	CV
Alanine	1557.67	1532.29	98.37
Arginine	3328.16	2534.90	76.17
Asparagine	517.38	409.37	79.12
Aspartic Acid	1668.35	790.55	47.39
Citrulline	228.98	651.77	284.64
GABA	684.98	1018.35	148.67
Glutamic Acid	5038.58	1710.90	33.96
Glutamine	138.33	182.84	132.17
Glycine	588.41	482.94	82.08
Histidine	314.78	329.33	104.62
Isoleucine	87.92	128.95	146.66
Leucine	175.64	168.77	96.09
L-Ornithine	81.85	86.23	105.35
Lysine	334.74	297.71	88.94
Phenylalanine	484.74	300.47	61.99
Proline	245.44	446.84	182.06
Serine	758.12	492.39	64.95
Threonine	269.61	202.36	75.06
Tryptophan	152.46	307.51	201.70
Tyrosine	286.80	182.18	63.52
Valine	333.90	283.05	84.77

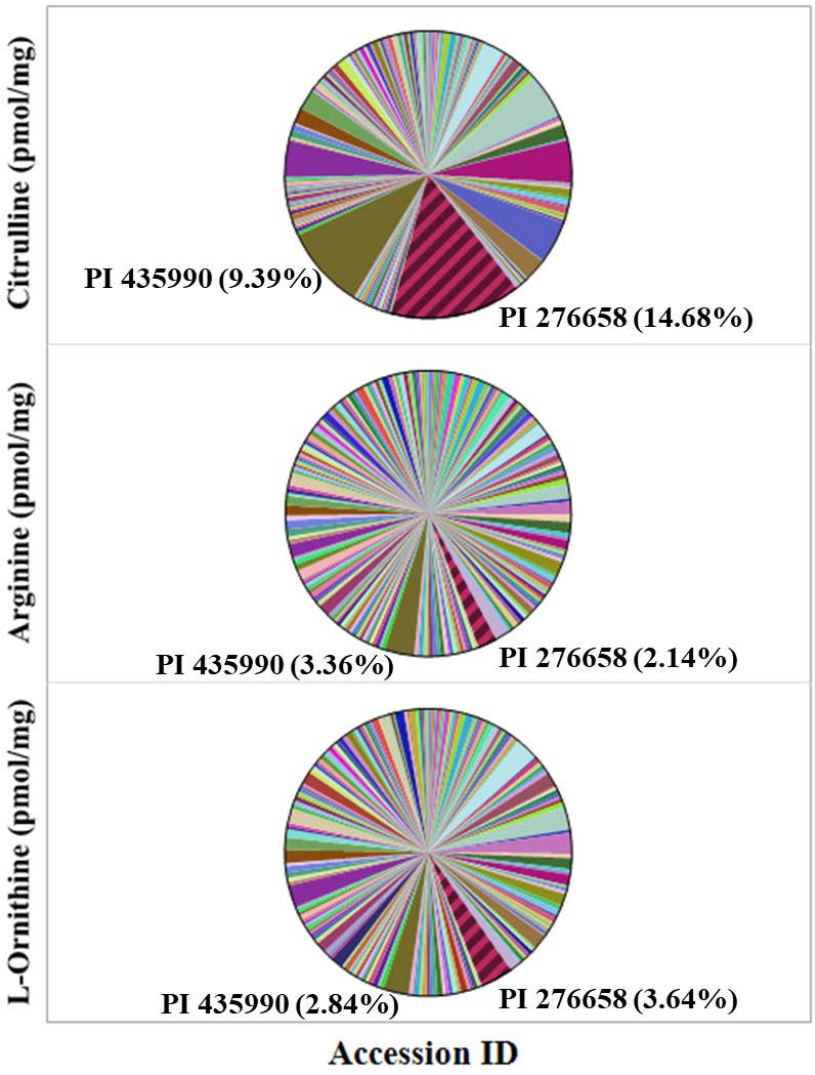

Figure 35. Distribution of citrulline, arginine, and L-ornithine content among all accessions.

4.3.1.2 Population structure of accessions by amino acid distribution

The details of geographical origin and continents are presented in Appendix A Table 12. We investigated the distribution of seed amino acids in a total of 211 watermelon accessions, including 2 *Citrullus. amarus*, 165 *Citrullus. lanatus* and 54 *Citrullus. mucosospermus* (egusi). The distribution of arginine and citrulline content in *C. lanatus and mucosospermus* are shown in Fig. 36. In general, a high variability ($P < 0.05$) for all amino acids among the accessions

analyzed was observed. The amino acid composition may be influenced by genotypic variability based on their center of origin or agronomic conditions such as soil fertility and postharvest processing that alters the ratio of seed components. The average arginine and citrulline contents by continents are presented in Fig. 37. Our data suggest that the citrulline content in selected domesticated European accessions was much higher than wild/landraces. Consistent with the previous report on fruit bound citrulline [207], the seed bound citrulline seems to be a domesticated trait. The average arginine content in European accessions was higher than the wild ones.

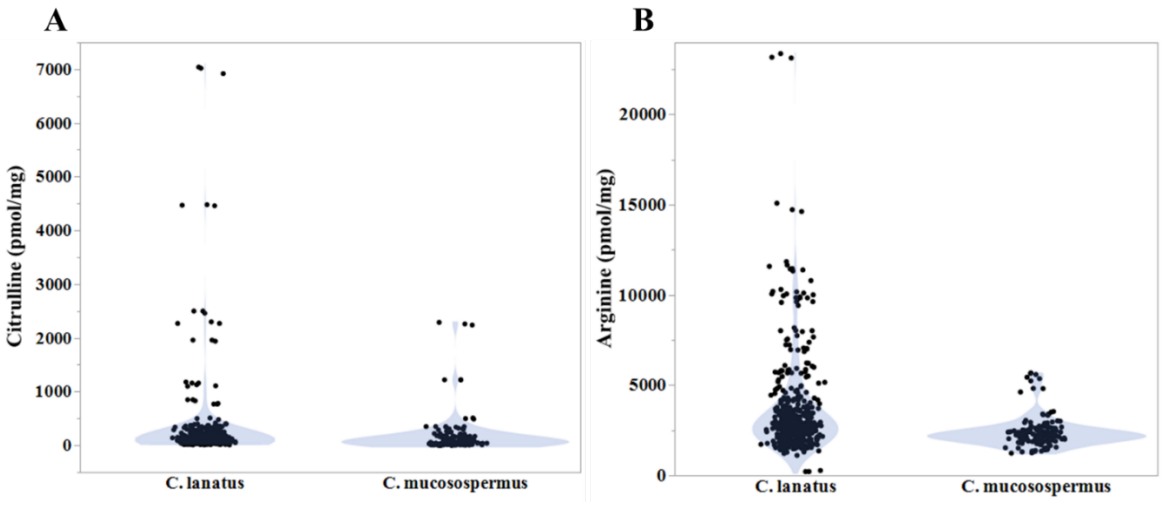

Figure 36. Distribution of citrulline (A) and arginine (B) content in *C. lanatus* and *mucosospermus*.

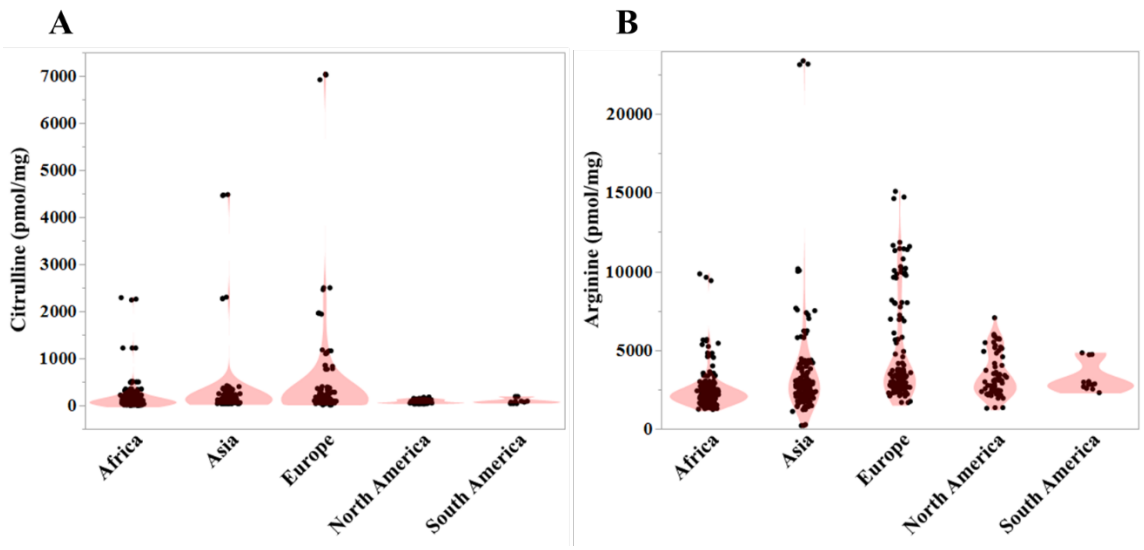

Figure 37. Geographical variation of citrulline (A) and arginine (B) content in seeds across accessions.

The principal component analysis (PCA) of citrulline content was conducted with the first (13.40) and second (4.71) principal components, which was based on the SNP dataset to test the separation across accessions during evolution. This PCA (Fig. 38) separated accession types (*Citrullus. amarus*, *Citrullus. lanatus*, and *Citrullus. mucosospermus*) as well as citrulline content levels (low, medium and high). Cultivars (*C. lanatus*) accumulated the highest content of citrulline compared to the medium level of egusi and landrace types further suggesting that a high amount of citrulline might be a characteristic of new cultivars.

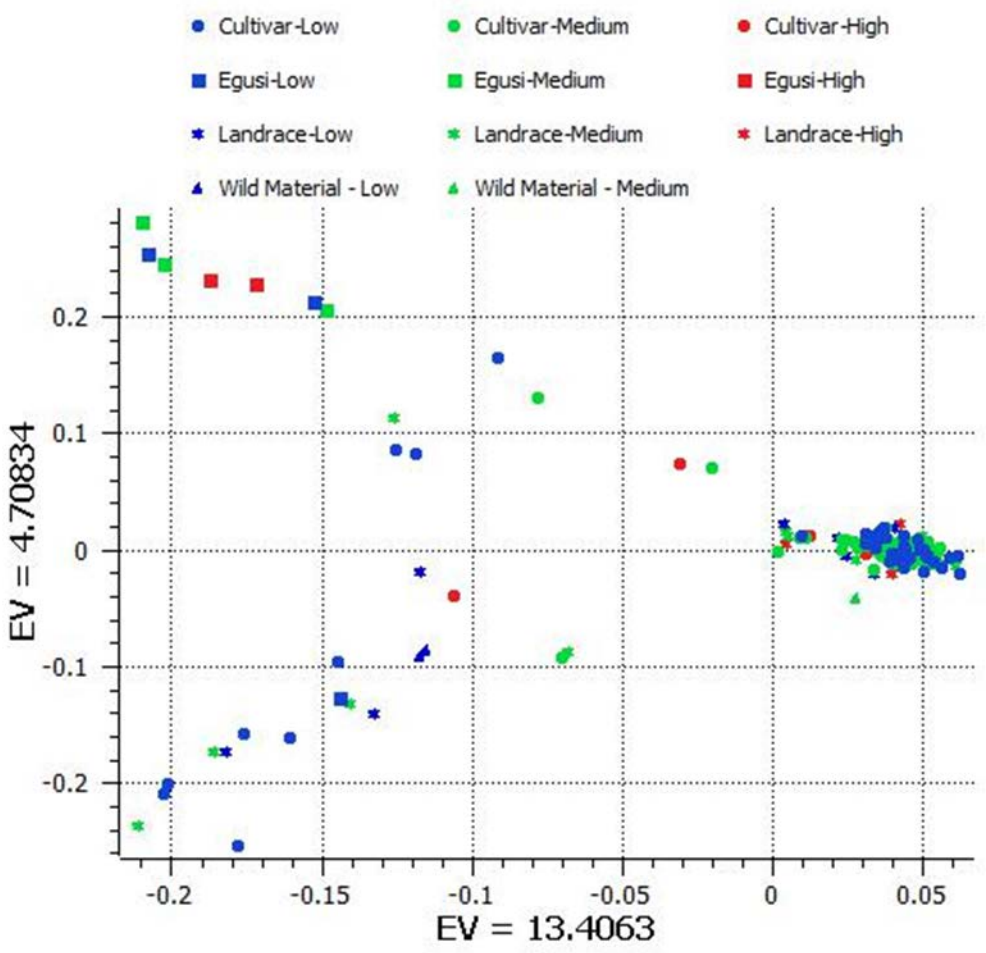

Figure 38. PCA showing the distribution of Cit. amarus, Cit. lanatus and Cit. mucosospermus as well as the low, medium and high levels of citrulline content in 211 watermelon accessions.

4.3.2 Variation and association mapping in protein

The total protein distribution across accessions is shown in Fig. 39. The highest protein content was measured in the accessions PI 172793 (19.51%). The percent coefficient of variation for protein content was 19.93. The accessions possessing exceptional high protein raises opportunities for their use in the watermelon breeding programs to enhance seedling vigor due to high stored protein and as a nutritional source for food and animal feed industries. The crude

seed protein content in the commercial cultivars (Black Diamond, Charleston Gray and Crimson Sweet) has been reported to range between 16- 17.7% [208].

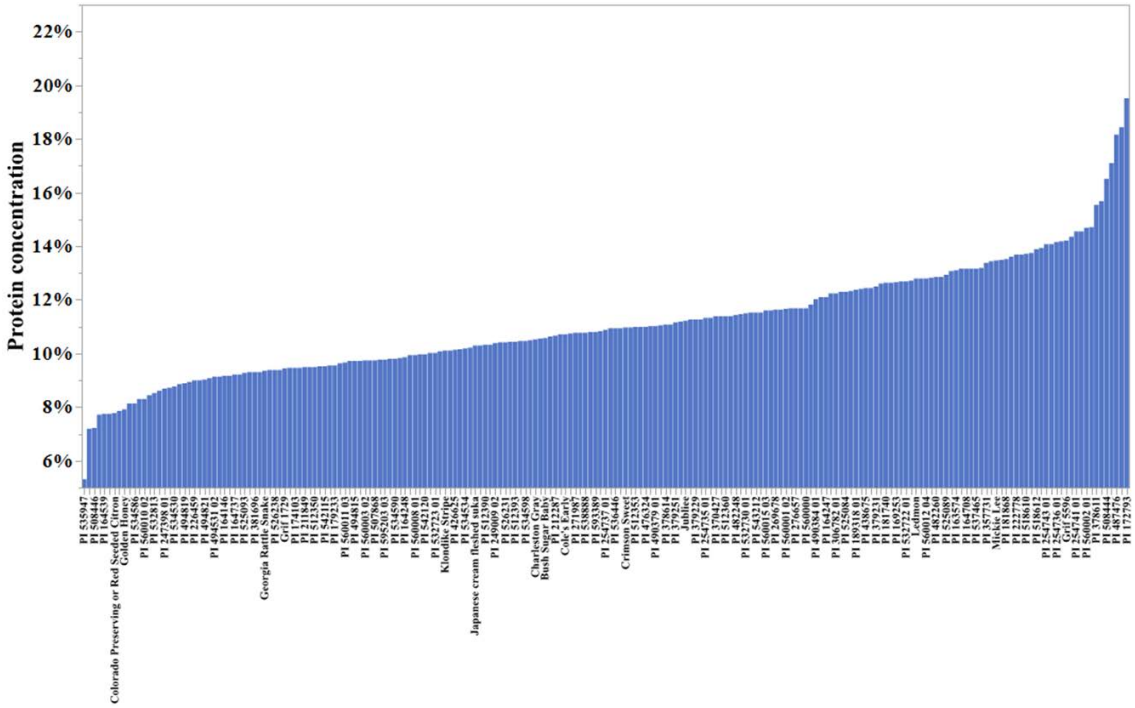

Figure 39. Variation of protein content in watermelon seeds across 211 accessions.

The distribution of protein content in *C. amarus*, *C. lanatus* and *C. mucosospermus* is summarized in Fig. 40. The average protein content in *C. mucosospermus* (11.37%) was higher than *Cit. lanatus* (10.99%) and by *Cit. amarus* (10.34%). The average protein content across accessions in different continents is shown in Fig. 41. The average protein concentration in the accessions from Europe (11.45%) was significantly higher than Asia (10.76%) and North America (10.57%). Accessions from Africa were significantly lower than in European or American accessions.

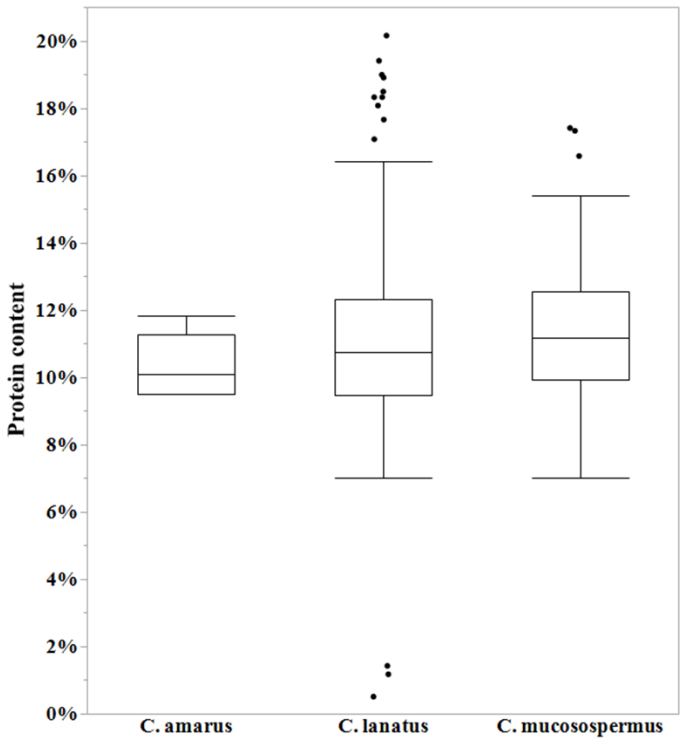

Figure 40. Box plot representing the distribution, mean and range of protein content in *Cit. amarus, lanatus and mucosospermus* types.

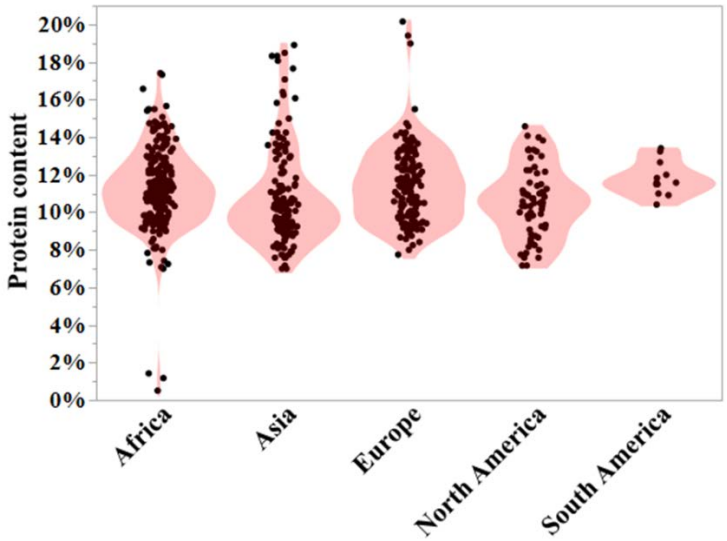

Figure 41. Contour graph showing geographic variation in protein content across accessions.

4.4 Conclusion

Watermelon seed proteins provide one of the most tangible paleo-friendly protein-rich and gluten-free dietary options. Besides proteins, the seeds are also a rich source of several amino acids including limiting amino acids. Our results demonstrated a significant amount of variation for the content of different amino acids and proteins across the accessions and geographies. Based on the geographic distribution of the accessions, the low protein in African accessions opens up the opportunities for breeding efforts for the improvement of the watermelon protein content and quality for supporting human nutrition. The accessions with high protein content and essential amino acids can be used for value-added benefits in the feed industry through biofortification. The phenotypic data collected for seed amino acids and proteins would allow genetic mapping using GWAS and identify SNP markers associated with these traits. Our results provided the required information on variability to guide introgression breeding of commercial diploid varieties using marker-based breeding. The data is already being used to identify causal genes associated with each amino acid and protein content using association mapping in collaboration with the Reddy lab at West Virginia State University.

CHAPTER V

SUMMARY

Citrulline, a non-protein amino acid, is synthesized from ornithine and carbamoyl phosphate in plants. In order to characterize the dynamics of citrulline accumulation during the development of watermelon, amino acids profilings of various plant tissues, such as cotyledon, leaf, stem, flower, fruit rind and pulp, were investigated. The highest amount of citrulline accumulation was found in fruit tissues, followed by stem and leaf tissues. The results showed a positive correlation between citrulline and the precursor (ornithine) and by-product (arginine) amino acids in fruits. Relatively moderate accumulation of citrulline in vegetative tissues (stem and leaf) suggests the possibility that citrulline was transported from the source (vegetative tissue) to the sink (developing fruits).

We evaluated the impact of abiotic stresses on citrulline accumulation in the vegetative tissues of watermelon plants. Under imposed drought stress, citrulline accumulation in leaf tissues was rapidly induced up to ~38-fold higher relative to control tissues during early stages (8 days of initiation of drought stress), indicating a potential role of citrulline as a biomarker in the drought-induced responses. During prolonged stress, citrulline abundance continued to increase in the drought-stressed leaf tissues, although the fold-change relative to control tissues was smaller (~16-fold). Consistent with the increase in citrulline, the concentration of arginine and ornithine also increased, emphasizing the significance of the ornithine-citrulline-arginine pathway in watermelons during drought stress. The drought-induced global transcriptomic profiling of the leaf tissues using RNA-seq analysis identified over 3900 differentially expressed genes (DEGs). Among these DEGs, up-regulation of biosynthetic genes (*AAT*, *AOD*, *OTC*, and *CPS2*) and the down-regulated catabolic genes (*ASS*, *ASL*, *ODC*, *OCD*) justified the increased

accumulation of citrulline during drought stress. Further studies evaluating biological relevance of citrulline in drought tolerance using the detailed characterization of genes involved in its metabolism would help in enhancing drought tolerance in other plant species. The watermelon seedlings also showed a rapid increase in the citrulline accumulation during salt stress. RNA-seq analysis identified over 7600 DEGs induced by salinity, and the salt-stressed seedlings showed inconsistent expression patterns of genes associated with citrulline metabolism. The complexity of salt-induced responses was apparent based on the high number of DEGs, accounting for more than 1/3 of the expressed transcriptome. It suggests that salt-induced responses are possibly spanned over several mechanisms rather than citrulline alone. Unlike drought and salt stress. no significant changes in citrulline accumulation were noticed in response to heat stress. Nonetheless, a significant increase in the accumulation of N-rich amino acids- Asparagine, Glutamine and Glutamic Acid, suggests the possibility of regulation of heat tolerance by new targets involved in the nitrogen assimilation.

Our data demonstrated that citrulline synthesis is regulated by the nitrogen status of the plant. Citrulline's role in translocating nitrogen in watermelon vegetative tissues was supported by the following results: (1) significant reduction in citrulline content along with its precursor (ornithine) and by-product (arginine) in nitrogen depleted leaf tissues (2) the percent distribution of citrulline in the nitrogen depleted leaves and stems (10-18%) , comparable to that of nitrogen carrying amino acids - aspartate and glutamate (3) reduction in NO_3-N of the phloem sap (*cv.* Crimson Sweet), and (4) down-regulation of the biosynthetic genes *AAT* and *CPS2* during nitrogen stress.

Watermelon seeds are rich sources of essential amino acids and proteins. We investigated the seed-specific amino acids and protein content in watermelon germplasms available at the

USDA germplasm repository. Our results demonstrated a significant amount of variation for both the traits across all the geographies and accessions. The low amount of protein in the African accessions suggests the need for improving the watermelon seed-bound protein content and quality via breeding programs. The accessions with high levels of protein and amino acids can be utilized for value-added benefits in the feed industry through biofortification. The phenotypic variation identified throughout this study will be used to identify candidate genes associated with seed-specific amino acids and proteins using Genome-wide Associationi Studies (GWAS) in collaboration with Dr. Umesh Reddy at West Virginia State University. The outcome of this research would enable the genetic improvement of these traits in cultivated watermelon varieties using classical and transgenic breeding.

REFERENCES

[1] KOGA and Yotaro, “Study report on the constituents of squeezed watermelon,” *Tokyo Kagaku Kaishi [Journal Tokyo Chem. Soc.*, vol. 35, pp. 519–528, 1914.

[2] M. Wada, “On the occurrence of a new amino acid in watermelon, citrullus vulgaris, schrad,” *J. Agric. Chem. Soc. Japan*, vol. 6, no. 1–5, pp. 32–34, 1930, doi: 10.1080/03758397.1930.10856930.

[3] E. Curis *et al.*, “Almost all about citrulline in mammals,” *Amino Acids*, vol. 29, no. 3, pp. 177–205, 2005, doi: 10.1007/s00726-005-0235-4.

[4] P. Crenn and L. Cynober, “Effect of intestinal resections on arginine metabolism: practical implications for nutrition support,” *Curr. Opin. Clin. Nutr. Metab. Care*, vol. 13, no. 1, pp. 65–69, 2010.

[5] S. Bahri *et al.*, “Citrulline: From metabolism to therapeutic use,” *Nutrition*, vol. 29, no. 3, pp. 479–484, 2013, doi: 10.1016/j.nut.2012.07.002.

[6] P. Alsop and D. Hauton, “Oral nitrate and citrulline decrease blood pressure and increase vascular conductance in young adults: a potential therapy for heart failure,” *Eur. J. Appl. Physiol.*, vol. 116, no. 9, pp. 1651–1661, 2016, doi: 10.1007/s00421-016-3418-7.

[7] C. Moinard *et al.*, “Arginine behaviour after arginine or citrulline administration in older subjects,” *Br. J. Nutr.*, vol. 115, no. 3, pp. 399–404, 2016, doi: 10.1017/S0007114515004638.

[8] G. A. Schellekens, “Pillars Article : Citrulline is an Essential Constituent of Antigenic Determinants Recognized by Rheumatoid Arthritis − specific,” *J Immunol*, vol. 195, pp. 8–16, 2015.

[9] M. Morita *et al.*, “Oral supplementation with a combination of L-citrulline and L-arginine rapidly increases plasma L-arginine concentration and enhances NO bioavailability,” *Biochem. Biophys. Res. Commun.*, vol. 454, no. 1, pp. 53–57, 2014, doi: 10.1016/j.bbrc.2014.10.029.

[10] N. Hao *et al.*, “Improvement of L-citrulline production in Corynebacterium glutamicum by ornithine acetyltransferase,” *J. Ind. Microbiol. Biotechnol.*, vol. 42, no. 2, pp. 307–313, 2015.

[11] D. Eberhardt, J. V. K. Jensen, and V. F. Wendisch, “L-citrulline production by metabolically engineered Corynebacterium glutamicum from glucose and alternative carbon sources,” *AMB Express*, vol. 4, no. 1, p. 85, 2014.

[12] W. W. Fish, “A reliable methodology for quantitative extraction of fruit and vegetable physiological amino acids and their subsequent analysis with commonly available HPLC systems,” *Food Nutr. Sci.*, vol. 3, no. 06, p. 863, 2012.

[13] J. L. Hartman, T. C. Wehner, G. Ma, and P. Perkins-Veazie, “Citrulline and Arginine Content of Taxa of Cucurbitaceae,” *Horticulturae*, vol. 5, no. 1, p. 22, 2019.

[14] W. W. Fish, “Process for the production of L-citrulline from watermelon flesh and rind.” Google Patents, 08-May-2012.

[15] W. W. Fish, “The Expression of Citrulline and other Members of the Arginine Metabolic Family in Developing Watermelon Fruit,” *Int. J. Agric. Innov. Res.*, vol. 2, no. 5, pp. 2319–1473, 2014.

[16] V. Joshi, M. Joshi, D. Silwal, K. Noonan, S. Rodriguez, and A. Penalosa, “Systematized biosynthesis and catabolism regulate citrulline accumulation in watermelon,” *Phytochemistry*, vol. 162, no. November 2018, pp. 129–140, 2019, doi:

10.1016/j.phytochem.2019.03.003.

[17] W. Liu, S. Zhao, Z. Cheng, X. Wan, Z. Yan, and S. R. King, “Lycopene and citrulline contents in watermelon (Citrullus lanatus) fruit with different ploidy and changes during fruit development,” *Acta Hortic.*, vol. 871, pp. 543–550, 2010.

[18] Y. Xu *et al.*, “The draft genome of watermelon (Citrullus lanatus) and resequencing of 20 diverse accessions,” *Nat. Genet.*, vol. 45, no. 1, pp. 51–58, 2013, doi: 10.1038/ng.2470.

[19] A. R. Davis, C. L. Webber, W. W. Fish, T. C. Wehner, S. King, and P. Perkins-Veazie, “L-citrulline levels in watermelon cultigens tested in two environments,” *HortScience*, vol. 46, no. 12, pp. 1572–1575, 2011, doi: 10.21273/hortsci.46.12.1572.

[20] D. E. Mitchell and M. A. Madore, “Patterns of assimilate production and translocation in muskmelon (Cucumis melo L.): II. Low temperature effects,” *Plant Physiol.*, vol. 99, no. 3, pp. 966–971, 1992.

[21] C. LEGRAIN *et al.*, “Structure and function of ornithine carbamoyltransferases,” *Eur. J. Biochem.*, vol. 80, no. 2, pp. 401–409, 1977.

[22] B. J. Micallef and B. J. Shelp, “Arginine metabolism in developing soybean cotyledons: I. Relationship to nitrogen nutrition,” *Plant Physiol.*, vol. 90, no. 2, pp. 624–630, 1989.

[23] S. Guo *et al.*, “Comparative transcriptome analysis of cultivated and wild watermelon during fruit development,” *PLoS One*, vol. 10, no. 6, pp. 1–22, 2015, doi: 10.1371/journal.pone.0130267.

[24] R. M. J. Palmer, D. S. Ashton, and S. Moncada, “Vascular endothelial cells synthesize nitric oxide from L-arginine,” *Nature*, vol. 333, no. 6174, p. 664, 1988.

[25] L. A. J. Mur, K. H. Hebelstrup, and K. J. Gupta, “Striking a balance: does nitrate uptake and metabolism regulate both NO generation and scavenging?,” *Front. Plant Sci.*, vol. 4,

p. 288, 2013.

[26] K. J. Gupta *et al.*, "The form of nitrogen nutrition affects resistance against Pseudomonas syringae pv. phaseolicola in tobacco," *J. Exp. Bot.*, vol. 64, no. 2, pp. 553–568, 2012.

[27] V. Joshi and A. R. Fernie, "Citrulline metabolism in plants," *Amino Acids*, vol. 49, no. 9, pp. 1543–1559, 2017, doi: 10.1007/s00726-017-2468-4.

[28] L. Bosch, A. Alegría, and R. Farré, "Application of the 6-aminoquinolyl-N-hydroxysccinimidyl carbamate (AQC) reagent to the RP-HPLC determination of amino acids in infant foods," *J. Chromatogr. B*, vol. 831, no. 1–2, pp. 176–183, Feb. 2006, doi: 10.1016/J.JCHROMB.2005.12.002.

[29] M. C. Gardener and M. P. Gillman, "Analyzing Variability in Nectar Amino Acids: Composition Is Less Variable Than Concentration," *J. Chem. Ecol.*, vol. 27, no. 12, pp. 2545–2558, 2001, doi: 10.1023/A:1013687701120.

[30] I. Boogers, W. Plugge, Y. Q. Stokkermans, and A. L. L. Duchateau, "Ultra-performance liquid chromatographic analysis of amino acids in protein hydrolysates using an automated pre-column derivatisation method," *J. Chromatogr. A*, vol. 1189, no. 1–2, pp. 406–409, May 2008, doi: 10.1016/J.CHROMA.2007.11.052.

[31] J. M. Armenta *et al.*, "Sensitive and rapid method for amino acid quantitation in malaria biological samples using AccQ • Tag ultra performance liquid chromatography-electrospray ionization-MS/MS with multiple reaction monitoring," *Anal. Chem.*, vol. 82, no. 2, pp. 548–558, 2010, doi: 10.1021/ac901790q.

[32] S. A. Cohen and D. P. Michaud, "Synthesis of a fluorescent derivatizing reagent, 6-aminoquinolyl-N-hydroxysuccinimidyl carbamate, and its application for the analysis of hydrolysate amino acids via high-performance liquid chromatography," *Anal. Biochem.*,

vol. 211, no. 2, pp. 279–287, 1993.

[33] K. Sandlin *et al.*, “Comparative mapping in watermelon [Citrullus lanatus (Thunb.) Matsum. et Nakai],” *Theor. Appl. Genet.*, vol. 125, no. 8, pp. 1603–1618, 2012.

[34] Y. Ren *et al.*, “An integrated genetic map based on four mapping populations and quantitative trait loci associated with economically important traits in watermelon (Citrullus lanatus),” *BMC Plant Biol.*, vol. 14, no. 1, p. 33, 2014.

[35] Q. Zhu *et al.*, “Comparative transcriptome analysis of two contrasting watermelon genotypes during fruit development and ripening,” *BMC Genomics*, vol. 18, no. 1, p. 3, 2017.

[36] P. Nimmakayala *et al.*, “Genome-wide differentiation of various melon horticultural groups for use in GWAS for fruit firmness and construction of a high resolution genetic map,” *Front. Plant Sci.*, vol. 7, p. 1437, 2016.

[37] A. Levi *et al.*, “Genetic diversity in the desert watermelon Citrullus colocynthis and its relationship with Citrullus species as determined by high-frequency oligonucleotides-targeting active gene markers,” *J. Am. Soc. Hortic. Sci.*, vol. 142, no. 1, pp. 47–56, 2017.

[38] H. Zhang, G. Gong, S. Guo, Y. Ren, Y. Xu, and K. S. Ling, “Screening the USDA watermelon germplasm collection for drought tolerance at the seedling stage,” *HortScience*, vol. 46, no. 9, pp. 1245–1248, 2011, doi: 10.21273/hortsci.46.9.1245.

[39] K. Akashi, Y. Mifune, K. Morita, S. Ishitsuka, H. Tsujimoto, and T. Ishihara, “Spatial accumulation pattern of citrulline and other nutrients in immature and mature watermelon fruits,” *J. Sci. Food Agric.*, vol. 97, no. 2, pp. 479–487, 2017, doi: 10.1002/jsfa.7749.

[40] A. M. Rimando and P. M. Perkins-Veazie, “Determination of citrulline in watermelon rind,” *J. Chromatogr. A*, vol. 1078, no. 1–2, pp. 196–200, 2005, doi:

10.1016/j.chroma.2005.05.009.

[41] I. Tlili, C. Hdider, M. S. Lenucci, I. Riadh, H. Jebari, and G. Dalessandro, “Bioactive compounds and antioxidant activities of different watermelon (Citrullus lanatus (Thunb.) Mansfeld) cultivars as affected by fruit sampling area,” *J. Food Compos. Anal.*, vol. 24, no. 3, pp. 307–314, May 2011, doi: 10.1016/J.JFCA.2010.06.005.

[42] J.-K. Zhu, “Abiotic stress signaling and responses in plants,” *Cell*, vol. 167, no. 2, pp. 313–324, 2016.

[43] A. Dixit, P. Tomar, E. Vaine, H. Abdullah, S. Hazen, and O. P. Dhankher, “A stress-associated protein, AtSAP13, from Arabidopsis thaliana provides tolerance to multiple abiotic stresses,” *Plant. Cell Environ.*, vol. 41, no. 5, pp. 1171–1185, 2018.

[44] S. Coolen *et al.*, “Transcriptome dynamics of Arabidopsis during sequential biotic and abiotic stresses,” *Plant J.*, vol. 86, no. 3, pp. 249–267, 2016.

[45] A. Pereira, “Plant abiotic stress challenges from the changing environment,” *Front. Plant Sci.*, vol. 7, p. 1123, 2016.

[46] B. Vinocur and A. Altman, “Recent advances in engineering plant tolerance to abiotic stress: achievements and limitations,” *Curr. Opin. Biotechnol.*, vol. 16, no. 2, pp. 123–132, 2005.

[47] M. Farooq, A. Wahid, N. Kobayashi, D. Fujita, and S. M. A. Basra, “Plant drought stress: effects, mechanisms and management,” in *Sustainable agriculture*, Springer, 2009, pp. 153–188.

[48] J. Zhang, “China’s success in increasing per capita food production,” *J. Exp. Bot.*, vol. 62, no. 11, pp. 3707–3711, 2011.

[49] K. Nahar, M. Hasanuzzaman, and M. Fujita, “Roles of osmolytes in plant adaptation to

drought and salinity," in *Osmolytes and plants acclimation to changing environment: Emerging omics technologies*, Springer, 2016, pp. 37–68.

[50] H. Kuşçu, A. Turhan, N. Özmen, P. Aydınol, H. Büyükcangaz, and A. O. Demir, "Deficit irrigation effects on watermelon (Citrullus Vulgaris) in a sub humid environment," *JAPS J. Anim. Plant Sci.*, vol. 25, no. 6, pp. 1652–1659, 2015.

[51] D. Harris, R. S. Tripathi, and A. Joshi, "On-farm seed priming to improve crop establishment and yield in dry direct-seeded rice," *Direct seeding Res. Strateg. Oppor. Int. Res. Institute, Manila, Philipp.*, pp. 231–240, 2002.

[52] M. D. Kaya, G. Okçu, M. Atak, Y. Cıkılı, and Ö. Kolsarıcı, "Seed treatments to overcome salt and drought stress during germination in sunflower (Helianthus annuus L.)," *Eur. J. Agron.*, vol. 24, no. 4, pp. 291–295, 2006.

[53] G. Okçu, M. D. Kaya, and M. Atak, "Effects of salt and drought stresses on germination and seedling growth of pea (Pisum sativum L.)," *Turkish J. Agric. For.*, vol. 29, no. 4, pp. 237–242, 2005.

[54] G. Cornic and A. Massacci, "Leaf Photosynthesis Under Drought Stress," in *Photosynthesis and the Environment*, N. R. Baker, Ed. Dordrecht: Springer Netherlands, 1996, pp. 347–366.

[55] D. I. Leskovar, H. Bang, K. Kolenda, J. A. Franco, and P. Perkins-Veazie, "Deficit irrigation influences yield and lycopene content of diploid and triploid watermelon," in *XXVI International Horticultural Congress: Issues and Advances in Postharvest Horticulture 628*, 2002, pp. 147–151.

[56] A. Yokota, S. Kawasaki, M. Iwano, C. Nakamura, C. Miyake, and K. Akashi, "Citrulline and DRIP-1 protein (ArgE homologue) in drought tolerance of wild watermelon," *Ann.*

Bot., vol. 89, no. SPEC. ISS., pp. 825–832, 2002, doi: 10.1093/aob/mcf074.

[57] S. Kawasaki, C. Miyake, T. Kohchi, S. Fujii, M. Uchida, and A. Yokota, "Responses of wild watermelon to drought stress: Accamulation of an ArgE homologue and citrulline in leaves during water deficits," *Plant Cell Physiol.*, vol. 41, no. 7, pp. 864–873, 2000, doi: 10.1093/pcp/pcd005.

[58] A. E. Hall, *Crop responses to environment*. CRC press, 2000.

[59] J. H. Christensen and O. B. Christensen, "A summary of the PRUDENCE model projections of changes in European climate by the end of this century," *Clim. Change*, vol. 81, no. 1, pp. 7–30, 2007.

[60] C. E. Bita and T. Gerats, "Plant tolerance to high temperature in a changing environment: Scientific fundamentals and production of heat stress-tolerant crops," *Front. Plant Sci.*, vol. 4, no. JUL, pp. 1–18, 2013, doi: 10.3389/fpls.2013.00273.

[61] B. Barnabás, K. Jäger, and A. Fehér, "The effect of drought and heat stress on reproductive processes in cereals," *Plant. Cell Environ.*, vol. 31, no. 1, pp. 11–38, 2008.

[62] D. B. Lobell and G. P. Asner, "Climate and management contributions to recent trends in US agricultural yields," *Science (80-.).*, vol. 299, no. 5609, p. 1032, 2003.

[63] C. Bita and T. Gerats, "Plant tolerance to high temperature in a changing environment: scientific fundamentals and production of heat stress-tolerant crops," *Front. Plant Sci.*, vol. 4, p. 273, 2013.

[64] A. Ahmad, H. Diwan, and Y. P. Abrol, "Global climate change, stress and plant productivity," in *Abiotic Stress Adaptation in Plants*, Springer, 2009, pp. 503–521.

[65] A. Smertenko, 1 2 P DRÁBER, V. Viklický, and Z. Opatrný, "Heat stress affects the organization of microtubules and cell division in Nicotiana tabacum cells," *Plant. Cell*

Environ., vol. 20, no. 12, pp. 1534–1542, 1997.

[66] G. Potters, T. P. Pasternak, Y. Guisez, and M. A. K. Jansen, “Different stresses, similar morphogenic responses: integrating a plethora of pathways,” *Plant. Cell Environ.*, vol. 32, no. 2, pp. 158–169, 2009.

[67] R. Rasheed, “Salinity and extreme temperature effects on sprouting buds of sugarcane (Saccharum officinarum L.): some histological and biochemical studies.” UNIVERSITY OF AGRICULTURE, FAISALABAD PAKISTAN, 2009.

[68] S. I. Allakhverdiev, V. D. Kreslavski, V. V Klimov, D. A. Los, R. Carpentier, and P. Mohanty, “Heat stress: an overview of molecular responses in photosynthesis,” *Photosynth. Res.*, vol. 98, no. 1–3, p. 541, 2008.

[69] D. T. Todorov, E. N. Karanov, A. R. Smith, and M. A. Hall, “Chlorophyllase activity and chlorophyll content in wild and mutant plants of Arabidopsis thaliana,” *Biol. Plant.*, vol. 46, no. 1, pp. 125–127, 2003.

[70] Y. P. Zhang, X. H. Zhu, H. D. Ding, S. J. Yang, and Y. Y. Chen, “Foliar application of 24-epibrassinolide alleviates high-temperature-induced inhibition of photosynthesis in seedlings of two melon cultivars,” *Photosynthetica*, vol. 51, no. 3, pp. 341–349, 2013.

[71] X. Zhao, Y. Nishimura, Y. Fukumoto, and J. Li, “Effect of high temperature on active oxygen species, senescence and photosynthetic properties in cucumber leaves,” *Environ. Exp. Bot.*, vol. 70, no. 2–3, pp. 212–216, 2011.

[72] W. Hou, A. H. Sun, H. L. Chen, F. S. Yang, J. L. Pan, and M. Y. Guan, “Effects of chilling and high temperatures on photosynthesis and chlorophyll fluorescence in leaves of watermelon seedlings,” *Biol. Plant.*, vol. 60, no. 1, pp. 148–154, 2016.

[73] S. Yan, F. Aili, and X. Weijun, “Effects of oxalate on photosynthetic apparatus and

xanthophyll cycle in leaves of cucumber seedlings under high temperature stress," *Sci. Agric. Sin.*, 2005.

[74] Y. C. Du and S. Tachibana, "Effect of supraoptimal root temperature on the growth, root respiration and sugar content of cucumber plants," *Sci. Hortic. (Amsterdam).*, vol. 58, no. 4, pp. 289–301, 1994.

[75] L. Zhou and C. Ye, "Effects of high temperature stress on metabolism of nitrogen and carbohydrates in seedlings of cucumber," *J. Fujian Agric. Univ.*, vol. 28, no. 3, pp. 289–293, 1999.

[76] J. J. Li, J. H. Yu, Y. J. Chang, X. Y. Xu, and S. M. Nei, "Influences of high temperature stress on membrane permeability and activity of cell defence enzymes in leaves of cucumber seedlings," 2007.

[77] M. Lingbo, Q. Zhiwei, and L. Shumin, "Effect of High Temperature Stress on the Root of Cucumber Seeding [J]," *Acta Hortic. Sin.*, vol. 6, 2003.

[78] M. Minmin, L. Quan, C. Beisheng, and C. Xuehao, "Effect of High Temperature on Reproductive Growth and Yield Formation of Cucumis sativus L," *Acta Hortic. Sin.*, vol. 27, no. 6, pp. 412–417, 2000.

[79] P. A. Lund, *Molecular chaperones in the cell*, vol. 37. Oxford University Press, USA, 2001.

[80] D. Whitley, S. P. Goldberg, and W. D. Jordan, "Heat shock proteins: a review of the molecular chaperones," *J. Vasc. Surg.*, vol. 29, no. 4, pp. 748–751, 1999.

[81] N. NS, A. SP, D. Sinha, V. B. Veedin Rajan, V. K. Esthaki, and P. D'Silva, "HSPIR: a manually annotated heat shock protein information resource," *Bioinformatics*, vol. 28, no. 21, pp. 2853–2855, 2012.

[82] E. Maestri, N. Klueva, C. Perrotta, M. Gulli, H. T. Nguyen, and N. Marmiroli, “Molecular genetics of heat tolerance and heat shock proteins in cereals,” *Plant Mol. Biol.*, vol. 48, no. 5–6, pp. 667–681, 2002.

[83] Y. Kim *et al.*, “Effects of sucrose on conformational equilibria and fluctuations within the native-state ensemble of proteins,” *Protein Sci.*, vol. 12, no. 6, pp. 1252–1261, 2003.

[84] R. K. Sairam and A. Tyagi, “Physiology and molecular biology of salinity stress tolerance in plants,” *Curr. Sci.*, pp. 407–421, 2004.

[85] R. R. Kumar *et al.*, “Differential expression of heat shock protein and alteration in osmolyte accumulation under heat stress in wheat,” *J. plant Biochem. Biotechnol.*, vol. 22, no. 1, pp. 16–26, 2013.

[86] V. V Kuznetsov, V. Y. U. Rakitin, and V. N. Zholkevich, “Effects of preliminary heat-shock treatment on accumulation of osmolytes and drought resistance in cotton plants during water deficiency,” *Physiol. Plant.*, vol. 107, no. 4, pp. 399–406, 1999.

[87] A. K. Parida and A. B. Das, “Salt tolerance and salinity effects on plants: a review,” *Ecotoxicol. Environ. Saf.*, vol. 60, no. 3, pp. 324–349, 2005.

[88] E. V Maas, “Salt tolerance of plants,” *Appl. Agric. Res.*, vol. 1, no. 1, pp. 12–25, 1986.

[89] E. V Maas and G. J. Hoffman, “Crop salt tolerance–current assessment,” *J. Irrig. Drain. Div.*, vol. 103, no. 2, pp. 115–134, 1977.

[90] M. A. Khan and D. J. Weber, *Ecophysiology of high salinity tolerant plants*, vol. 40. Springer Science & Business Media, 2006.

[91] G. Colla, Y. Rouphael, M. Cardarelli, and E. Rea, “Effect of salinity on yield, fruit quality, leaf gas exchange, and mineral composition of grafted watermelon plants,” *HortScience*, vol. 41, no. 3, pp. 622–627, 2006, doi: 10.21273/hortsci.41.3.622.

[92] J. Cuartero and R. Fernández-Muñoz, “Tomato and salinity,” *Sci. Hortic. (Amsterdam).*, vol. 78, no. 1–4, pp. 83–125, 1998.

[93] A. Bybordi, “The influence of salt stress on seed germination, growth and yield of canola cultivars,” *Not. Bot. Horti Agrobot. Cluj-Napoca*, vol. 38, no. 1, pp. 128–133, 2010.

[94] K. Nahar and M. Hasanuzzaman, “Germination, growth, nodulation and yield performance of three mungbean varieties under different levels of salinity stress,” *Green Farming*, vol. 2, no. 12, pp. 825–829, 2009.

[95] Z. Khodarahmpour, M. Ifar, and M. Motamedi, “Effects of NaCl salinity on maize (Zea mays L.) at germination and early seedling stage,” *African J. Biotechnol.*, vol. 11, no. 2, pp. 298–304, 2012.

[96] A. Dolatabadian, S. A. M. M. SANAVY, and F. Ghanati, “Effect of salinity on growth, xylem structure and anatomical characteristics of soybean,” *Not. Sci. Biol.*, vol. 3, no. 1, pp. 41–45, 2011.

[97] A. Läuchli, “Responses and adaptations of crops to salinity,” in *Symposium on Tomato Production on Arid Land 190*, 1984, pp. 243–246.

[98] H. Marschner, “Mineral nutrition of higher plants. 2nd,” *Edn. Acad. Pres*, 1995.

[99] R. Munns and A. Termaat, “Whole-plant responses to salinity,” *Funct. Plant Biol.*, vol. 13, no. 1, pp. 143–160, 1986.

[100] S. R. Grattan and C. M. Grieve, “Mineral nutrient acquisition and response by plants grown in saline environments,” *Handb. plant Crop Stress*, vol. 2, pp. 203–229, 1999.

[101] L. P. Lapina and B. A. Popov, “The effect of sodium chloride on the photosynthetic apparatus of tomatoes.,” *Fiziol. Rastenii*, vol. 17, pp. 580–584, 1970.

[102] A. M. Hamada and A. E. El-Enany, “Effect of NaCl salinity on growth, pigment and

mineral element contents, and gas exchange of broad bean and pea plants," *Biol. Plant.*, vol. 36, no. 1, pp. 75–81, 1994.

[103] G. Demetriou, C. Neonaki, E. Navakoudis, and K. Kotzabasis, "Salt stress impact on the molecular structure and function of the photosynthetic apparatus—the protective role of polyamines," *Biochim. Biophys. Acta (BBA)-Bioenergetics*, vol. 1767, no. 4, pp. 272–280, 2007.

[104] P. M. Hasegawa, R. A. Bressan, J.-K. Zhu, and H. J. Bohnert, "Plant cellular and molecular responses to high salinity," *Annu. Rev. Plant Biol.*, vol. 51, no. 1, pp. 463–499, 2000.

[105] R. Munns, "Comparative physiology of salt and water stress," *Plant. Cell Environ.*, vol. 25, no. 2, pp. 239–250, 2002.

[106] M. Ashraf and M. Shahbaz, "Assessment of genotypic variation in salt tolerance of early CIMMYT hexaploid wheat germplasm using photosynthetic capacity and water relations as selection criteria," *Photosynthetica*, vol. 41, no. 2, pp. 273–280, 2003.

[107] M. Ashraf and P. J. C. Harris, "Potential biochemical indicators of salinity tolerance in plants," *Plant Sci.*, vol. 166, no. 1, pp. 3–16, 2004.

[108] E. Marrè and O. Ciferri, "Regulation of cell membrane activities in plants," in *International Workshop on the Regulation of Cell Membrane Activities in Plants (1976: Istituto italiano di idrobiologia)*, 1977.

[109] M. Briens and F. Larher, "Osmoregulation in halophytic higher plants: a comparative study of soluble carbohydrates, polyols, betaines and free proline," *Plant. Cell Environ.*, vol. 5, no. 4, pp. 287–292, 1982.

[110] D. Rhodes and A. D. Hanson, "Quaternary ammonium and tertiary sulfonium compounds

in higher plants," *Annu. Rev. Plant Biol.*, vol. 44, no. 1, pp. 357–384, 1993.

[111] A. D. Hanson, B. Rathinasabapathi, B. Chamberlin, and D. A. Gage, "Comparative physiological evidence that β-alanine betaine and choline-O-sulfate act as compatible osmolytes in halophytic Limonium species," *Plant Physiol.*, vol. 97, no. 3, pp. 1199–1205, 1991.

[112] A. D. Hanson, B. Rathinasabapathi, J. Rivoal, M. Burnet, M. O. Dillon, and D. A. Gage, "Osmoprotective compounds in the Plumbaginaceae: a natural experiment in metabolic engineering of stress tolerance," *Proc. Natl. Acad. Sci.*, vol. 91, no. 1, pp. 306–310, 1994.

[113] J. Peñuelas *et al.*, "Evidence of current impact of climate change on life: a walk from genes to the biosphere," *Glob. Chang. Biol.*, vol. 19, no. 8, pp. 2303–2338, 2013.

[114] M. Ashraf and M. R. Foolad, "Roles of glycine betaine and proline in improving plant abiotic stress resistance," *Environ. Exp. Bot.*, vol. 59, no. 2, pp. 206–216, 2007.

[115] A. K. Parida, A. B. Das, and P. Mohanty, "Investigations on the antioxidative defence responses to NaCl stress in a mangrove, Bruguiera parviflora: differential regulations of isoforms of some antioxidative enzymes," *Plant Growth Regul.*, vol. 42, no. 3, pp. 213–226, 2004.

[116] P. Saha, P. Chatterjee, and A. K. Biswas, "NaCl pretreatment alleviates salt stress by enhancement of antioxidant defense system and osmolyte accumulation in mungbean (Vigna radiata L. Wilczek)," 2010.

[117] M. R. Amirjani, "Pigments and Enzyme Activity of Rice," *Int. J. Bot.*, vol. 7, no. 1, pp. 73–81, 2011.

[118] E. A. N. Greenwood, "Nitrogen stress in plants," in *Advances in Agronomy*, vol. 28, Elsevier, 1976, pp. 1–35.

[119] R. K. Pandey, J. W. Maranville, and A. Admou, “Deficit irrigation and nitrogen effects on maize in a Sahelian environment: I. Grain yield and yield components,” *Agric. water Manag.*, vol. 46, no. 1, pp. 1–13, 2000.

[120] Y. A. I. Kirrilov and V. D. Pavlov, “Effect of fertilizer on yield and protein contents in wheat grain,” *Agrochimiya*, vol. 1, pp. 49–51, 1989.

[121] W. W. Wilhelm, “Dry-matter partitioning and leaf area of winter wheat grown in a long-term fallow tillage comparisons in the US Central Great Plains,” *Soil Tillage Res.*, vol. 49, no. 1–2, pp. 49–56, 1998.

[122] V. P. N. Singh, S. K. Uttam, and J. D. Laddin, “Response of wheat cultivars to different N levels under early sown conditions,” *Crop Res*, vol. 5, pp. 82–86, 1992.

[123] G. R. dos Santos *et al.*, “Effect of nitrogen doses on disease severity and watermelon yield,” *Hortic. Bras.*, vol. 27, no. 3, pp. 330–334, 2009.

[124] M. A. Nawaz *et al.*, “Genome-wide expression profiling of leaves and roots of watermelon in response to low nitrogen,” *BMC Genomics*, vol. 19, no. 1, p. 456, 2018.

[125] M. A. Nawaz *et al.*, “Pumpkin rootstock improves nitrogen use efficiency of watermelon scion by enhancing nutrient uptake, cytokinin content, and expression of nitrate reductase genes,” *Plant Growth Regul.*, vol. 82, no. 2, pp. 233–246, 2017.

[126] P. J. Lea and R. A. de Azevedo, “Nitrogen use efficiency. 1. Uptake of nitrogen from the soil,” *Ann. Appl. Biol.*, vol. 149, no. 3, pp. 243–247, 2006.

[127] B. G. Forde and P. J. Lea, “Glutamate in plants: metabolism, regulation, and signalling,” *J. Exp. Bot.*, vol. 58, no. 9, pp. 2339–2358, 2007.

[128] J. Luo, H. Li, T. Liu, A. Polle, C. Peng, and Z.-B. Luo, “Nitrogen metabolism of two contrasting poplar species during acclimation to limiting nitrogen availability,” *J. Exp.*

Bot., vol. 64, no. 14, pp. 4207–4224, 2013.

[129] B. Hirel, J. Le Gouis, B. Ney, and A. Gallais, “The challenge of improving nitrogen use efficiency in crop plants: towards a more central role for genetic variability and quantitative genetics within integrated approaches,” *J. Exp. Bot.*, vol. 58, no. 9, pp. 2369–2387, 2007.

[130] M. Tabuchi, T. Abiko, and T. Yamaya, “Assimilation of ammonium ions and reutilization of nitrogen in rice (Oryza sativa L.),” *J. Exp. Bot.*, vol. 58, no. 9, pp. 2319–2327, 2007.

[131] P. J. Lea, L. Sodek, M. A. J. Parry, P. R. Shewry, and N. G. Halford, “Asparagine in plants,” *Ann. Appl. Biol.*, vol. 150, no. 1, pp. 1–26, Feb. 2007, doi: 10.1111/j.1744-7348.2006.00104.x.

[132] P. J. Lea and R. A. Azevedo, “Nitrogen use efficiency. 2. Amino acid metabolism,” *Ann. Appl. Biol.*, vol. 151, no. 3, pp. 269–275, 2007.

[133] K. Akashi, C. Miyake, and A. Yokota, “Citrulline, a novel compatible solute in drought-tolerant wild watermelon leaves, is an efficient hydroxyl radical scavenger,” *FEBS Lett.*, vol. 508, no. 3, pp. 438–442, 2001, doi: 10.1016/S0014-5793(01)03123-4.

[134] S. Kawasaki, C. Miyake, T. Kohchi, S. Fujii, M. Uchida, and A. Yokota, “Responses of Wild Watermelon to Drought Stress: Accumulation of an ArgE Homologue and Citrulline in Leaves during Water Deficits,” *Plant Cell Physiol.*, vol. 41, no. 7, pp. 864–873, Jul. 2000, doi: 10.1093/pcp/pcd005.

[135] S. Kusvuran, H. Y. Dasgan, and K. Abak, “Citrulline is an important biochemical indicator in tolerance to saline and drought stresses in melon,” *Sci. World J.*, vol. 2013, 2013.

[136] R. Garg *et al.*, “Transcriptome analyses reveal genotype- and developmental stage-

specific molecular responses to drought and salinity stresses in chickpea," *Sci. Rep.*, vol. 6, no. September 2015, pp. 1–15, 2016, doi: 10.1038/srep19228.

[137] R. Minocha, R. Majumdar, and S. C. Minocha, "Polyamines and abiotic stress in plants: a complex relationship1," *Front. Plant Sci.*, vol. 5, p. 175, 2014.

[138] E. Planchet and W. M. Kaiser, "Nitric oxide production in plants: facts and fictions," *Plant Signal. Behav.*, vol. 1, no. 2, pp. 46–51, 2006.

[139] C. M. Pérez Delgado de Torres, M. García Calderón, A. J. Márquez Cabeza, and M. Betti, "Reassimilation of photorespiratory ammonium in Lotus japonicus plants deficient in plastidic glutamine synthetase," *Plos One, 10 (6), e0130438-1-e0130438-20.*, 2015.

[140] D. Igarashi, H. Tsuchida, M. Miyao, and C. Ohsumi, "Glutamate: glyoxylate aminotransferase modulates amino acid content during photorespiration," *Plant Physiol.*, vol. 142, no. 3, pp. 901–910, 2006.

[141] F. Potel *et al.*, "Assimilation of excess ammonium into amino acids and nitrogen translocation in Arabidopsis thaliana–roles of glutamate synthases and carbamoylphosphate synthetase in leaves," *FEBS J.*, vol. 276, no. 15, pp. 4061–4076, 2009.

[142] R. A. Ludwig, "Arabidopsis chloroplasts dissimilate L-arginine and L-citrulline for use as N source," *Plant Physiol.*, vol. 101, no. 2, pp. 429–434, 1993.

[143] R. Kasting and C. C. Delwiche, "Ornithine, Citrulline, and Arginine Metabolism in Watermelon Seedlings.," *Plant Physiol.*, vol. 33, no. 5, p. 350, 1958.

[144] D. E. Mitchell, M. V. Gadus, and M. A. Madore, "Patterns of assimilate production and translocation in muskmelon (Cucumis melo L.): I. Diurnal patterns," *Plant Physiol.*, vol. 99, no. 3, pp. 959–965, 1992, doi: 10.1104/pp.99.3.959.

[145] Q. Kong *et al.*, “Evaluation of appropriate reference genes for gene expression normalization during watermelon fruit development,” *PLoS One*, vol. 10, no. 6, 2015.

[146] M. K. Bartlett *et al.*, “Rapid determination of comparative drought tolerance traits: Using an osmometer to predict turgor loss point,” *Methods Ecol. Evol.*, vol. 3, no. 5, pp. 880–888, 2012, doi: 10.1111/j.2041-210X.2012.00230.x.

[147] G. Sakthivelu *et al.*, “Drought-induced alterations in growth, osmotic potential and in vitro regeneration of soybean cultivars,” *Gen. Appl. Plant Physiol.*, vol. 34, no. 1–2, pp. 103–112, 2008.

[148] A. Patakas, N. Nikolaou, E. Zioziou, K. Radoglou, and B. Noitsakis, “The role of organic solute and ion accumulation in osmotic adjustment in drought-stressed grapevines,” *Plant Sci.*, vol. 163, no. 2, pp. 361–367, 2002.

[149] J. Galmés, A. Abadía, H. Medrano, and J. Flexas, “Photosynthesis and photoprotection responses to water stress in the wild-extinct plant Lysimachia minoricensis,” *Environ. Exp. Bot.*, vol. 60, no. 3, pp. 308–317, Jul. 2007, doi: 10.1016/J.ENVEXPBOT.2006.12.016.

[150] C. Signarbieux and U. Feller, “Non-stomatal limitations of photosynthesis in grassland species under artificial drought in the field,” *Environ. Exp. Bot.*, vol. 71, no. 2, pp. 192–197, 2011.

[151] J. M. Escalona, J. Flexas, and H. Medrano, “Stomatal and non-stomatal limitations of photosynthesis under water stress in field-grown grapevines,” *Funct. Plant Biol.*, vol. 27, no. 1, p. 87, 2000.

[152] M. R. B. Siddique, A. Hamid, and M. S. Islam, “Drought stress effects on photosynthetic rate and leaf gas exchange of wheat,” *Bot. Bull. Acad. Sin.*, vol. 40, 1999.

[153] B. Sarabi *et al.*, “Stomatal and non-stomatal limitations are responsible in down-regulation of photosynthesis in melon plants grown under the saline condition: Application of carbon isotope discrimination as a reliable proxy,” *Plant Physiol. Biochem.*, vol. 141, pp. 1–19, 2019.

[154] T. Brodribb, “Dynamics of changing intercellular CO2 concentration (ci) during drought and determination of minimum functional Ci,” *Plant Physiol.*, vol. 111, no. 1, pp. 179–185, 1996, doi: 10.1104/pp.111.1.179.

[155] M. C. Dias and W. Brüggemann, “Limitations of photosynthesis in Phaseolus vulgaris under drought stress: gas exchange, chlorophyll fluorescence and Calvin cycle enzymes,” *Photosynthetica*, vol. 48, no. 1, pp. 96–102, Mar. 2010, doi: 10.1007/s11099-010-0013-8.

[156] M. J. CORREIA, M. M. C. CHAVES, and J. S. PEREIRA, “Afternoon Depression In Photosynthesis in Grapevine Leaves—Evidence for a High Light Stress Effect,” *J. Exp. Bot.*, vol. 41, no. 4, pp. 417–426, Apr. 1990, doi: 10.1093/jxb/41.4.417.

[157] A. K. Sinha, P. A. Shirke, U. Pathre, and P. V Sane, “Midday depression in photosynthesis: Effect on sucrose-phosphate synthase and ribulose-1,5-bisphosphate carboxylase in leaves of Prosopis juliflora (Swartz) DC,” *Photosynthetica*, vol. 34, no. 1, pp. 115–124, 1998, doi: 10.1023/A:1006872003291.

[158] O. . Ommen, A. Donnelly, S. Vanhoutvin, M. van Oijen, and R. Manderscheid, “Chlorophyll content of spring wheat flag leaves grown under elevated CO2 concentrations and other environmental stresses within the ‘ESPACE-wheat’ project,” *Eur. J. Agron.*, vol. 10, no. 3–4, pp. 197–203, Apr. 1999, doi: 10.1016/S1161-0301(99)00011-8.

[159] N. Sionit, H. Hellmers, and B. R. Strain, “Growth and Yield of Wheat under CO2

Enrichment and Water Stress1," *Crop Sci.*, vol. 20, pp. 687–690, 1980, doi: 10.2135/cropsci1980.0011183X002000060003x.

[160] P. Manivannan *et al.*, "Growth, biochemical modifications and proline metabolism in Helianthus annuus L. as induced by drought stress," *Colloids Surfaces B Biointerfaces*, vol. 59, no. 2, pp. 141–149, Oct. 2007, doi: 10.1016/J.COLSURFB.2007.05.002.

[161] N. SMIRNOFF, "The role of active oxygen in the response of plants to water deficit and desiccation," *New Phytol.*, vol. 125, no. 1, pp. 27–58, Sep. 1993, doi: 10.1111/j.1469-8137.1993.tb03863.x.

[162] C. H. FOYER, P. DESCOURVIÈRES, and K. J. KUNERT, "Protection against oxygen radicals: an important defence mechanism studied in transgenic plants," *Plant. Cell Environ.*, vol. 17, no. 5, pp. 507–523, May 1994, doi: 10.1111/j.1365-3040.1994.tb00146.x.

[163] G. Noctor and C. H. Foyer, "ASCORBATE AND GLUTATHIONE: Keeping Active Oxygen Under Control," *Annu. Rev. Plant Physiol. Plant Mol. Biol.*, vol. 49, no. 1, pp. 249–279, Jun. 1998, doi: 10.1146/annurev.arplant.49.1.249.

[164] K. Asada, "THE WATER-WATER CYCLE IN CHLOROPLASTS: Scavenging of Active Oxygens and Dissipation of Excess Photons," *Annu. Rev. Plant Physiol. Plant Mol. Biol.*, vol. 50, no. 1, pp. 601–639, Jun. 1999, doi: 10.1146/annurev.arplant.50.1.601.

[165] D. G. Routley, "Proline Accumulation in Wilted Ladino Clover Leaves1," *Crop Sci.*, vol. 6, pp. 358–361, 1966, doi: 10.2135/cropsci1966.0011183X000600040019x.

[166] Z. Wang, H. Hu, L. R. Goertzen, J. S. McElroy, and F. Dane, "Analysis of the Citrullus colocynthis transcriptome during water deficit stress," *PLoS One*, vol. 9, no. 8, 2014.

[167] L. Rizhsky, H. Liang, J. Shuman, V. Shulaev, S. Davletova, and R. Mittler, "When

defense pathways collide. The response of Arabidopsis to a combination of drought and heat stress," *Plant Physiol.*, vol. 134, no. 4, pp. 1683–1696, 2004.

[168] M. B. Herrera-Rodríguez, R. Pérez-Vicente, and J. M. Maldonado, "Expression of asparagine synthetase genes in sunflower (Helianthus annuus) under various environmental stresses," *Plant Physiol. Biochem.*, vol. 45, no. 1, pp. 33–38, 2007, doi: 10.1016/j.plaphy.2006.12.002.

[169] R. Jin, Y. Wang, R. Liu, J. Gou, and Z. Chan, "Physiological and metabolic changes of purslane (Portulaca oleracea L.) in response to drought, heat, and combined stresses," *Front. Plant Sci.*, vol. 6, no. JAN2016, 2016, doi: 10.3389/fpls.2015.01123.

[170] G. Bongi and F. Loreto, "Gas-Exchange Properties of Salt-Stressed Olive (Olea europea L.) Leaves," *Plant Physiol.*, vol. 90, no. 4, pp. 1408 LP – 1416, Aug. 1989, doi: 10.1104/pp.90.4.1408.

[171] R. Belkhodja, F. Morales, A. Abadia, J. Gomez-Aparisi, and J. Abadia, "Chlorophyll Fluorescence as a Possible Tool for Salinity Tolerance Screening in Barley (Hordeum vulgare L.)," *Plant Physiol.*, vol. 104, no. 2, pp. 667 LP – 673, Feb. 1994, doi: 10.1104/pp.104.2.667.

[172] J. D. Everard, R. Gucci, S. C. Kann, J. A. Flore, and W. H. Loescher, "Gas Exchange and Carbon Partitioning in the Leaves of Celery (Apium graveolens L.) at Various Levels of Root Zone Salinity," *Plant Physiol.*, vol. 106, no. 1, pp. 281 LP – 292, Sep. 1994, doi: 10.1104/pp.106.1.281.

[173] M. Ashraf and P. J. C. Harris, "Potential biochemical indicators of salinity tolerance in plants," *Plant Sci.*, vol. 166, no. 1, pp. 3–16, 2004, doi: 10.1016/j.plantsci.2003.10.024.

[174] Y. Yoshiba, T. Kiyosue, K. Nakashima, K. Yamaguchi-Shinozaki, and K. Shinozaki,

"Regulation of Levels of Proline as an Osmolyte in Plants under Water Stress," *Plant Cell Physiol.*, vol. 38, no. 10, pp. 1095–1102, Jan. 1997, doi: 10.1093/oxfordjournals.pcp.a029093.

[175] H. Y. Dasgan, S. Kusvuran, K. Abak, L. Leport, F. Larher, and A. Bouchereau, "The relationship between citrulline accumulation and salt tolerance during the vegetative growth of melon (Cucumis melo L.)," *Plant, Soil Environ.*, vol. 55, no. 2, pp. 51–57, 2009, doi: 10.17221/316-pse.

[176] M. M. F. Mansour, "Nitrogen Containing Compounds and Adaptation of Plants to Salinity Stress," *Biol. Plant.*, vol. 43, no. 4, pp. 491–500, Dec. 2000, doi: 10.1023/A:1002873531707.

[177] P. J. Lea, L. Sodek, M. A. J. Parry, P. R. Shewry, and N. G. Halford, "Asparagine in plants," *Ann. Appl. Biol.*, vol. 150, no. 1, pp. 1–26, 2007, doi: 10.1111/j.1744-7348.2006.00104.x.

[178] S. Kusvuran, H. Y. Dasgan, N. Sari, and İ. Solmaz, "Citrulline can be used as a Biochemical Marker in Watermelon Screening Studies for Tolerance to Drought and Salinity," no. 2008, pp. 1–6, 2011.

[179] R. G. Wyn Jones, "Salt tolerance. In 'Physiological Processes Limiting Plant Productivity'.(Ed. CB Johnson.) pp. 271–292." Butterworths: Boston, Durban, London, Sydney, Toronto, Wellington, 1981.

[180] A. S. Rudolph, J. H. Crowe, and L. M. Crowe, "Effects of three stabilizing agents—proline, betaine, and trehalose—on membrane phospholipids," *Arch. Biochem. Biophys.*, vol. 245, no. 1, pp. 134–143, 1986.

[181] M. M. F. Mansour, "Protection of plasma membrane of onion epidermal cells by

glycinebetaine and proline against NaCl stress," *Plant Physiol. Biochem.*, vol. 36, no. 10, pp. 767–772, 1998.

[182] L. Taiz and E. Zeiger, "Plant Physiology (Sinauer, Sunderland, MA)." 2006.

[183] Z. Wang, M. Gerstein, and M. Snyder, "RNA-Seq: a revolutionary tool for transcriptomics," *Nat. Rev. Genet.*, vol. 10, no. 1, pp. 57–63, 2009.

[184] C. Trapnell *et al.*, "Differential gene and transcript expression analysis of RNA-seq experiments with TopHat and Cufflinks," *Nat. Protoc.*, vol. 7, no. 3, pp. 562–578, 2012, doi: 10.1038/nprot.2012.016.

[185] C. Trapnell, L. Pachter, and S. L. Salzberg, "TopHat: Discovering splice junctions with RNA-Seq," *Bioinformatics*, vol. 25, no. 9, pp. 1105–1111, 2009, doi: 10.1093/bioinformatics/btp120.

[186] S. Anders, P. T. Pyl, and W. Huber, "HTSeq—a Python framework to work with high-throughput sequencing data," *Bioinformatics*, vol. 31, no. 2, pp. 166–169, 2015.

[187] M. Love, S. Anders, and W. Huber, "Differential analysis of count data–the DESeq2 package," *Genome Biol*, vol. 15, no. 550, pp. 10–1186, 2014.

[188] H. Li *et al.*, "Transcriptomic and physiological analyses reveal drought adaptation strategies in drought-tolerant and-susceptible watermelon genotypes," *Plant Sci.*, vol. 278, pp. 32–43, 2019.

[189] Y. Yang *et al.*, "Transcriptome profiling of watermelon root in response to short-term osmotic stress," *PLoS One*, vol. 11, no. 11, 2016.

[190] Y. C. Altunoglu, M. C. Baloglu, P. Baloglu, E. N. Yer, and S. Kara, "Genome-wide identification and comparative expression analysis of LEA genes in watermelon and melon genomes," *Physiol. Mol. Biol. plants*, vol. 23, no. 1, pp. 5–21, 2017.

[191] J.-B. Chen, F.-R. Zhang, D.-F. Huang, L.-D. Zhang, and Y.-D. Zhang, “Transcriptome analysis of transcription factors in two melon (Cucumis melo L.) cultivars under salt stress,” *Plant Physiol. J.*, vol. 50, no. 2, pp. 150–158, 2014.

[192] L. M. Wang, L. D. Zhang, J. B. Chen, D. F. Huang, and Y. D. Zhang, “Physiological analysis and transcriptome comparison of two muskmelon (Cucumis melo L.) cultivars in response to salt stress,” *Genet. Mol. Res*, vol. 15, pp. 1–18, 2016.

[193] C. Trapnell *et al.*, “Transcript assembly and quantification by RNA-Seq reveals unannotated transcripts and isoform switching during cell differentiation,” *Nat. Biotechnol.*, vol. 28, no. 5, pp. 511–515, 2010, doi: 10.1038/nbt.1621.

[194] N. Sreenivasulu and U. Wobus, “Seed-development programs: a systems biology–based comparison between dicots and monocots,” *Annu. Rev. Plant Biol.*, vol. 64, 2013.

[195] R. Angelovici, A. Fait, A. R. Fernie, and G. Galili, “A seed high-lysine trait is negatively associated with the TCA cycle and slows down Arabidopsis seed germination,” *New Phytol.*, vol. 189, no. 1, pp. 148–159, 2011.

[196] X. Zhu, G. Tang, F. Granier, D. Bouchez, and G. Galili, “A T-DNA insertion knockout of the bifunctional lysine-ketoglutarate reductase/saccharopine dehydrogenase gene elevates lysine levels in Arabidopsis seeds,” *Plant Physiol.*, vol. 126, no. 4, pp. 1539–1545, 2001.

[197] G. Galili and R. Höfgen, “Metabolic engineering of amino acids and storage proteins in plants,” *Metab. Eng.*, vol. 4, no. 1, pp. 3–11, 2002.

[198] J. F. A. H. E. Committee, *Energy and protein requirements*. FAO/WHO, 1973.

[199] T. A. El-Adawy and K. M. Taha, “Characteristics and composition of different seed oils and flours,” *Food Chem.*, vol. 74, no. 1, pp. 47–54, Jul. 2001, doi: 10.1016/S0308-8146(00)00337-X.

[200] P. Kaul, “Nutritional potential, bioaccessibility of minerals and functionality of watermelon (Citrullus vulgaris) seeds,” *LWT-Food Sci. Technol.*, vol. 44, no. 8, pp. 1821–1826, 2011.

[201] A. A. Wani, D. S. Sogi, P. Singh, I. A. Wani, and U. S. Shivhare, “Characterisation and functional properties of watermelon (Citrullus lanatus) seed proteins,” *J. Sci. Food Agric.*, vol. 91, no. 1, pp. 113–121, 2011.

[202] M. L. S. de Melo, N. Narain, and P. S. Bora, “Characterisation of some nutritional constituents of melon (Cucumis melo hybrid AF-522) seeds,” *Food Chem.*, vol. 68, no. 4, pp. 411–414, Mar. 2000, doi: 10.1016/S0308-8146(99)00209-5.

[203] A. A. Wani, D. Kaur, I. Ahmed, and D. S. Sogi, “Extraction optimization of watermelon seed protein using response surface methodology,” *LWT - Food Sci. Technol.*, vol. 41, no. 8, pp. 1514–1520, Nov. 2008, doi: 10.1016/J.LWT.2007.10.001.

[204] D. S. Galitz, “Uptake and assimilation of nitrogen by plants,” 1979.

[205] T. J. Jacks, T. P. Hensarling, and L. Y. Yatsu, “Cucurbit seeds: I. Characterizations and uses of oils and proteins. A review,” *Econ. Bot.*, vol. 26, no. 2, pp. 135–141, Apr. 1972, doi: 10.1007/BF02860774.

[206] M. M. Ige, A. O. Ogunsua, and O. L. Oke, “Functional properties of the proteins of some Nigerian oilseeds: conophor seeds and three varieties of melon seeds,” *J. Agric. Food Chem.*, vol. 32, no. 4, pp. 822–825, Jul. 1984, doi: 10.1021/jf00124a031.

[207] V. Joshi *et al.*, “Haplotype networking of GWAS hits for citrulline variation associated with the domestication of watermelon,” *Int. J. Mol. Sci.*, vol. 20, no. 21, pp. 1–15, 2019, doi: 10.3390/ijms20215392.

[208] B. Tabiri, “Watermelon Seeds as Food: Nutrient Composition, Phytochemicals and

Antioxidant Activity," *Int. J. Nutr. Food Sci.*, vol. 5, no. 2, p. 139, 2016, doi: 10.11648/j.ijnfs.20160502.18.

APPENDIX A

Table 9. Information of primers designed for genes associated with citrulline metabolism pathway.

Gene Name	Gene ID	Forward Primer	Reverse Primer
Actin	ClCG02G000680	CCATGTATGTTGCCATCCAG	GGATAGCATGGGGTAGAGCA
α-tubulin5	ClCG02G024360	GATGGTATGATGCCCAGTGA	CCGGTAGGCTCCAGTTCTAA
N-acetylornithine Aminotransferase (AAT)	ClCG09G003180	CTC GAA GGG CGA GAG TAT TTA G	GTA TTC GCC TGC TCT GTT ACT
N-acetylornithine deacetylase (AOD2)	ClCG09G012030	TTG TCT CCT TCG TTG GAA GTC	GTC CCA CGA CCT CTT AGT TTA TC
N-acetylornithine deacetylase (AOD3)	ClCG09G012020	AGG GAG TTT GCC GGT TAT TC	CAT TCT GGG CAT GGT ATG TAT CT
Arginine decarboxylase (ArgD)	ClCG11G003830	GGT GGT CTG GGT ATT GAC TAT G	ACA GCG GAC TGC ATT AAC A
Arginosuccinate lyase (ASL1)	ClCG08G011660	GAT GAG ATC GAG AGG CGT ATT C	GCT CGC CAA TCA AAT CAG TAA G
Argininosuccinate lyase (ASL2)	ClCG11G014580	CGT TCC GGG CTA TAC ACA TTT A	GAC AAA CGA CCA GCA TCT CT
Argininosuccinate lyase (ASL1)	ClCG08G011660	GAT GAG ATC GAG AGG CGT ATT C	GCT CGC CAA TCA AAT CAG TAA G
Arginosuccinate synthase (ASS1)	ClCG06G017780	CAG GAG GAA CCA TCC TAT TCA C	ACA CCA GCT CGG CAT ATT T
Carbamoyl phosphate synthase (CPS1)	ClCG11G013120	GGG TAC AGT TCA GAG ACC TTT C	CTG ATG CAG CCC ATG TAG AA
Carbamoyl phosphate synthase (CPS2)	ClCG09G021680	ATT TGA GGA GGA TGG CTC TTG	CTC GCC TTC AGG CTC TTT ATT
Ornithine carbamoyl transferase (OTC)	ClCG05G018820	CTA CCT ACG GGT CGT CAT ACT A	TGT AAT CCG TCA GGC CAT TTA T
Ornithine decarboxylase (ODC)	ClCG08G013990	TTC CGG CAA ACC CAA AGA	GAG GAG GCC ATG TTG AGA AA
Ornithine cyclodeaminase (OCD)	ClCG05G008460	GGC ACT GCC TTG ACT CTT TA	CAC CAT AAC CAT GAC CCT ACT ATC

Table 10. Information of DEGs in response to drought stress

Regulation	Gene Name	Gene ID	Chromosome	Strand	gene_start	gene_end	Gene length	Description	log2FoldChange	pvalue
Up	N-acetylornithine deacetylase	ClCG09G012030	CG_Chr09	+	13134974	13140976	1313	Acetylornithine deacetylase, putative	7.4424	1.95E-33
Up	Carbamoyl phosphate synthase, large subunit	ClCG09G021680	CG_Chr09	+	38651143	38656426	3935	Carbamoyl-phosphate synthase large chain	1.8449	7.22E-10
Up	N-acetylornithine deacetylase	ClCG09G012020	CG_Chr09	+	13094295	13098888	1689	Acetylornithine deacetylase, putative	1.1365	0.00061122
Up	Nitric-oxide synthase, putative	ClCG01G004960	CG_Chr01	+	5240548	5248670	1938	Nitric-oxide synthase, putative	0.81193	0.0052014
Up	N-acetylornithine aminotransferase	ClCG09G003180	CG_Chr09	+	2753768	2756078	1815	Acetylornithine aminotransferase, putative	0.78922	0.0097721
Up	Ornithine δ-aminotransferase	ClCG03G006680	CG_Chr03	-	7492010	7499334	2005	Ornithine aminotransferase, putative	0.70555	0.0024195
Up	Arginine decarboxylase	ClCG11G003830	CG_Chr11	+	4073782	4075935	2154	Arginine decarboxylase	0.62965	0.0056197
Down	Argininosuccinate synthase	ClCG06G017780	CG_Chr06	-	30873887	30876957	1827	Argininosuccinate synthase	-1.5812	0.0033967
Down	Pyrroline-5-carboxylate synthase	ClCG11G006600	CG_Chr11	+	7251774	7259871	3017	Gamma-glutamyl phosphate reductase	-1.6746	0.00031253
Down	Ornithine cyclodeaminase	ClCG05G008460	CG_Chr05	+	9117244	9118886	1381	Ornithine cyclodeaminase/mu-crystallin family protein, putative, expressed	-1.9315	0.00085113
Down	Argininosuccinate synthase	ClCG03G003670	CG_Chr03	-	4036767	4040520	1835	Argininosuccinate synthase, putative	-2.2531	4.74E-11
Down	Ornithine decarboxylase	ClCG08G013990	CG_Chr08	+	26828171	26829454	1284	Ornithine decarboxylase	-2.4865	0.0075579

Table 11. Information of DEGs in response to salt stress

Regulation	Gene Name	Gene ID	Chromosome	Strand	gene_start	gene_end	Gene length	Description	log2FoldChange	pvalue
Up	N-acetylornithine deacetylase	ClCG09G012030	CG_Chr09	+	13134974	13140976	1313	Acetylornithine deacetylase, putative	4.1885	1.19E-08
Up	Argininosuccinate synthase	ClCG06G017780	CG_Chr06	-	30873887	30876957	1827	Argininosuccinate synthase	3.523	4.99E-11
Up	Ornithine decarboxylase	ClCG08G013990	CG_Chr08	+	26828171	26829454	1284	Ornithine decarboxylase	1.5285	0.019256
Up	Ornithine cyclodeaminase	ClCG05G008460	CG_Chr05	+	9117244	9118886	1381	Ornithine cyclodeaminase/mu-crystallin family protein, putative, expressed	1.3767	0.0038898
Up	N-acetyl-γ-glutamyl-Preductase	ClCG09G017590	CG_Chr09	+	34490303	34496002	1641	N-acetyl-gamma-glutamyl-phosphate reductase	1.2117	0.0053694
Up	P5C dehydrogenase	ClCG01G014440	CG_Chr01	-	28755860	28761222	2103	Methylmalonate semialdehyde dehydrogenase [acylating], putative	0.93856	0.0049511
Down	N-acetyl Glu synthase	ClCG01G017650	CG_Chr01	-	32158551	32164711	2712	Amino acid acetyltransferase, putative, expressed	-1.0866	0.00093878
Down	N-acetylglutamate Kinase	ClCG08G012830	CG_Chr08	+	25713606	25714655	1050	Acetylglutamate kinase-like protein	-1.1651	0.00012922
Down	P-II	ClCG09G004810	CG_Chr09	+	4254114	4257387	1172	Nitrogen regulatory protein P-II	-1.1848	0.00051207
Down	N-acetylornithine deacetylase	ClCG09G012020	CG_Chr09	+	13094295	13098888	1689	Acetylornithine deacetylase, putative	-1.3756	0.0000166
Down	N-acetylornithineglutamate acetyltransferase	ClCG10G020940	CG_Chr10	-	35721951	35726221	1629	Arginine biosynthesis bifunctional protein ArgJ	-1.44	0.0000441
Down	Urease	ClCG11G013850	CG_Chr11	+	27054415	27080559	5349	Urease subunit alpha	-1.5965	0.00000652
Down	Ornithine δ-aminotransferase	ClCG03G006680	CG_Chr03	-	7492010	7499334	2005	Ornithine aminotransferase, putative	-1.7134	0.00019705
Down	Pyrroline-5-carboxylate synthase	ClCG11G006600	CG_Chr11	+	7251774	7259871	3017	Gamma-glutamyl phosphate reductase	-2.247	2.62E-14
Down	Carbamoyl phosphate synthase, large subunit	ClCG09G021680	CG_Chr09	+	38651143	38656426	3935	Carbamoyl-phosphate synthase large chain	-2.6234	0.000000439

Table 12. Information of accessions for GWAS

Accession ID	species	Country	Continent
PI 254742 02- S9	C. mucosospermus	Senegal	Africa
PI 249009 02- S9	C. mucosospermus	Nigeria, Kaduna	Africa
PI 184800 02- S9	C. mucosospermus	Nigeria	Africa
PI 494529 03- S9	C. mucosospermus	Nigeria, Oyo	Africa
PI 595203 03- S9	C. mucosospermus	United States, Georgia	North America
PI 560010 02- S9	C. mucosospermus	Nigeria, Ogun	Africa
PI 560005 02- S9	C. mucosospermus	Nigeria, Oyo	Africa
PI 560004 02- S9	C. mucosospermus	Nigeria, Oyo	Africa
PI 560003 02- S9	C. mucosospermus	Nigeria, Oyo	Africa
PI 494531 02- S9	C. mucosospermus	Nigeria, Oyo	Africa
PI 560014 03- S9	C. mucosospermus	Nigeria, Ogun	Africa
PI 560013 03- S9	C. mucosospermus	Nigeria, Ogun	Africa
PI 560011 03- S9	C. mucosospermus	Nigeria, Ogun	Africa
PI 560009 03- S9	C. mucosospermus	Nigeria, Oyo	Africa
PI 560015 03- S9	C. mucosospermus	Nigeria, Oyo	Africa
PI 560012 04- S9	C. mucosospermus	Nigeria, Ogun	Africa
PI 560001 02- S9	C. mucosospermus	Nigeria, Oyo	Africa
PI 532733 01- S9	C. mucosospermus	Democratic Republic of the Congo, Bandundu	Africa

Table 12 Continued

Accession ID	species	Country	Continent
PI 532732 01- S9	C. mucosospermus	Democratic Republic of the Congo, Bandundu	Africa
PI 532730 01- S9	C. mucosospermus	Democratic Republic of the Congo, Bandundu	Africa
PI 532722 01- S9	C. mucosospermus	Democratic Republic of the Congo, Bas-Zaire	Africa
PI 532723 01- S9	C. mucosospermus	Democratic Republic of the Congo, Bas-Zaire	Africa
PI 326516 01- S9	C. mucosospermus	Ghana	Africa
PI 490386 01- S9	C. mucosospermus	Mali	Africa
PI 490384 01- S9	C. mucosospermus	Mali	Africa
PI 490381 01- S9	C. mucosospermus	Mali	Africa
PI 490380 01- S9	C. mucosospermus	Mali	Africa
PI 490379 01- S9	C. mucosospermus	Mali	Africa
PI 490377 01- S9	C. mucosospermus	Mali	Africa
PI 560020 01- S9	C. mucosospermus	Nigeria, Oyo	Africa
PI 560016 01- S9	C. mucosospermus	Nigeria, Oyo	Africa
PI 560008 01- S9	C. mucosospermus	Nigeria, Oyo	Africa
PI 560007 01- S9	C. mucosospermus	Nigeria, Oyo	Africa
PI 560002 01- S9	C. mucosospermus	Nigeria, Oyo	Africa

Table 12 Continued

Accession ID	species	Country	Continent
PI 494528 01- S9	C. mucosospermus	Nigeria, Oyo	Africa
PI 494527 01- S9	C. mucosospermus	Nigeria, Ogun	Africa
PI 457916 01- S9	C. mucosospermus	Liberia	Africa
PI 306782 01- S9	C. mucosospermus	Nigeria	Africa
PI 254743 01- S9	C. mucosospermus	Senegal	Africa
PI 254741 01- S9	C. mucosospermus	Senegal	Africa
PI 254740 01- S9	C. mucosospermus	Senegal	Africa
PI 254737 01- S9	C. mucosospermus	Senegal	Africa
PI 254736 01- S9	C. mucosospermus	Senegal	Africa
PI 254735 01- S9	C. mucosospermus	Senegal	Africa
PI 248178 01- S9	C. mucosospermus	Democratic Republic of the Congo	Africa
PI 247398 01- S9	C. mucosospermus	Greece	Europe
PI 189318 01- S9	C. mucosospermus	Nigeria	Africa
PI 186975 01- S9	C. mucosospermus	Ghana	Africa
PI 186489 01- S9	C. mucosospermus	Nigeria	Africa
PI 164248 01- S9	C. mucosospermus	Liberia	Africa
PI 482248	C. lanatus	Zimbabwe	Africa
PI 482250	C. lanatus	Zimbabwe	Africa

Table 12 Continued

Accession ID	species	Country	Continent
PI 494819	C. lanatus	Zambia	Africa
PI 494821	C. lanatus	Zambia	Africa
PI 500318	C. lanatus	Zambia	Africa
PI 525084	C. lanatus	Egypt	Africa
PI 525089	C. lanatus	Egypt	Africa
PI 525093	C. lanatus	Egypt	Africa
PI 525098	C. lanatus	Egypt	Africa
PI 526238	C. lanatus	Zimbabwe	Africa
PI 535947	C. lanatus	Cameroon	Africa
PI 542115	C. amarus	Botswana	Africa
PI 542120	C. lanatus	Botswana	Africa
PI 559993	C. mucosospermus	Nigeria	Africa
PI 560000	C. mucosospermus	Nigeria	Africa
PI 164247	C. lanatus	Liberia	Africa
PI 164248	C. mucosospermus	Liberia	Africa
PI 271752	C. lanatus	Ghana	Africa
PI 271987	C. lanatus	Somalaia	Africa
PI 306366	C. lanatus	Gabon	Africa
PI 319212	C. lanatus	Egypt	Africa

Table 12 Continued

Accession ID	species	Country	Continent
PI 378611	C. lanatus	Zaire	Africa
PI 378614	C. lanatus	Zaire	Africa
PI 392291	C. lanatus	Kenya	Africa
PI 459074	C. lanatus	Botswana	Africa
PI 482260	C. lanatus	Zimbabwe	Africa
PI 490376	C. lanatus	Mali	Africa
PI 494815	C. lanatus	Zambia	Africa
PI 505590	C. lanatus	Zambia	Africa
PI 500302	C. lanatus	Zambia	Africa
PI 525095	C. lanatus	Egypt	Africa
PI 560024	C. mucosospermus	Nigeria	Africa
PI 535948	C. lanatus	Cameroon	Africa
PI 535947	C. lanatus	Cameroon	Africa
PI 526231	C. lanatus	Zimbabwe	Africa
PI 487476	C. lanatus	Israel	Asia
PI 105445	C. lanatus	Turkey	Europe
PI 113326	C. lanatus	China	Asia
PI 508444	C. lanatus	South Korea	Asia
PI 161373	C. lanatus	South Korea	Asia

Table 12 Continued

Accession ID	species	Country	Continent
PI 508446	C. lanatus	South Korea	Asia
PI 512332	C. lanatus	China	Asia
PI 163202	C. lanatus	India	Asia
PI 163203	C. lanatus	India	Asia
PI 532813	C. lanatus	China	Asia
PI 534530	C. lanatus	Syria	Asia
PI 534534	C. lanatus	Syria	Asia
PI 534586	C. lanatus	Syria	Asia
PI 534590	C. lanatus	Syria	Asia
PI 534598	C. lanatus	Syria	Asia
PI 536446	C. lanatus	Maldives	Asia
PI 536451	C. lanatus	Maldives	Asia
PI 536453	C. lanatus	Maldives	Asia
PI 537265	C. lanatus	Pakistan	Asia
PI 537299	C. lanatus	Uzbekistan	Asia
PI 593389	C. lanatus	China	Asia
Grif 1729	C. lanatus	China	Asia
PI 164708	C. lanatus	India	Asia
PI 164737	C. lanatus	India	Asia

Table 12 Continued

Accession ID	species	Country	Continent
PI 164977	C. lanatus	Turkey	Europe
PI 165024	C. lanatus	Turkey	Europe
PI 169251	C. lanatus	Turkey	Europe
PI 169253	C. lanatus	Turkey	Europe
Grif 1730	C. lanatus	China	Asia
PI 172793	C. lanatus	Turkey	Europe
PI 172799	C. lanatus	Turkey	Europe
PI 179233	C. lanatus	Turkey	Europe
PI 181740	C. lanatus	Lebanon	Asia
Grif 1731	C. lanatus	China	Asia
PI 211849	C. lanatus	Iran	Asia
PI 211851	C. lanatus	Iran	Asia
PI 212287	C. lanatus	Afghanistan	Asia
Grif 5595	C. lanatus	India	Asia
Grif 5596	C. lanatus	India	Asia
PI 222775	C. lanatus	Iran	Asia
PI 222778	C. lanatus	Iran	Asia
PI 226459	C. lanatus	Iran	Asia
PI 227202	C. lanatus	Japan	Asia
PI 270307	C. lanatus	Philippines	Asia
PI 319236	C. lanatus	Japan	Asia

Table 12 Continued

Accession ID	species	Country	Continent
Grif 5599	C. lanatus	India	Asia
Grif 12336	C. lanatus	China	Asia
PI 426625	C. lanatus	Pakistan	Asia
PI 435990	C. lanatus	China	Asia
PI 470246	C. lanatus	Indonesia	Asia
Grif 14199	C. lanatus	India	Asia
PI 164539	C. lanatus	India	Asia
PI 381696	C. lanatus	India	Asia
PI 536453	C. lanatus	Maldives	Asia
PI 212289	C. lanatus	Afghanistan	Asia
PI 536449	C. lanatus	Maldives	Asia
PI 534584	C. lanatus	Syria	Asia
PI 164146	C. lanatus	India	Asia
PI 169261	C. lanatus	Turkey	Europe
PI 181868	C. lanatus	Syria	Asia
PI 174103	C. lanatus	Turkey	Europe
PI 507861	C. lanatus	Hungary	Europe
PI 507865	C. lanatus	Hungary	Europe
PI 507867	C. lanatus	Hungary	Europe

Table 12 Continued

Accession ID	species	Country	Continent
PI 507868	C. lanatus	Hungary	Europe
PI 508441	C. lanatus	South Korea	Europe
PI 512339	C. lanatus	Spain	Europe
PI 512343	C. lanatus	Spain	Europe
PI 512346	C. lanatus	Spain	Europe
PI 512353	C. lanatus	Spain	Europe
PI 512356	C. lanatus	Spain	Europe
PI 512360	C. lanatus	Spain	Europe
PI 512363	C. lanatus	Spain	Europe
PI 512390	C. lanatus	Spain	Europe
PI 512393	C. lanatus	Spain	Europe
PI 512395	C. lanatus	Spain	Europe
PI 512407	C. lanatus	Spain	Europe
PI 518606	C. lanatus	Russian federation	Europe
PI 518612	C. lanatus	Former Soviet Union	Europe
PI 537465	C. lanatus	Spain	Europe
PI 538888	C. lanatus	Russian federation	Europe
PI 561138	C. lanatus	Kazakhstan	Europe

Table 12 Continued

Accession ID	species	Country	Continent
PI 270144	C. lanatus	Greece	Europe
PI 270145	C. lanatus	Greece	Europe
PI 276657	C. lanatus	Russian federation	Europe
PI 276658	C. lanatus	Russian federation	Europe
PI 276659	C. lanatus	Russian federation	Europe
PI 357743	C. lanatus	Former Serbia and Montenegro	Europe
PI 370427	C. lanatus	Former Serbia and Montenegro	Europe
PI 370430	C. lanatus	Former Serbia and Montenegro	Europe
PI 379223	C. lanatus	Former Serbia and Montenegro	Europe
PI 379229	C. lanatus	Former Serbia and Montenegro	Europe
PI 379231	C. lanatus	Former Serbia and Montenegro	Europe
PI 379251	C. amarus	Former Serbia and Montenegro	Europe
PI 476324	C. lanatus	Former Soviet Union	Europe
PI 512350	C. lanatus	Spain	Europe

Table 12 Continued

Accession ID	species	Country	Continent
PI 357731	C. lanatus	Former Serbia and Montenegro	Europe
PI 518610	C. lanatus	Former Soviet Union	Europe
PI 212208	C. lanatus	Greece	Europe
PI 379237	C. lanatus	Former Serbia and Montenegro	Europe
PI 163574	C. lanatus	Guatemala	South America
PI 269678	C. lanatus	Belize	South America
PI 438675	C. lanatus	Mexico	North America
Cole's Early	C. lanatus	United States	North America
Garrisonian	C. lanatus	United States	North America
Klondike Stripe	C. lanatus	United States	North America
Fairfax	C. lanatus	United States	North America
Klecky Sweet	C. lanatus	United States	North America
Mickie Lee	C. lanatus	United States	North America
Calhoun Gray	C. lanatus	United States	North America
Sweet Princess	C. lanatus	United States	North America
Georgia Rattle Snake	C. lanatus	United States	North America
Orange Tender Sweet	C. lanatus	United States	North America
Bush Sugar Baby	C. lanatus	United States	North America

Table 12 Continued

Accession ID	species	Country	Continent
Crimson Sweet	C. lanatus	United States	North America
Sugarbaby	C. lanatus	United States	North America
Jubliee	C. lanatus	United States	North America
PI 458739	C. lanatus	Paraguay	South America
PI 543212	C. lanatus	Bolivia	South America
Golden Honey	C. lanatus	United States	North America
Missouri Heirloom Yellow Flesh	C. lanatus	United States	North America
Colorado Preserving or Red Seeded Citron	C. lanatus	United States	North America
Hopi Yellow	C. lanatus	United States	North America
Japanese cream fleshed suka	C. lanatus	Japan	Asia
Ledmon	C. lanatus	United States	North America
Charleston Gray	C. lanatus	United States	North America